STRUCTURE-BASED GENERALIZED MODELS FOR PURE-FLUID SATURATION PROPERTIES AND ACTIVITY COEFFICIENTS

By

DEVIPRIYA RAVINDRANATH

Bachelor of Technology

University College of Technology
Osmania University

Hyderabad, India

2002

Submitted to the Faculty of the
Graduate College of the
Oklahoma State University
in partial fulfillment of
the requirements for
the Degree of
MASTER OF SCIENCE
December, 2005

STRUCTURE-BASED GENERALIZED MODELS FOR

PURE-FLUID SATURATION PROPERTIES AND

ACTIVITY COEFFICIENTS

Thesis Approved:

Khaled A.M. Gasem

Thesis Advisor

Robert L. Robinson, Jr.

James Smay

A. Gordon Emslie

Dean of Graduate College

PREFACE

Structure-based generalized models were developed for *a priori* predictions of pure-fluid saturation properties, and for vapor-liquid equilibrium (VLE) of binary mixtures. Specifically, Quantitative Structure-Property Relationships (QSPR) modeling was used to provide structure-based parameters for (a) the Scaled-Variable-Reduced-Coordinate (SVRC) saturation property model, and (b) the Non-Random Two-Liquid (NRTL) and the Universal Quasi-Chemical (UNIQUAC) activity coefficient models. A representative database comprised of diverse molecular species was utilized for these generalizations

The SVRC-QSPR model generalizations for vapor pressure and saturated phase densities yielded predictions with absolute average deviation (AAD) of 1%. Similarly, the NRTL-QSPR and UNIQUAC-QSPR activity coefficient models produced VLE predictions within twice the AAD of the data regressions.

The results of this preliminary study demonstrate the efficacy of using theory-framed QSPR modeling for generalizing saturation property and phase equilibrium models.

ACKNOWLEDGMENTS

Many people have been a part of my graduate education, as friends, teachers, and colleagues. Dr. Khaled Gasem has been all of these. The best advisor and teacher I could have wished for, he is actively involved in the work of all his students, and clearly has their best interest in mind. He has made my learning experience at Oklahoma State University interesting and worthwhile.

Many thanks to the members of my thesis committee, Dr. Robert Robinson and Dr. James Smay for helping to supervise me, and for offering useful directions through many insightful discussions. In addition, I would like to thank my colleagues Dr. James Fitzgerald and Dr. Srinivasa Godavarthy for their valuable input.

I would like to thank my all friends at OSU for making my stay at Stillwater memorable. Special thanks to Satish Gundawar and Venkat Padmanabhan for their constant encouragement and support, and for always being there for me. I cannot end without thanking my father P.V. Ravindranath, my mother Indra Ravindranath, and my brother Rajiv on whose constant love and memory I have relied throughout my time at OSU.

TABLE OF CONTENTS

CHAPTER PAGE

LIST OF TABLES

LIST OF FIGURES

FIGURE PAGE

FIGURE PAGE

NOMENCLATURE

Symbols

$\hat{A}_{12}$	one-parameter Margules constant
A_{12}	one-parameter Margules constant (temperature dependant)
AAD	average absolute deviation
A, B, C	correlation constants
$\hat{f}$	fugacity
G^E	excess Gibbs energy
g_{ij}	energy of interaction between a i-j pair of molecules
K_1, K_2	equilibrium constants
P	pressure
q_i	van der Waals surface area
r_i	van der Waals volume
R	universal gas constant
RMSE	root mean square error
S	objective function defined by Equation (3.13)
T	temperature
x, y	mole fractions in the liquid and vapor phase
Y	saturation property

Greek Symbols

α	scaling exponent
$\Delta\alpha$	α_c-α_t
α_{12}	non-randomness factor in the NRTL model
β	coefficient of molecular descriptor
Δ_{ij}	NRTL interaction parameters modeled
ε	reduced variable for property Y
γ	activity coefficient
ϕ_i	area fraction in the UNIQUAC model
θ_i	volume fraction in the UNIQUAC model
Θ	correlating function
τ_{ij}	interaction parameters of the NRTL and the UNIQUAC model
ω	acentric factor

Subscripts and Superscripts

b	normal boiling point state
c	critical point state
cal	calculated
expt	experimental
l	liquid phase
r	reduced property
t	triple point state
v	vapor phase
0	reference state

CHAPTER 1

INTRODUCTION

Knowledge of thermodynamic properties and phase equilibria of mixtures is critical in the design of industrial processes such as distillation, extraction and other phase-contacting operations. In addition to optimization of existing processes, there is also an increasing demand for the design of new cost-effective processes and the synthesis of new improved materials. The traditional industrial approach has been to determine experimentally the properties of these new materials. However, this has proven to be time consuming and expensive. An alternate approach is to use theoretical and empirical thermodynamic property models; however, such models depend on the availability of experimental data, and the predictive ability of most of these models is limited when applied to systems with little or no reliable experimental data. Hence there is a need for reliable generalized property models capable of giving *a priori* predictions of pure-fluid properties and phase behavior of diverse systems thereby reducing the burden of experimentation.

1.1 Need for Generalized Pure-Fluid Saturation Property Models

Several equation-of-state (EOS) and empirical models [1] are available in the literature for prediction of pure-fluid saturation properties. However, many of these models suffer from a limited range of applicability and poor generalizations when applied

to systems with limited or no data. Also, the need for specialized correlations for each saturation property amplifies the usefulness of a unified and generalized framework for the prediction of pure-fluid saturation properties. The Scaled-Variable-Reduced-Coordinate (SVRC) model developed at OSU [2, 3], based on corresponding states theories (CST) and scaling-laws, provides precise representations of the pure-fluid behavior. Generalized equations were developed for the model parameters based on traditional physical properties (e.g., critical properties, acentric factor, etc.). The SVRC model provides accurate predictions for normal fluids. However, generalizations for polar fluids such as alcohols, ketones and aldehydes were less accurate, as the SVRC model generalizations do not account fully through traditional physical properties for the structural variations of the different classes of compounds. Nevertheless, the results obtained show that the trends produced by the SVRC model parameters can be further utilized in developing a reliable predictive model.

The use of *ab initio* approaches is being explored by several researchers [4, 5] to develop improved generalized models for fluid property prediction. Among the currently available approaches, Quantitative Structure-Property Relationships (QSPR) modeling has proven to be effective in correlating the properties of compounds with their structures. Studies based on QSPR models to correlate pure-fluid properties like vapor pressure, critical properties, liquid density, etc. [6, 7, 8] have been published in the literature. However, most current QSPR models are limited to predictions at a single temperature, and a need exists to extend this structure-based modeling to describe the entire saturation range.

This work presents an integrated approach for developing generalized models capable of accurate *a priori* predictions of pure-fluid properties over the full saturation range. The QSPR models provide effective parameter generalizations for the SVRC framework which can then represent the fluid behavior over the full saturation range (from the triple point to the critical point temperature).

1.2 Need for Generalized Activity Coefficient Models

Phase equilibria models are required for the design and optimization of numerous chemical processes. Fluid phase equilibrium pressure, temperature and composition for multicomponent systems can be measured using a variety of methods; however, these measurements are both cost and time intensive. Hence, EOS and excess Gibbs energy solution models are widely used to describe the equilibrium properties of mixtures. Compared to the EOS models, the excess Gibbs energy models have found wide application because of their ability to handle highly non-ideal systems. However, both these approaches have limited abilities for *a priori* predictions. The earliest attempt for a generalized, predictive activity coefficient model was made by Hildebrand and Scatchard [9, 10], based on the van Laar theory. They developed the regular solution theory, which gives semi-quantitative representations of activity coefficients for non-polar solutions. Most current studies attempt to estimate vapor-liquid equilibrium (VLE) properties from molecular structure, so as to obtain *a priori* predictions for systems with little or no experimental data. Among these, the group contribution concept has found considerable success and wide usage. It is based on the concept that a solution is made up of functional groups rather than molecules. The generalized-parameter prediction based on the

UNIQUAC model through the group contribution approach, the UNIFAC model [9, 10], is widely used owing to its large range of applicability and reliable predictions compared to existing activity coefficient models. However, the limitation of this model is that it accounts only for first-order structural dependence and hence cannot account for the group proximity effects within molecules. The model is also based on the assumption that the interaction energy of the mixture is the sum of functional group interaction energies; thus, it is limited by the availability of group interaction parameters. It also lacks an *a priori* method for defining the functional groups.

QSPR modeling has shown potential in providing accurate predictions of fluid properties based on the molecular structure. The goal of this work is to generalize the interaction parameters of the widely used theoretical excess Gibbs energy models like the NRTL and the UNIQUAC models using QSPR modeling; thereby, a predictive, structure-based model capable of describing the phase behavior of diverse systems at various conditions can be developed.

1.3 Objectives

The goal of this work is to develop structure-based generalized models for the *a priori* predictions of (a) pure-fluid vapor pressures and saturated phase densities, and (b) of vapor-liquid equilibrium of binary mixtures. The specific objectives for accomplishing this goal are to:

1. Assemble a reliable database of pure-fluid vapor pressures and saturated phase densities and for binary vapor-liquid equilibrium for model development and validation.

2. Develop QSPR models to provide structure-based parameters for the SVRC, NRTL and UNIQUAC models.
3. Ascertain that the QSPR generalized models are capable of predicting the saturation properties within 1% absolute average deviation (AAD) and the VLE properties within two to three times the precision of the experimental data.

1.4 Thesis Organization

This thesis is written in the manuscript style and is divided into two separate manuscripts. Chapter 1 of the thesis provides the rationale and the objectives of this work. Chapter 2 presents the development of linear and non-linear QSPR models to obtain structure-based parameters of the SVRC model. The results for vapor pressure, liquid density and vapor density are presented and discussed in this chapter. Chapter 3 deals with the structure-based generalization of the NRTL and the UNIQUAC model parameters. Finally, Chapter 4 presents a summary of conclusions based on the results from Chapters 2 and 3, and possible directions for future research are outlined.

References

1. Reid, R.C., Prausnitz, J.M., Poling, B.E., The Properties of Gases and Liquids, 4th Ed., McGraw –Hill, 1987.
2. Shaver, R.D., Robinson, R.L., Jr., Gasem, K.A.M., A Framework for the Prediction of Saturation Properties: Vapor Pressures, *Fluid Phase Equilibria*, 64, 141-163 (1991).
3. Shaver, R.D., Robinson, R.L., Jr., Gasem, K.A.M., A Framework for the Prediction of Saturation Properties: Liquid Density, *Fluid Phase Equilibria*, 64, 81-98 (1992).
4. Eckert, F., Klamt, A., Fast Solvent Screening via Quantum Chemistry: COSMO-RS Approach, *AIChE Journal*, 48(2), 369-385 (2002).
5. Prausnitz, J.M., Macknick, A.B., Vapor Pressure of Heavy Liquid Hydrocarbons by a Group-Contribution Method, *Ind. Chem. Eng. Fundamentals*, 18(4), 348-351 (1979).
6. Katritzky, R.A., Wang, Y., Sild, S., Tamm, T., QSPR Studies on Vapor Pressure, Aqueous Solubility, and the Prediction of Water-Air Partition Coefficients, *Journal of Chemical Information and Computer Sciences,* 38, 720-725 (1998).
7. McClelland, E.H., Jurs, C.P., Quantitative Structure-Property Relationships for the Prediction of Vapor Pressures of Organic Compounds from Molecular Structure, *Journal of Chemical Information and Computer Sciences,* 40, 967-975 (2000).
8. Karelson, M., Perkson, A., QSPR Prediction of Densities of Organic Liquids, *Computers & Chemistry*, 23, 49-59 (1999).

9. Prausnitz, J.M., Tavares, F.W., Thermodynamics of Fluid Phase Equilibria for Standard Chemical Engineering Operations, *AIChE Journal*, 50(4), 739-761 (2004).
10. Walas, S.M., Phase Equilibrium in Chemical Engineering, Butterworth Publishers, Boston, 1985.

CHAPTER 2

PURE-FLUID SATURATION PROPERTY PREDICTION: THE SVRC-QSPR MODEL

2.1 Introduction

Accurate knowledge of saturation properties of pure fluids is essential for the theoretical understanding of fluid phase behavior and for the effective design, development and operation of numerous industrial processes. Often in the industry the saturated properties of the fluid of interest are determined experimentally. This approach, however, is both time and cost intensive. An alternative approach is to develop accurate theoretical models based on first principles. However, these models depend on the availability of experimental data, and in most cases model generalizations fail to give accurate property estimations. Furthermore, the need for specialized correlations for each saturation property and for different types of compounds amplifies the usefulness of an efficient and reliable framework for property predictions.

The theoretical methods available in literature are predominantly fluid-specific equation of state (EOS) or generalized corresponding states theories (CST) approaches. The disadvantage of the EOS approach is that it has a limited range of applicability, e.g., the temperature and pressure range to which the EOS can be applied. Also, these EOSs cannot be generalized for a wide range of fluids. In previous work done by the research group at OSU [1, 2], the CST was used in developing a framework capable of correlating

the saturation properties over a temperature range extending from the triple to the critical point. The Scaled-Variable-Reduced-Coordinate (SVRC) framework thus developed [1, 2] provides good representations of pure-fluid saturation properties of diverse chemical species and has demonstrated potential for generalized predictions. However, the generalized predictions for highly polar fluids such as alcohols are less accurate since the current SVRC model generalizations do not fully account for the structural variations of the different classes of compounds.

Accurate generalizations can be obtained when the property models account fully for molecular structural variations. Currently, several *ab initio* methods are being used for structure-based property prediction. Models based on Molecular Dynamics (MD) and Monte Carlo (MC) simulation techniques are being researched, but these techniques are time-consuming, computationally intensive and are not at a stage where they can be applied routinely to a wide range of compounds. Sandler and co-workers [3] and Eckert and co-workers [4] have used the conductor-like screening model for real solvents (COSMOS-RS) approach for the calculation of vapor pressures. However, their work is limited to prediction of vapor pressure at a single temperature. Prausnitz and co-workers [5] utilized the group contribution method to estimate the parameters of the AMP [6] equation used to calculate vapor pressure. Olsen and co-workers [7] use the UNIQUAC functional groups activity coefficients (UNIFAC) method for predicting vapor pressures, which is implemented in a program P_PREDICT. However, their study again is limited to single temperature property estimation.

Another *ab initio* approach that has gained significant prominence is the use of Quantitative Structure-Property Relationships (QSPR) and artificial neural networks (ANN) models to correlate the desired property with molecular structure. Several studies based on the QSPR models for the correlation of vapor pressure [8, 9, 10, 11], aqueous solubilities [10], and phase densities [12] have been published. Although these studies were successful in correlating the property with structure, they were limited to estimating properties at a single temperature, i.e., they do not account for the temperature dependence of the fluid properties.

In this work, we seek to overcome the above drawbacks of current QSPR modeling. Specifically, we propose to generalize the parameters of a *theory-based* model using the QSPR methodology. As the SVRC model has proven to be a model capable of correlating precisely the fluid saturation properties over the entire saturation range and has demonstrated generalization capabilities, the goal of this work is to combine the SVRC saturation property model with the parameter-generalization QSPR model. We use QSPR modeling to develop structure-based generalizations of the SVRC model parameters, thus providing a generalized model capable of *a priori* predictions of the saturation properties for a diverse set of organic compounds and accounting for the fluid behavior over the entire saturation range.

2.2 Overview of the SVRC and QSPR Modeling

2.2.1 The SVRC Model

In previous studies [1, 2], the SVRC framework was used to correlate saturation properties of a wide variety of organic molecules over the entire saturation range. The SVRC model utilizes corresponding states theory (CST) and scaling-law behavior. The SVRC model with two regressed parameters per molecule was able to represent the vapor pressure of most molecules within 0.1%. The previous modeling efforts, which involved a limited database of aliphatic compounds and alcohols, showed that the SVRC model yeilds accurate generalized predictions for saturation properties of normal and slightly polar fluids with average errors of less than 1% based on available physical properties.

The general SVRC formulation for correlating thermo-physical properties between the triple and the critical points may be given as [1, 2]:

$$Y = \left\{ Y_c^{\alpha} - \left(Y_c^{\alpha} - Y_t^{\alpha} \right) \Theta \right\}^{(1/\alpha)} \tag{2.1}$$

where Θ = correlating function, α = scaling exponent, Y = saturation property at given T, and the subscripts c and t represent critical and triple points, respectively. The values of Θ and α are dependent on the saturation property being calculated:

For vapor pressure

$$\Theta(\varepsilon) = \frac{\left(1 - A^{\varepsilon^B}\right)}{(1 - A)} \tag{2.2}$$

$$\alpha = \alpha_c - \Delta\alpha \frac{\varepsilon(1 + C\varepsilon)}{(1 + C)} \tag{2.3}$$

For liquid density

$$\Theta(\varepsilon) = \frac{\left(1 - A^{\varepsilon^B}\right)}{(1 - A)} \tag{2.4}$$

$$\alpha = \alpha_c - \Delta\alpha \frac{\left(1 - A^{\varepsilon}\right)}{(1 - A)} \tag{2.5}$$

For vapor density

$$\Theta = \frac{\left(2 - A_1^{\varepsilon^{B_1}} - A_2^{\varepsilon^{B_2}}\right)}{(2 - A_1 - A_2)} \tag{2.6}$$

$$\alpha = \alpha_c - \Delta\alpha \frac{\left(2 - A_1^{\varepsilon^C} - A_2^{\varepsilon}\right)}{(2 - A_1 - A_2)} \tag{2.7}$$

where

$$\varepsilon = \frac{T_c - T}{T_c - T_t} \tag{2.8}$$

$$\Delta\alpha = \alpha_c - \alpha_t \tag{2.9}$$

and A, B and C are correlation constants, α_c and α_t are the limiting values of α at the critical temperature and triple point temperatures, respectively. The SVRC model accounts for the effects of temperature and chemical structure through the correlating

function (Θ) and the scaling function (α). The parameters α_c and α_t have been found to be highly structure dependent [1, 2]. The normal boiling point (T_b), critical compressibility factor (Z_c) and the accentric factor (ω) were used for parameter generalization. The SVRC model gives accurate descriptions of the properties considered over the full saturation region (including the near critical region) and demonstrates the effectiveness of using structure-based parameters. However, current generalizations fail to account for structural variation of complex and highly polar compounds.

2.2.2 QSPR Modeling

Computational techniques have improved drastically over the last two decades, along with the revolutionary advances in computing power. They are routinely used to address more complex engineering and design problems in chemical processing. Computation intensive models are also being used to complement, guide and sometimes replace experimental measurements, thus reducing the amount of time and money spent on research to bring ideas from the lab to practical application.

The QSPR approach is among the computational methods gaining wide use. It is based on the assumption that there exists a relationship between the structure of a substance and its physical and chemical properties. QSPR uses quantum mechanics to define the structure of the molecule in terms of a series of molecular descriptors and then correlates the property in terms of these descriptors. Molecular descriptors are variables which describe the structural characteristics of the molecule and its interactions. They are classified as follows [13]:

Constitutional Descriptors: These are simple descriptors based on the chemical composition of the compound. Example constitutional descriptors include number of atoms, number of bonds, number of rings, and molecular weight.

Topological Descriptors: These descriptors describe the atomic connectivity in the molecule. Example topological descriptors include molecular connectivity indices, substructure counts, molecular distance edge descriptors, kappa indices, and electro topological state indices.

Geometric Descriptors: These descriptors are derived from the three-dimensional structure of the compound. Example geometric descriptors include moments of inertia, solvent-accessible surface area, length-to-breadth ratios, shadow areas, and gravitational index.

Electrostatic Descriptors: These descriptors give the charge distribution of the entire molecule. Example electrostatic descriptors include polarity indices, charged partial surface area, and partial charges.

Quantum Chemical Descriptors: These descriptors are derived from quantum chemical calculations and provide an accurate description of electronic distribution, and they account for the partial charges of fragments of molecules. The descriptors also provide the value of the partial charge of the atoms in the molecule (e.g., dHmin represents the minimum partial charge on a hydrogen atom).

Thermodynamic Descriptors: These descriptors are calculated on the basis of the total partition function (Q) of the molecule and its electronic, translational, rotational, and vibrational components.

The QSPR approach has found wide applications in the calculation of thermo-physical properties, aqueous solubilities, partition coefficients and in the design of new chemicals [9, 10, 14]. This approach has the potential of providing predictions for as-yet unknown or unmeasured compounds based on structural information. Several QSPR studies exist for the calculation of vapor pressures of pure compounds [8, 9, 10, 11]. The correlation of liquid densities by Karelson[12] is the only available QSPR study on liquid densities, and to our knowledge no work has been done on the correlation of vapor densities using QSPR models. However, these models are limited to the prediction of properties at a single temperature. A study by Yaffe and co-workers [8] uses a neural network/QSPR model to predict vapor pressures of simple hydrocarbons as a function of temperature. This study was moderately sucessful; overall absolute average deviations (AAD) of around 10% was observed for the database considered and large errors were observed for complex aromatic and polar compounds. The work previously done by the research group at OSU on aqueous solubility and normal boiling points of pure compounds [15] demonstrates that the QSPR modeling provides an effective tool in correlating and predicting properties from structural information.

In this work, we use the integrated SVRC-QSPR model to describe the fluid behavior over the entire saturation range and to obtain effective parameter generalizations based on the chemical structural information; in turn, these QSPR generalized models

will provide accurate *a priori* predictions of saturation properties of diverse organic compounds in the absence of experimental data.

2.3 QSPR Methodology

2.3.1 Linear Model

A brief overview of the QSPR methodology is shown in Figure 2.1. The database is compiled and the names of the individual molecules are stored in EXCEL and 2-D structures are generated using ChemDraw [16]. Then the 3-D structures are generated and the structures are optimized in Chem 3D Ultra [16]. These optimized structures are further optimized and refined in AMPAC 6.0 [17]. The output of AMPAC serves as the input to the QSPR model. The entire data available is split into training and prediction

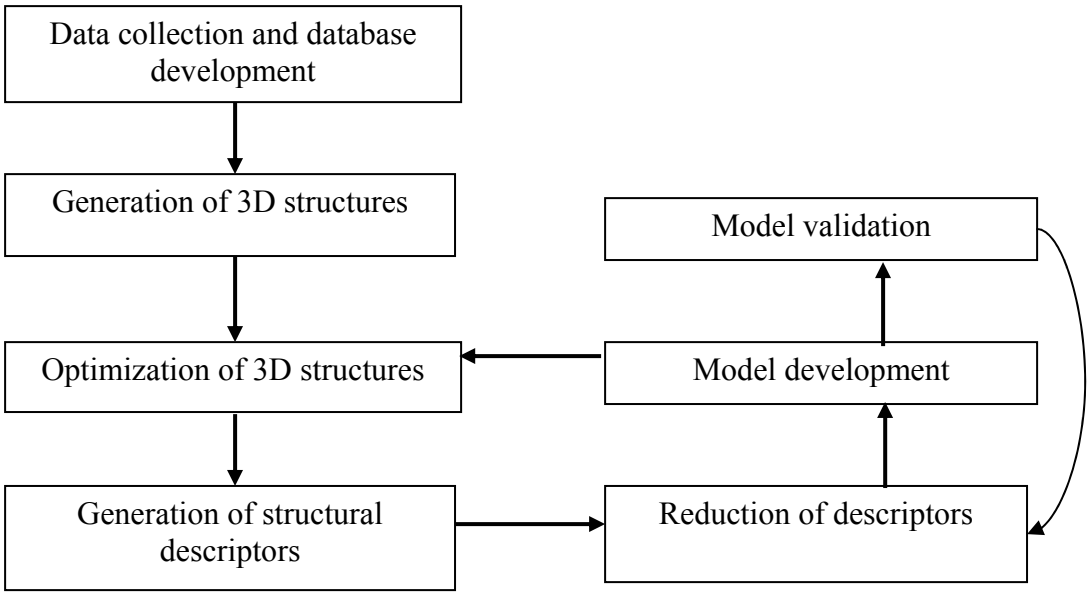

Figure 2.1 Overview of QSPR Methodology

sets. A commercial QSPR package, CODESSA [18] is used for the descriptor generation. Over 1400 molecular descriptors are calculated for each compound. Insignificant

descriptors are eliminated by statistical methods available in CODESSA. A multi-linear regression (MLR) model is then used to relate the molecular descriptors to the property of interest, i.e., the model parameters. The generalized model parameters thus obtained are used to predict the property.

In this study, a multi-linear model was developed relating the molecular descriptors to the property of interest. The general form of the correlation is given as:

$$y = \beta_o + \sum_{i=1}^{N} \beta_i x_i \qquad (2.10)$$

where, y = property of interest (e.g., a model parameter), β_o = intercept, N = number of molecular descriptors, β_i = coefficient for descriptor 'i' and x_i = molecular descriptor 'i'. The multi-parameter regression that maximizes the predicting ability is determined using the following strategy:

1. All orthogonal pairs of descriptors i and j are found in a given data set.
2. The property analyzed is treated by using the two-parameter regression with the pairs of descriptors, obtained in Step 1.
3. For each descriptor pair obtained in the previous step, a non-collinear descriptor, k is added, and the respective three-parameter regression treatment is performed.
4. For each descriptor set chosen in the previous step, an additional non-collinear descriptor scale is added, and the respective (n+1) parameter regression treatment is performed.

The final product of the above steps is a linear relationship between the molecular structure and the property of interest containing n parameters.

2.3.2 Non-Linear Model

The *CODESSA program* is used to develop a linear relationship between the descriptors and the parameters. If accurate generalizations are not obtained with a linear model, then the descriptors from the linear model are used as input to develop a non-linear model. A wide range of non-linear architectures are available; often, the network is chosen based on a trial-and-error process. Available literature suggests that a back-propagation network, although it has a simple architecture, is well suited for property prediction models. The number of hidden neurons and hidden layers are again chosen based on a trial-and-error process. As a rule of thumb, the ratio of the number of molecules to the number of adjustable parameters should be greater than two to obtain a robust non-linear model [19].

Once, suitable network architecture has been identified, the next step is to determine the adjustable weights on the network connections. The usual procedure is to initialize randomly these weights multiple times and determine which set of weights provides the lowest training error. A common problem encountered in neural network model development is over training. The root mean square error (RMSE) for the training set usually decreases as the number of training cycles increases; however, the ability of the network to predict eventually decreases. This is called over-fitting, which typically results in larger RMSE for the prediction set than for the training set.

To identify the optimum number of training cycles, where the training and prediction sets exhibit their lowest errors, a procedure known as cross validation (CV) is commonly employed. The entire data are split into training and cross validation sets. The

network is trained using only the training dataset. Periodically, the training is halted and error values for the cross validation set are predicted. Any training beyond the minimum error in the CV set indicates that the network is being over trained. At the onset of an increase in the CV set RMSE, the network has essentially learned all of the general information from the training set and has just started to memorize their individual characteristics. Since the goal of network training is not only to produce small errors in the training set but also to produce reasonable prediction results (referred to as the ability to generalize), the training cycle corresponding to the minimum CV RMSE corresponds to the termination point for training. The model parameters obtained from the non-linear model are then used in the theoretical frameworks to predict the properties considered.

2.4 Database Employed

A property database of pure fluids including, alkanes, refrigerants, aromatics and alcohols was used in the SVRC vapor pressure, liquid density and vapor density model development, respectively. The database contained over 8673 saturated vapor pressure points involving 90 fluids, 6806 saturated liquid density points involving 80 fluids, and 5203 saturated vapor density points involving 27 fluids. The databases used for vapor pressure and liquid density were diverse and nearly 50% of the compounds in both the databases were highly polar (dipole moment values ranging from 3.0-1.0 Debye). However, reliable vapor density data are rather limited and a database of 27 compounds, consisting mostly of aliphatic compounds and a few refrigerants was compiled. The data used in this study were compiled mainly from the NIST [20] and DIPPR [21] databases and were screened to include quality experimental data.

The data for each compound, to the extent possible, cover the full saturation range from the triple point to the critical point. Since the SVRC model requires the triple point and the critical point properties as input, these values were treated as adjustable parameters, and the quality of these physical properties and their effect on the overall regressions were evaluated. Data points with %AAD greater than twice the overall regression %AAD of a compound were eliminated from the database in an effort to remove erroneous data. Appendix A presents the complete list of the physical properties, the ranges and the sources of all data used in the model development.

2.5 Results and Discussion

The entire database for the vapor pressure and the saturated phase densities were correlated using the two-parameter SVRC model. Tables 2.1-2.3 present the results of the SVRC model regressions and generalizations for the three saturation properties under consideration. The SVRC model was able to correlate the vapor pressure, liquid density and vapor density within 0.2%, 0.1% and 0.3% AAD, respectively. These results are in agreement with those obtained from the previous SVRC modeling efforts [1, 2, 22] and proves the efficacy of the SVRC model in providing precise representations of the saturation properties for diverse chemical species over the full saturation range. However, as in previous studies [1, 2], the model generalizations obtained were not accurate when applied to highly polar compounds. The large errors obtained for some of the compounds, was attributed to the error in the physical properties. For example, a change in the physical properties of hydrogen reduced the AAD for hydrogen from 17% to 1% and the overall SVRC generalization results of vapor pressure from 2.9% AAD to 2.5% AAD.

Table 2.1: Results of the SVRC-QSPR vapor pressure model development

Compound	SVRC regressed %AAD	SVRC generalization %AAD [1, 2]	SVRC-QSPR linear %AAD	SVRC-QSPR NN %AAD	No. of pts.
Methane	0.02	0.42	1.5	0.92	199
Ethane	0.01	1.1	0.31	0.70	200
Ethylene	0.04	0.73	1.3	0.28	200
Propane	0.04	1.3	0.37	0.16	199
Butane	0.04	1.2	1.0	0.31	199
Pentane	0.07	0.55	1.9	0.11	200
Hexane	0.10	1.4	1.8	0.33	200
Oxygen	0.05	0.56	1.0	0.22	199
Fluorine	0.07	0.25	0.31	0.39	199
Nitrogen	0.03	0.40	0.67	0.30	198
Carbon dioxide	0.01	0.89	0.33	0.01	201
Benzene	0.02	0.68	2.8	1.3	42
Acetylene	0.28	1.0	0.67	0.28	27
1,3-Butadiene	0.22	1.3	1.3	1.1	45
Carbon disulfide	0.71	1.9	16.7	1.9	42
Carbon tetrachloride	0.34	0.45	1.2	0.98	81
Chlorine	0.44	0.44	0.75	0.50	40
Cyclopentane	0.21	2.0	7.2	0.62	35
Propylene	0.03	0.51	1.7	1.2	201
Isobutane	0.10	2.2	0.45	0.24	201
Heptane	0.04	1.4	2.1	0.24	201
Hydrogen	0.07	1.0	0.07	0.07	199
1-Butene	0.16	0.88	1.6	1.3	75
Cumene	0.28	11.5	8.6	2.0	62
Cyclohexane	0.39	1.1	2.1	1.1	66
Cyclohexene	0.27	2.8	1.9	2.3	58
1-Decene	0.38	7.9	7.9	1.4	88
Ethylbenzene	0.15	6.6	1.5	0.26	100
Indene	0.31	8.4	6.4	2.0	33
Isobutene	0.53	1.4	2.5	1.3	55
Naphthalene	0.49	2.1	1.8	1.0	90
n-Nonane	0.11	4.5	2.3	2.2	65

Table 2.1: Results of the SVRC-QSPR vapor pressure model development (Contd.)

Compound	SVRC regressed %AAD	SVRC generalization %AAD [1, 2]	SVRC-QSPR linear %AAD	SVRC-QSPR NN %AAD	No. of pts.
n-Octane	0.30	2.5	1.7	1.0	85
Toluene	0.23	5.8	2.0	1.1	80
o-Xylene	0.24	0.58	2.5	1.2	99
p-Xylene	0.24	1.4	1.2	0.48	93
Phenanthrene	1.08	1.1	0.94	0.97	22
Nitric oxide	0.29	2.0	1.1	0.29	42
Ammonia	0.04	0.16	0.72	0.55	201
Water	0.05	0.45	5.7	0.05	201
Acetone	0.05	0.34	0.72	0.62	47
Methanol	0.19	7.5	4.1	2.7	19
Ethanol	0.28	3.8	1.8	0.28	26
R-22	0.05	0.50	4.2	4.3	201
R-32	0.04	0.84	3.6	1.1	201
R-125	0.03	4.9	1.4	0.57	201
R-123	0.05	1.6	1.0	0.73	201
R-124	0.03	4.3	0.65	0.24	201
R-134a	0.04	5.9	5.2	2.3	201
R-143a	0.05	0.60	0.69	2.4	201
R-152a	0.04	0.44	3.2	1.6	201
1-Butanol	1.1	13.2	10.9	5.5	55
Chloroform	0.62	3.4	6.1	0.97	72
Diethyl ether	0.48	4.9	7.1	2.8	50
Ethyl acetate	0.58	2.9	0.58	2.0	78
Ethyl mercaptan	0.44	2.2	6.0	4.3	43
Ethylamine	0.54	1.9	1.7	1.0	54
Ethylene glycol	0.45	3.7	13.5	0.47	26
Formaldehyde	0.24	0.78	5.6	5.5	32
Hydrogen chloride	0.30	2.8	1.2	0.38	25
Cyclopropane	0.03	0.63	0.16	0.04	201
Methyl acetate	0.49	4.4	1.9	2.9	67
Methyl chloride	0.20	1.2	2.3	2.0	27
Methyl ethyl ketone	0.34	1.6	0.52	0.65	54
Methylamine	0.59	13.0	1.5	0.69	36

Table 2.1: Results of the SVRC-QSPR vapor pressure model development (Contd.)

Compound	SVRC regressed %AAD	SVRC generalization %AAD [1, 2]	SVRC-QSPR linear %AAD	SVRC-QSPR NN %AAD	No. of pts.
Nitric acid	0.73	44.8	1.9	0.74	30
Terephthalic acid	0.18	32.6	1.4	0.18	21
Diisopropyl ether	0.50	3.6	1.8	2.0	22
n-Propyl mercaptan	0.14	7.3	0.64	2.0	61
1-Butyl acetate	0.51	5.9	4.5	0.58	113
1,2-Dichloropropane	0.96	2.3	1.9	1.3	77
Isopentane	0.12	1.0	0.60	0.22	94
Glyoxal	0.12	1.0	0.89	0.13	21
n-Butylamine	0.06	4.0	1.0	0.76	10
Ethyl formate	0.32	0.32	1.5	0.92	45
1-Heptanol	0.47	6.2	3.7	0.56	57
1-Hexanol	0.87	7.9	14.2	0.85	43
2-Butanol	0.41	4.1	4.2	0.44	64
Diphenyl ether	0.49	6.6	3.8	0.51	29
Isobutylbenzene	0.44	2.6	3.7	2.2	36
n-Heptylamine	0.84	12.9	15.0	4.7	58
n-Hexylamine	0.23	0.36	2.4	2.6	31
2-Methyl propanol	0.79	1.1	1.4	2.3	35
Benzaldehyde	0.26	8.8	1.2	0.98	20
2-Heptanone	0.31	1.5	0.60	0.60	214
n-Octanol	0.39	4.3	13.2	0.41	74
Methyl benzoate	0.40	1.5	5.2	1.7	52
Cyclohexanol	0.49	6.6	10.9	0.50	35
Ethylene diamine	0.96	12.3	1.5	1.4	54
o-Methyl styrene	0.24	1.5	2.64	0.90	34
Overall %AAD	**0.19**	**2.5**	**2.4**	**0.99**	**8673**

Table 2.2: Results of the SVRC-QSPR liquid density model development

Compound	SVRC regressed %AAD	SVRC generalization %AAD [1, 2]	SVRC-QSPR linear %AAD	No. of pts.
R22	0.03	0.17	0.27	201
R32	0.02	0.54	1.0	201
R123	0.03	0.21	0.24	201
R125	0.03	0.45	0.42	201
R124	0.02	0.12	0.25	201
R134a	0.03	0.54	0.15	201
R152a	0.03	0.39	0.42	201
R143a	0.02	0.41	0.91	201
Methane	0.04	0.15	0.80	201
Ethane	0.03	0.10	0.20	201
Ethylene	0.02	0.25	0.79	201
Propane	0.06	0.11	0.35	201
Propylene	0.07	0.40	1.0	199
Butane	0.05	0.22	0.09	201
Isobutane	0.09	0.11	0.09	201
Pentane	0.07	0.33	0.18	201
Hexane	0.06	0.43	0.31	198
Heptane	0.08	0.56	0.27	189
Oxygen	0.05	0.22	0.10	201
Fluorine	0.08	0.63	0.14	186
Nitrogen	0.03	0.13	0.31	201
Ammonia	0.06	1.2	0.59	201
Water	0.38	5.1	0.38	47
Carbon dioxide	0.02	0.42	1.4	201
Hydrogen	0.14	2.1	0.21	186
Acetic acid	0.11	1.4	0.42	43
Benzene	0.13	0.19	1.7	124
Ethanol	0.18	8.3	0.26	56
Methanol	0.14	0.47	1.5	46
Acetone	0.05	0.20	0.30	9
1,3-Butadiene	0.06	0.11	1.1	88
Carbon disulfide	0.00	0.34	0.02	16
Carbon tetrachloride	0.06	0.18	0.31	51

Table 2.2: Results of the SVRC-QSPR liquid density model development(Contd.)

Compound	SVRC regressed %AAD	SVRC generalization %AAD [1, 2]	SVRC-QSPR linear %AAD	No. of pts.
Cyclopentane	0.28	2.2	1.4	30
1-Butene	0.18	0.33	0.46	49
Cumene	0.11	0.12	0.19	43
Cyclohexane	0.03	0.11	0.27	23
Cyclohexene	0.09	0.10	0.24	47
1-Decene	0.08	0.28	0.61	18
Ethylbenzene	0.03	0.15	0.31	82
Indene	0.40	0.40	0.50	17
Isobutene	0.15	0.28	0.31	55
Naphthalene	0.01	0.47	0.16	17
n-Nonane	0.09	0.28	0.31	47
n-Octane	0.16	0.20	0.96	24
Toluene	0.05	0.21	0.20	101
o-Xylene	0.05	0.63	0.57	63
p-Xylene	0.14	0.72	1.1	72
Phenanthrene	0.03	0.73	0.21	14
1-Butanol	0.16	1.2	0.66	39
Chloroform	0.10	0.52	0.21	61
Diethyl ether	0.10	0.28	1.2	31
Ethyl acetate	0.12	0.35	1.3	28
Ethyl mercaptan	0.16	0.50	0.37	19
Ethylamine	0.03	0.08	0.42	14
Ethylene glycol	0.06	1.8	0.26	92
Hydrogen chloride	0.17	1.4	0.22	15
Cyclopropane	0.27	5.4	0.44	63
Methyl acetate	0.15	0.61	1.6	26
Methyl chloride	0.08	0.32	0.63	41
Methylamine	0.02	1.2	0.97	14
Diisopropyl ether	0.22	0.28	0.26	6
o-Methyl styrene	0.00	0.05	0.02	16
Ethylene diamine	0.09	0.26	0.56	18
Ethyl formate	0.13	0.38	0.80	50

Table 2.2: Results of the SVRC-QSPR liquid density model development(Contd.)

Compound	SVRC regressed %AAD	SVRC generalization %AAD [1, 2]	SVRC-QSPR linear %AAD	No. of pts.
1-Heptanol	0.08	0.92	0.30	26
1-Hexanol	0.02	1.0	0.73	19
n-Octanol	0.16	1.9	0.25	38
Diphenyl ether	0.04	0.39	0.75	8
Methyl benzoate	0.02	0.04	0.03	16
n-Heptylamine	0.01	0.11	0.06	13
n-Hexylamine	0.08	0.85	0.28	17
Benzaldehyde	0.12	0.16	0.22	24
2-Heptanone	0.06	0.12	0.30	19
n-Propyl mercaptan	0.08	0.11	0.14	19
1-Butyl acetate	0.05	0.13	0.06	33
Isopentane	0.09	0.15	0.33	59
n-Butylamine	0.23	0.31	0.25	9
2-Butanol	0.06	3.6	0.50	14
Overall %AAD	**0.07**	**0.60**	**0.48**	**3205**

Table 2.3: Results of the SVRC-QSPR vapor density model development

Compound	SVRC regressed %AAD	SVRC generalization %AAD [1, 2]	SVRC-QSPR linear %AAD	SVRC-QSPR NN %AAD	No. of pts.
R-22	0.11	15.1	0.57	0.17	201
R-32	0.17	2.5	0.28	0.28	201
R-123	0.29	6.1	0.49	0.32	201
R-125	0.15	8.1	0.71	0.25	201
R-124	0.06	11.4	0.75	0.43	201
R-134a	0.12	9.5	0.57	0.14	201
R-152a	0.29	4.8	0.36	0.35	201
R-143a	0.14	5.7	0.22	0.15	201
methane	0.07	3.8	0.10	0.08	201
ethane	0.08	10.7	0.30	0.38	201
ethylene	0.20	4.9	0.53	0.24	201
propane	0.04	6.5	0.70	0.25	201
Propylene	0.82	1.9	0.93	0.83	201
butane	0.15	5.5	0.65	0.56	201
Isobutane	0.14	7.5	1.1	0.27	201
Pentane	0.14	2.9	0.81	0.57	201
Hexane	0.23	3.1	0.28	0.26	201
Heptane	0.44	2.4	0.60	0.47	201
oxygen	0.21	6.3	0.27	0.24	201
fluorine	0.66	8.8	1.0	0.67	201
nitrogen	0.12	2.8	0.46	0.14	201
ammonia	0.68	2.2	0.92	0.68	201
water	0.72	6.4	0.97	0.72	201
Carbon dioxide	0.11	1.5	0.12	0.11	201
hydrogen	1.8	4.7	1.8	1.8	199
Benzene	0.54	2.3	0.67	0.54	62
CO	0.13	3.9	0.16	0.13	191
Overall %AAD	**0.31**	**5.6**	**0.61**	**0.41**	**5203**

The entire database for vapor pressure, liquid density and vapor density were split into a 70:30 ratio of training and prediction sets. The regressed parameters obtained from the SVRC model were used as the input for a linear QSPR model developed using the commercial software CODESSA. The heuristic analysis available in CODESSA was used to eliminate redundant and insignificant descriptors and generate the most significant descriptors. Tables 2.4-2.6 list the descriptors used to develop the linear model for the vapor pressure, liquid density and vapor density, respectively. Sets of 12 molecular descriptors (consisting of quantum chemical, electrostatic and topological descriptors) were used to develop the linear models for vapor pressure and liquid density, and a set of 10 descriptors was used to develop the linear model for vapor density.

Tables 2.1-2.3 also present the results of the linear QSPR models for vapor pressure, liquid density and vapor density. Utilizing the parameters obtained from the linear QSPR models, the SVRC model was able to predict the vapor pressure, liquid density and vapor density within AAD of 2.4%, 0.48% and 0.61%, respectively. Figures 2.2 and 2.3 show the typical comparision plot of the calculated α_c and α_t obtained from the linear QSPR model and the regressed α_c and α_t obtained from the SVRC model for liquid density. The linear QSPR and SVRC model parameters for liquid density are in good agreement. Table 2.2 presents the overall results of the liquid density models. The SVRC-QSPR model generalizations were within 0.48%, which are more accurate than the original SVRC model generalizations (%AAD of 0.6). Also, the deviations for all the data points considered were within 3% AAD, as shown in Figure 2.4. Hence, the need for a non-linear QSPR model for liquid density was ruled out.

The results presented in Tables 2.1 and 2.3 clearly indicate that the linear QSPR models for vapor pressure and vapor density (%AAD of 2.4 and 0.61 for vapor pressure and vapor density, respectively) are more accurate than the original SVRC model

Table 2.4: Molecular descriptors used in SVRC-QSPR vapor pressure model development

Coefficient	Molecular Descriptors
α_c	
41.463	Intercept
35.265	Reduced temperature
-24.751	Acentric factor
13.953	Min resonance energy for a H-H bond
-1.627	Min net atomic charge for a H atom
11.467	exch. eng. + e-e repulsion for a H-O bond
-8.676	FHASA Fractional HASA
3.491	1X BETA polarizability (DIP)
3.042	Max SIGMA - PI bond order
4.471	RPCS Relative positive charged surface area
-4.640	WNSA-2 Weighted partial negative surface area
-3.670	Number of aromatic bonds
2.774	FNSA-3 Fractional negative surface area
α_t	
5.492	Intercept
47.457	Reduced temperature
-19.961	Acentric factor
15.049	Min resonance energy for a H-H bond
-9.418	FHBCA Fractional HBSA
6.990	HDSA H-donors surface area
3.682	Min partial charge (Qmin)
4.685	RPCS Relative positive charged surface area
4.275	Max SIGMA - PI bond order
-2.993	YZ Shadow
-4.561	WNSA-2 Weighted partial negative surface area
-3.471	Number of rings
-2.662	Max partial charge for a H atom

Table 2.5: Molecular descriptors used in SVRC-QSPR liquid density model development

Coefficient	Molecular Descriptors
α_c	
-2.069	Intercept
6.090	Max nucleophilic reactive index for a N atom
-12.098	Avg 1-electron reactive index for a N atom
-1.954	HACA-2/TMSA
-2.621	Max bond order of a N atom
2.482	Min total interaction for a H-O bond
3.075	YZ Shadow / YZ Rectangle
-4.179	Topographic electronic index (all pairs)
3.665	Acentric factor
-2.900	Total hybridization comp. of the molecular dipole
2.006	HASA-2/TMSA
2.976	DPSA-3 Difference in Charged partial surface areas
2.666	Relative number of H atoms
α_t	
3.161	Intercept
-6.041	Principal moment of inertia A / # of atoms
8.217	Min nucleophilic reactive index for a N atom
-8.314	Max 1-electron reactive index for a N atom
-2.840	Lowest normal mode vibrational frequency
2.564	Max atomic state energy for a C atom
-2.989	Principal moment of inertia C / # of atoms
-1.700	HASA-1/TMSA
2.135	Max electrophilic reactive index for a C atom
3.665	1X GAMMA polarizability (DIP)
-3.306	Randic index (order 1)
2.756	WPSA-1 Weighted positive partial surface area
1.374	Total molecular 1-center E-E repulsion

Table 2.6: Molecular descriptors used in SVRC-QSPR vapor density model development

Coefficient	Molecular Descriptors
α_c	
24.934	Intercept
-11.520	Acentric factor
16.542	ALFA polarizability (DIP)
7.369	Total hybridization comp. of the molecular dipole
-7.684	FPSA-2 Fractional positive partial surface area
-9.762	Translational entropy (300K)
-8.479	Normal boiling temperature
-4.259	RPCS Relative positive charged surface area
-4.872	ZX Shadow / ZX Rectangle
5.711	Min partial charge (Qmin)
4.820	Min electrophilic reactive index for a F atom
α_t	
22.974	Intercept
-19.538	Acentric factor
42.990	Reduced temperature
-11.743	Total entropy (300K) / # of atoms
5.281	Min e-e repulsion for a C atom
-6.920	Avg 1-electron reactive index for a O atom
9.896	Lowest normal mode vibrational frequency
6.737	Polarity parameter / square distance
-6.528	Total entropy (300K)
4.617	Wiener index
-3.425	Max nucleophilic reactive index for a F atom

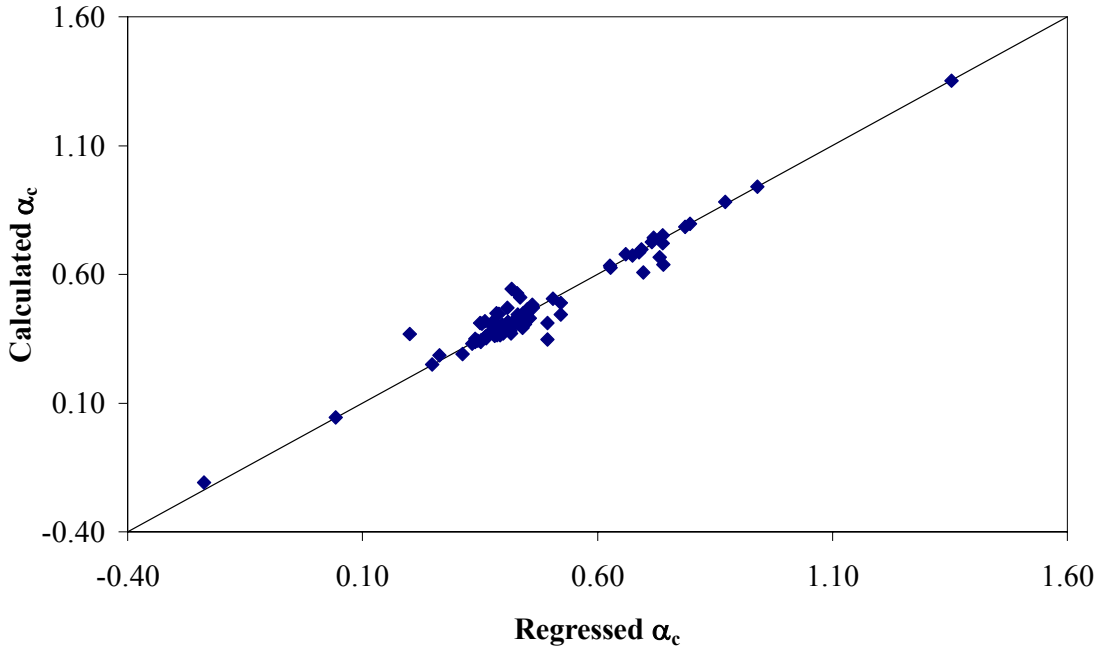

Figure 2.2: Comparison plot of regressed α_c and calculated α_c of the SVRC-QSPR model for liquid density

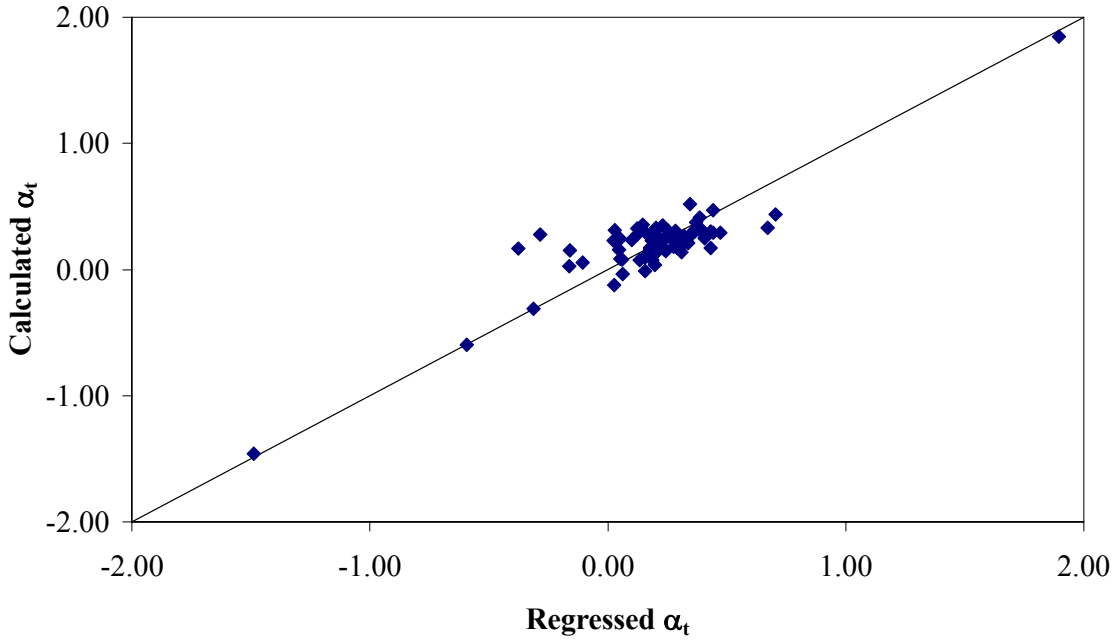

Figure 2.3: Comparison plot of regressed α_t and calculated α_t of the SVRC-QSPR model for liquid density

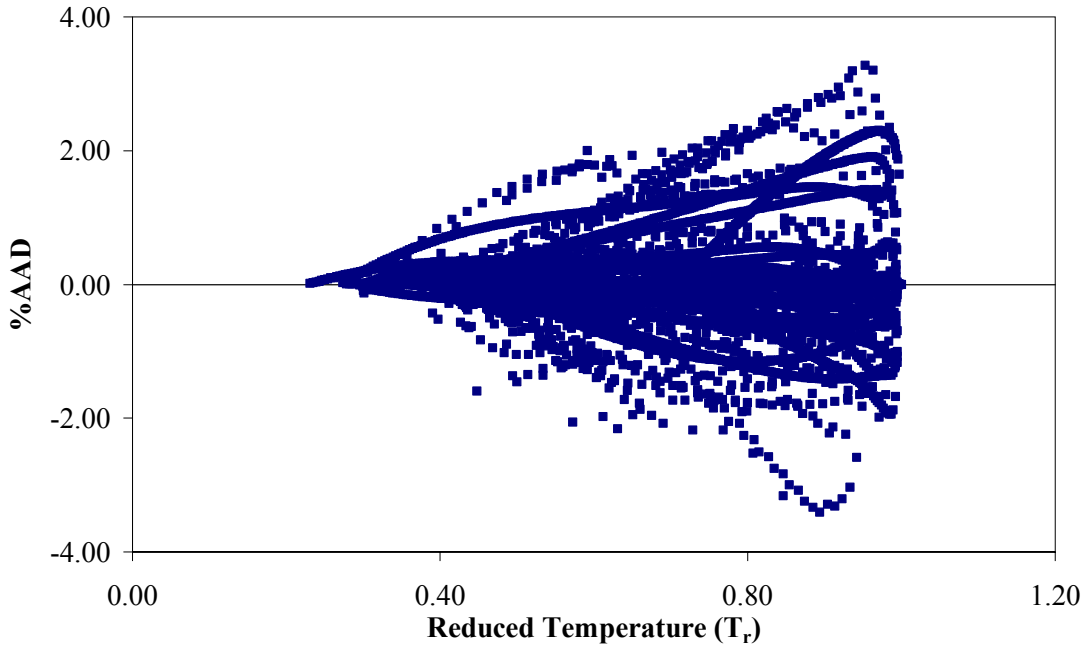

Figure 2.4: Percentage deviation (%AAD) in predicted liquid densities

generalizations (%AAD of 2.9 and 5.6 for vapor pressure and vapor density, respectively). However, for some of the data points considered, errors as large as 10-15 % are observed. Therefore, the QSPR models for vapor pressure and vapor density required further refinement, and hence, non-linear QSPR models were undertaken.

The non-linear QSPR models were developed using a back propagation neural network architecture [19]. A three-layer network with four neurons in the hidden layer was used for the vapor pressure and the vapor density correlations. This network yielded accurate predictions of α_c and α_t for both the training and the prediction sets. Figures 2.5-2.8 are the typical comparison plots of the regressed α_c and α_t and the calculated α_c and α_t obtained from the non-linear QSPR models developed for vapor pressures and vapor density, respectively. The non-linear QSPR model for vapor pressure yielded an R^2 of

0.998 for the training set and an R^2 of 0.997 for the prediction set. Similarly, for vapor density an R^2 of 0.992 for the training set and an R^2 of 0.988 for the prediction set were obtained.

Tables 2.1 and 2.3 present the results obtained from the SVRC-QSPR models for vapor pressure and vapor density. The outliers seen for the vapor pressure model were mostly for compounds in the prediction set which did not have sufficient representation in the training set. These compounds were formaldehyde (%AAD of 5.5), 1-butanol (%AAD of 5.5) and n-heptylamine (%AAD of 4.8). Hydrogen was the only compound with a large deviation (%AAD of 1.83) which was similar to the deviation obtained from the SVRC model regressions. Overall, for vapor density, errors of less than 1% AAD were obtained for all the compounds considered.

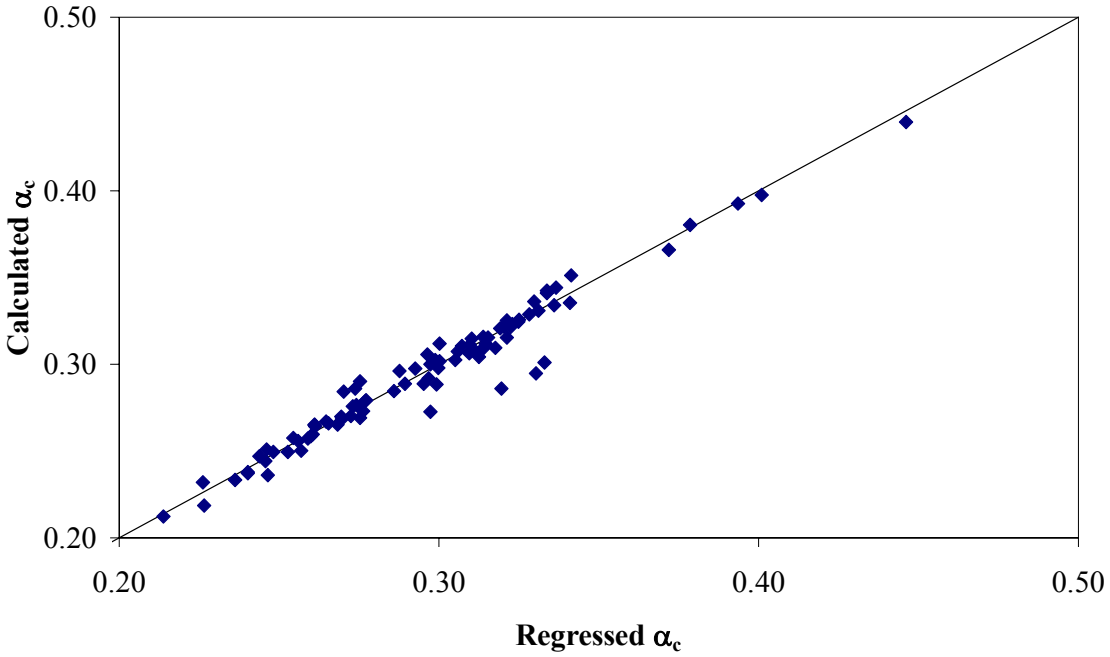

Figure 2.5: Comparison plot of regressed α_c and calculated α_c of the SVRC-QSPR model for vapor pressure

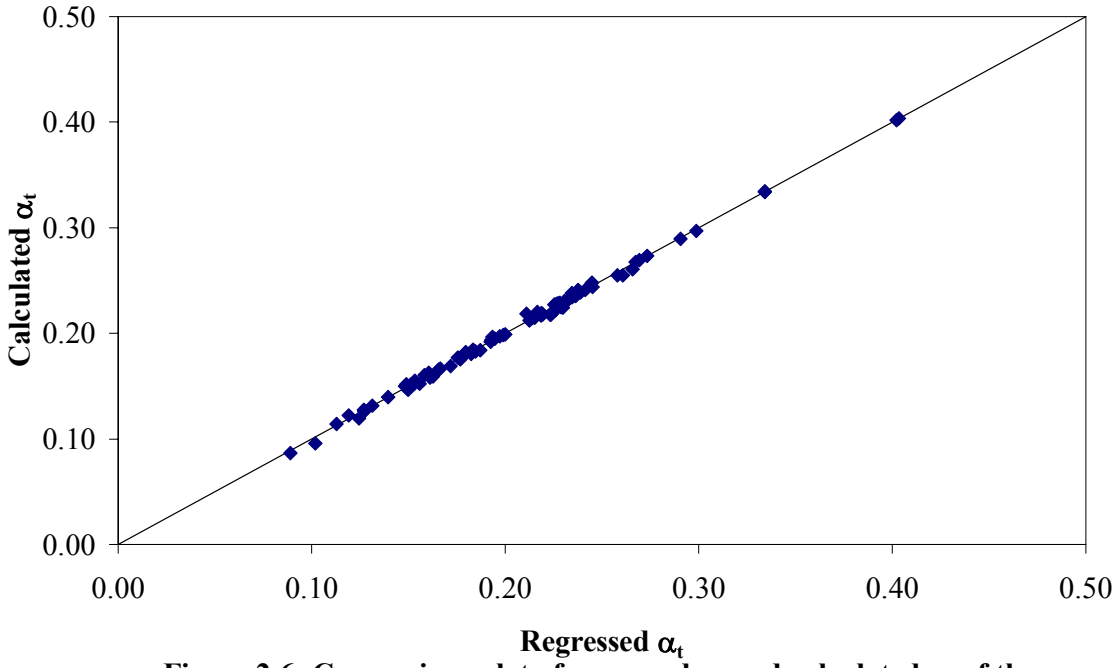

Figure 2.6: Comparison plot of regressed α_t and calculated α_t of the SVRC-QSPR model for vapor pressure

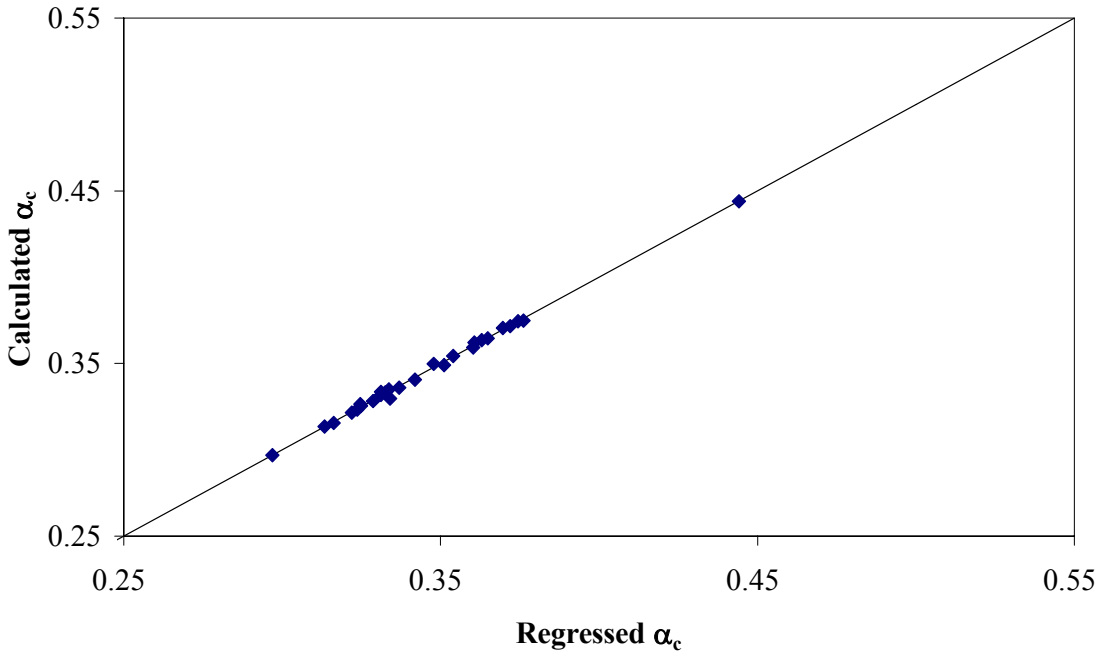

Figure 2.7: Comparison plot of regressed α_c and calculated α_c of the SVRC-QSPR model for vapor density

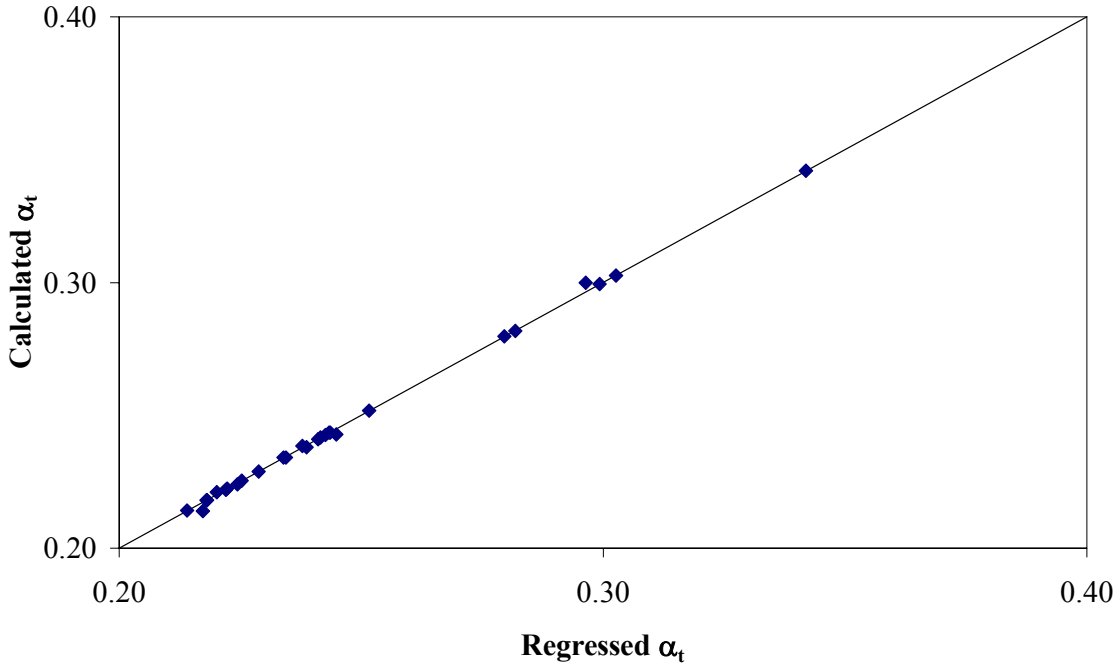

Figure 2.8: Comparison plot of regressed α_t and calculated α_t of the SVRC-QSPR model for vapor density

Figures 2.9 and 2.10 present the deviation plots for vapor pressure and vapor density, respectively. For vapor pressure, the largest deviations are within ±8%, for all data points. Figures 2.4 and 2.10 (the deviation plots for liquid density and vapor density), show that large deviations in the near-critical region are observed for some of the compounds. The source of this error could be attributed to the critical properties used. As discussed by Span and Wagner [23], the variation in the critical density and pressure could be as much as 3% depending on the experimental techniques used. Nevertheless, the observed deviations for all the liquid and vapor density data were within ±3 and ±4%, respectively.

The overall accuracy of generalization-to-precision of representation ratios (A/P ratio) are 5.3, 6.3, and 1.3, for vapor pressure, liquid density and vapor density,

respectively. This translates to generliazed prediction AAD of 1% or less for the three properties, as shown in Tables 2.1-2.3. Although the vapor pressure and the liquid density databases contained several complex compounds and some of the classes of compounds did not have sufficient representation in the training set, the QSPR models developed have been successful in providing relatively accurate generalizations for a diverse set of compounds. Nevetheless, additional work would be required to realize the full benefit of the QSPR modeling undertaken.

The databases used for the vapor pressure and the liquid density models had a diverse and a more representative set of chemical compounds, consisting of around 46

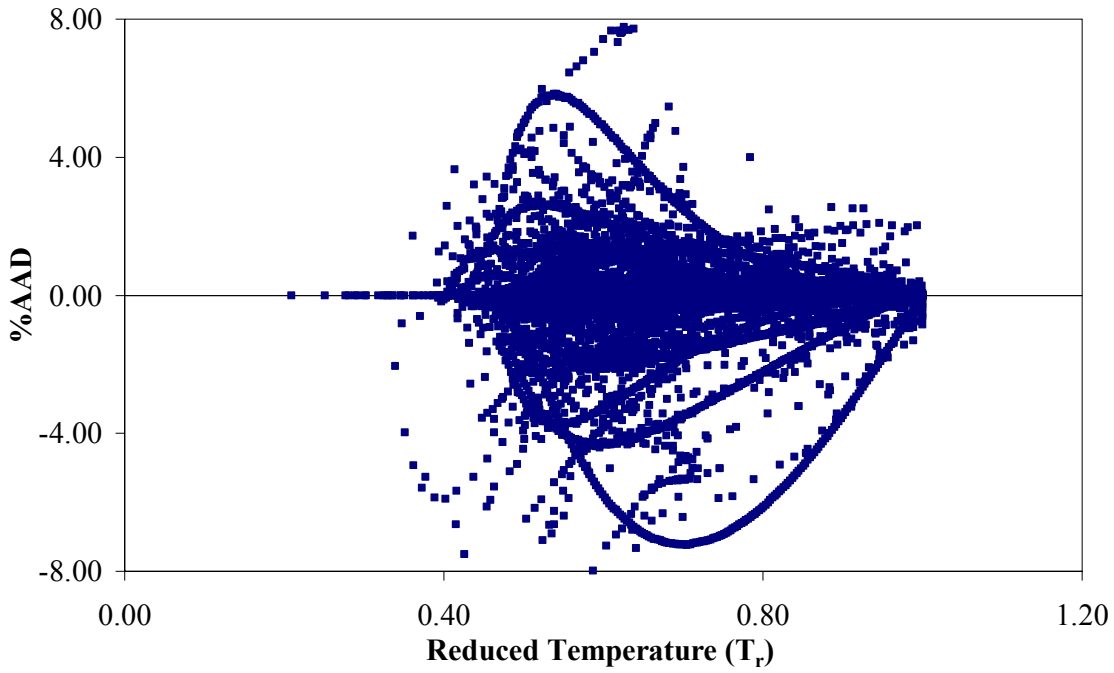

Figure 2.9: Percentage deviation (%AAD) in predicted vapor pressures

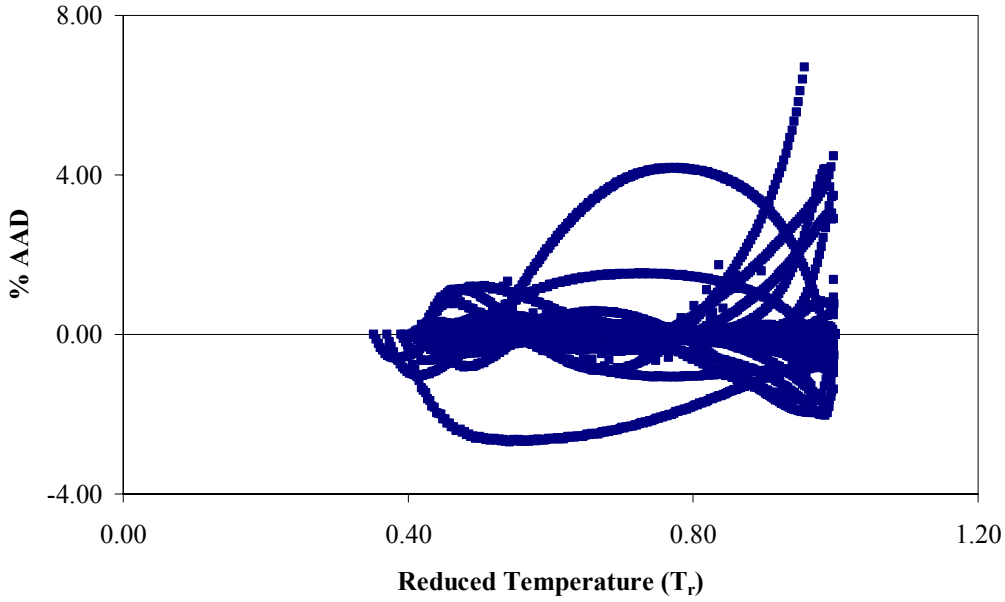

Figure 2.10: Percentage deviation (%AAD) in predicted vapor densities

and 42 highly polar compounds, respectively. For these polar compounds the overall SVRC-QSPR model predictions obtained were about 1.5% AAD for vapor pressure and 0.5% AAD for liquid density, which are better than the generalizations obtained from the original SVRC model. This shows that the SVRC-QSPR model is capable of providing reliable predictions for highly polar compounds.

Table 2.7 presents the overall %AAD of the QSPR generalized parameters and the resulting overall %AAD of the SVRC model predictions for the three properties. For liquid density models, deviations of 0.8% and 0.6% in α_c and α_t, translates into an overall %AAD of 0.49 for the property. However, for the vapor pressure model, deviations within 0.3% in α_c and α_t translate to overall property errors of 0.98% and 0.4%,

respectively. This indicates that the vapor pressure correlation is more sensitive to variations in the model parameters.

Figures 2.11, 2.12 and 2.13 show the %AAD distribution of the vapor pressure, liquid density, and vapor density predictions, respectively. The SVRC-QSPR model yields generalized predictions within 1% AAD for 68%, 72%, and 89% of the data points considered, for vapor pressure, liquid density, and vapor density, respectively. Moreover, deviations greater than 2% are observed for 12% of the data or less for the three saturation properties.

Table 2.7: Overall %AAD in SVRC-QSPR model parameters and saturation properties

Property	%AAD α_c	%AAD α_t	%AAD property
Vapor Pressure	0.28	0.15	0.98
Liquid Density	0.86	0.60	0.49
Vapor Density	0.32	0.84	0.40

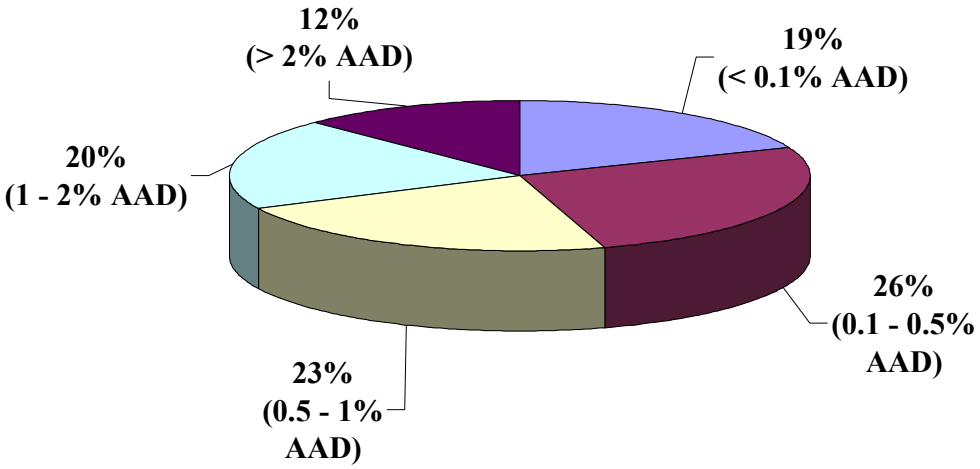

Figure 2.11: %AAD distribution for the SVRC-QSPR model vapor pressure predictions

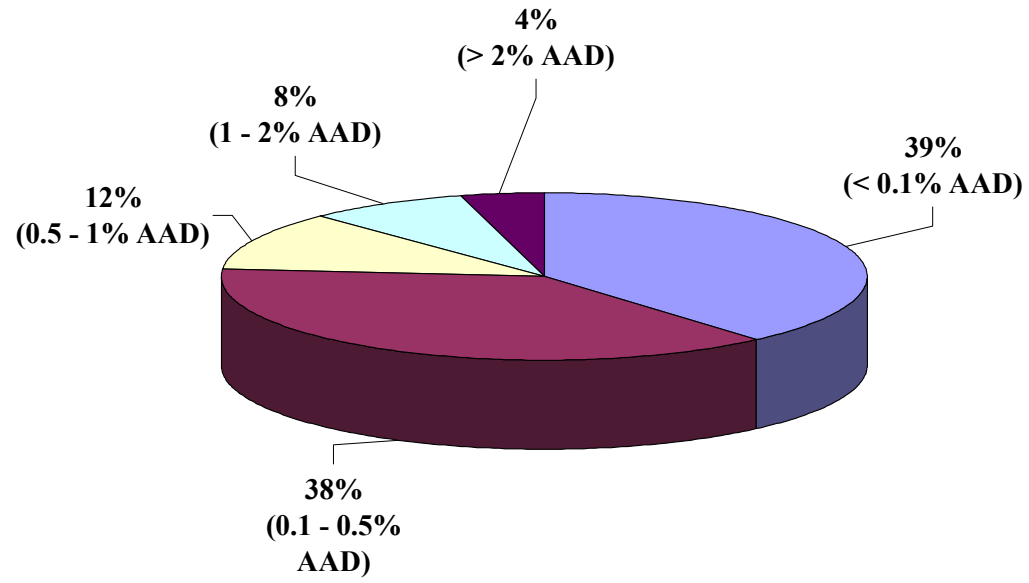

Figure 2.12: %AAD distribution for the SVRC-QSPR model liquid density predictions

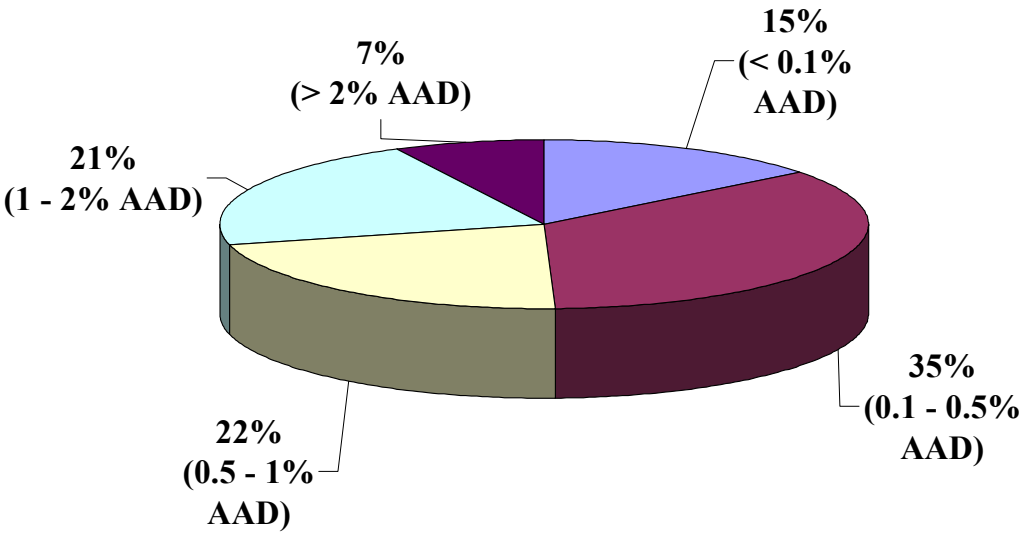

Figure 2.13: %AAD distribution for the SVRC-QSPR model vapor density predictions

The goal of this work has been to develop a generalized model for pure-fluid saturation properties, capable of *a priori* predictions for diverse chemical species, over

the full saturation range. Previous QSPR modeling efforts in the literature [8] accounting for the temperature dependence of saturation properties, using a limited database, have resulted in less accurate models than the present work. Overall errors of about 10% were observed for the database considered, with larger errors for complex aromatic and polar compounds. In comparision, the current study involves a heterogenous dataset which increases the complexity of the QSPR model. Also, the results for this study and previous studies involving the SVRC model [1, 2] indicate that the integrated SVRC-QSPR model is capable of producing better generalized predictions than the recommended literature models [24].

Overall, the results of the QSPR models developed in this study demonstrate that the use of structure-based parameters provides reliable generalizations for the SVRC model parameters of different molecular species encompassing an extended database. Also, the approach of integrating a theoretical model with an *ab inito* QSPR model is an effective methodology for the generalization of fluid saturation properties over the entire saturation range.

2.6 Conclusions

The current generalizations of the SVRC model cannot account for all structural variations of diverse organic compounds in the database, and the QSPR models alone cannot account for the fluid behavior over the entire saturation range. The objective of this study was to improve the SVRC generalizations of the saturation properties by incorporating structure-based generalizations of the model parameters using QSPR modeling. An extended database has been used, consisting of alcohols, amines,

aldehydes, ethers and other complex organic compounds, involving a total of 90 compounds for vapor pressure and 80 compounds for liquid density. The models developed have shown good generalization abilities. For vapor density, the paucity of experimental data constrained the model generalization effort. The present results demonstrates that the proposed approach has the potential for developing generalized pure-fluid saturation property predictions. This work, however, constitutes the initial effort in our quest to develop more accurate models based on a larger database.

References

1. Shaver, R.D., Robinson, R.L., Jr., Gasem, K.A.M., A Framework for the Prediction of Saturation Properties: Vapor Pressures, *Fluid Phase Equilibria*, 64, 141-163 (1991).
2. Shaver, R.D., Robinson, R.L., Jr., Gasem, K.A.M., A Framework for the Prediction of Saturation Properties: Liquid Density, *Fluid Phase Equilibria*, 64, 81-98 (1992).
3. Lin, S., Chang, J., Wang, S., Goddard III, A. W., Sandler, I. S., Prediction of Vapor Pressures and Enthalpies of Vaporization Using the COSMO Solvation Model, *Journal of Physical Chemistry A*, 108, 7429-7439 (2004).
4. Eckert, F., Klamt, A., Fast Solvent Screening via Quantum Chemistry: COSMO-RS Approach, *AIChE Journal*, 48(2), 369-385 (2002).
5. Prausnitz, J. M., Macknick, A. B., Vapor Pressure of Heavy Liquid Hydrocarbons by a Group-Contribution Method, *Ind. Chem. Eng. Fundamentals*, 18(4), 348-351 (1979).
6. Prausnitz, J. M., Abrams, D. S., Massaldi, H. A., Vapor Pressure of Liquids as a Function of Temperature: Two-Parameter Equation Based on Kinetic Theory of Fluids, *Ind. Chem. Eng. Fundamentals***,** 13(3), 259-262 (1974).
7. Olsen, E., Nielsen, F., Predicting Vapor Pressures of Organic Compounds from their Chemical Structure for Classification According to the VOC Directive and Risk Assessment in General, *Molecules*, 6, 370-389 (2001).

8. Yaffe, D., Cohen, Y., Neural Network Based Temperature-Dependent Quantitative Structure Property Relationships (QSPRs) for Predicting Vapor Pressures of Hydrocarbons, *Journal of Chemical Information and Computer Sciences,* 41, 463-477 (2001).
9. Basak, C. S., Mills, D., Quantitative Structure-Property Relationships (QSPRs) for the Estimation of Vapor Pressure: A Hierarchical Approach Using Mathematical Structural Descriptors, *Journal of Chemical Information and Computer Sciences,* 41, 692-701 (2001).
10. Katritzky, R. A., Wang, Y., Sild, S., Tamm, T., QSPR Studies on Vapor Pressure, Aqueous Solubility, and the Prediction of Water-Air Partition Coefficients, *Journal of Chemical Information and Computer Sciences,* 38, 720-725 (1998).
11. McClelland, E. H., Jurs, C. P., Quantitative Structure-Property Relationships for the Prediction of Vapor Pressures of Organic Compounds from Molecular Structure, *Journal of Chemical Information and Computer Sciences,* 40, 967-975 (2000).
12. Karelson, M., Perkson, A., QSPR Prediction of Densities of Organic Liquids, *Computers & Chemistry*, 23, 49-59 (1999).
13. Karelson, M., Molecular Descriptors in QSAR/QSPR, Wiley-Interscience, 2000.
14. Katritzky, A. R., Lobanov, V. S., Karelson, M., QSPR: The Correlation and Quantitative Prediction of Chemical and Physical Properties from Structure, *Chemical Society Reviews,* 1995.
15. Neely, J. B., Godavarthy, S. S., Robinson Jr., L. R., Gasem, K. A. M., Improved Quantitative Structure Property Relationship Models for Infinite Dilution Activity

Coefficients of Aqueous Systems, *Proceedings of the Sixth International Petroleum Environmental Conference*, Albuquerque, November, 2004.

16. ChemDraw 8.0, Cambridge Software (2004).
17. AMPAC 6.0, Semichem Inc., 7128 Summit, Shawnee, KS (1997).
18. CODESSA 2.63, Semichem Inc., 7128 Summit, Shawnee, KS (1998).
19. Schneider, G., Wrede, P., Artificial Neural Networks for Computer-based Molecular Design, *Progress in Biophysics & Molecular Biology*, 70, 175-222 (1998).
20. NIST Standard Reference Database 69; Thermophysical Properties for Fluid Systems, 2005.
21. DIPPR Project 801; Physical and Thermodynamic Properties of Pure Chemicals, 2005.
22. Godavarthy, S., Ravindranath, D., Gasem, K.A.M., Robinson, R.L., Jr., Generalized SVRC-QSPR Model for Prediction of Vapor Pressures and Phase Densities, *Proceedings of the AIChE Spring Annual Meeting*, New Orleans, 2005.
23. Span, R., Wagner, W., *Journal of Physical Chemistry Reference Data*, 25, 1509 (1996).
24. Reid, R.C., Prausnitz, J.M., Poling, B.E., The Properties of Gases and Liquids, 4th Ed., McGraw-Hill, 1987.

CHAPTER 3

PHASE EQUILIBRIA MODELING: THE NRTL-QSPR AND THE UNIQUAC-QSPR MODEL

3.1 Introduction

Multiphase equilibrium calculations are an integral part of the design and optimization of any industrial process. Practitioners typically rely on experimental measurements or generalized thermodynamic models to determine the phase equilibria of the systems under consideration. The models used for phase equilibria calculations can be broadly classified as equation-of-state (EOS) models, which are capable of handling subclasses of fluid behavior such as that exhibited by normal fluid mixtures, and excess Gibbs energy (G^E) models, which are capable of handling highly non-ideal mixtures. However, current EOS and G^E model generalizations are not uniformly accurate and are of insufficient accuracy for many systems of interest. Hence, there is a need for reliable predictive thermodynamic models capable of giving *a priori* predictions of the phase behavior of diverse systems in the absence of experimental data.

Activity coefficient models like the Non Random Two-Liquid (NRTL) and universal quasi-chemical (UNIQUAC) models [1, 2] are widely used in the chemical and petrochemical industry today. These are found to be useful especially for highly non-ideal vapor-liquid equilibrium (VLE) systems. The NRTL model developed by Renon in 1968 [2] is based on the local composition and the two-liquid solution theories. It uses

three adjustable parameters per binary system and can be generalized to multi-component mixtures without additional parameters. The model gives precise representation of highly non-ideal VLE systems and liquid-liquid equilibrium (LLE) systems. However, the model fails to provide reliable generalizations for systems with limited or no data. Further, the model parameters tend to be highly correlated.

The UNIQUAC model developed by Abrams and Prausnitz in 1975 [1, 5] is also based on the local composition and the two-liquid theories, and it postulates that G^E is the sum of combinatorial and residual terms. The model gives precise representations of VLE and LLE behavior, and it is also applicable to mixtures of widely different molecular sizes. Like the NRTL model, the UNIQUAC model currently lacks accurate parameter generalizations beyond those provided by group contributions; thus, it cannot be applied to many systems for which experimental data are not available.

Accurate model generalizations can be obtained by accounting for the molecular structural variations and interactions of the systems considered. The earliest and significant theoretical work in the literature for development of generalized models for VLE prediction using activity coefficients is the van Laar theory, wherein the activity coefficients are expressed as a function of pure-component molar volume, the volume fractions and the solubility parameters of each species. The model is limited by the number of available solubility parameters and fails when extended to multicomponent mixtures. This was followed by the regular solution theory proposed by Hildebrand and Scatchard in 1929 [1, 3], which gave semi-quantitative representations of activity coefficients for non-polar solutions. However, this model could not be extended effectively to solutions containing polar components [3].

In the last few decades, studies based on the group contribution method have had considerable success in *a priori* prediction of VLE behavior. The method is based on the concept that a solution is composed of a mixture of functional groups rather than molecules. The ASOG (Analytical Solution of Groups) model [4, 5] is one such model, which allows for the calculation of activity coefficients at low pressures for liquid mixtures containing neither electrolytes nor polymers. This model is limited by poor predictions for systems with compounds of different sizes [6] and the relatively small number of interaction parameters available.

The modified UNIFAC (UNIQUAC Functional Group Activity Coefficient) is another widely used group contribution model. The UNIQUAC model provides the theoretical framework for the UNIFAC, which attempts to account for the structural variations and interactions of diverse chemical systems through first-order group contribution approximations. The popularity of the UNIFAC model is due to its wide range of applicability and ability to provide reasonable predictions without the need for experimental mixture data. However, this model also suffers from some limitations, including its inability to account for the group proximity effects within molecules [5]. Currently, second and third-order approaches are being investigated by two research groups [7]. Also, this model assumes that the interaction energy of the mixture is the sum of functional group interaction energies; thus, it is limited by the availability of group interaction parameters. Further, it lacks an *a priori* method for defining the functional groups.

Several other studies based on *ab initio* approaches for *a priori* predictions of VLE also exist in the literature. Considerable work has been done on developing models

utilizing direct Molecular Dynamics / Monte Carlo simulation techniques. However, these approaches are highly time-consuming, require enormous computational burden, involve several approximations, and are yet to be applied to a wide range of systems. Another *a priori* predictive model, the COnductor like Screening MOdel for Real Solvents (COSMOS-RS) [8, 9, 10], provides reliable estimate of vapor-liquid and liquid-liquid equilibria based on quantum chemical calculations for the chemical species involved. It is a relatively new approach which utilizes unimolecular quantum chemical calculations of the individual species and does not consider the mixture itself. COSMOS-RS uses eight adjustable parameters and one additional parameter for each element. Although the theory of COSMOS-RS [9, 10] resolves the issue of isomers, can handle rare molecules, and gives accurate representations of LLE; it sometimes fails to describe the VLE of even simple organic systems.

Sandler and co-workers [11], using the Gaussian 94 program, explored the *ab initio* computation of the energy parameters in the UNIQUAC and the Wilson equation. The approach has only been applied to four binary systems and further studies are needed for further development of this method. Similar work was done by Fermeglia and Pricl [12], where they modeled the PHSCT EOS parameters to predict the VLE behavior of binary systems using quantum/COSMO and molecular dynamics simulations. These studies demonstrate that integrating *ab initio* approaches with theoretical models is effective in obtaining *a priori* VLE predictions.

Quantitative Structure-Property Relationship (QSPR) modeling has the potential to provide reliable property estimates based on detailed chemical structure information. Various studies for the correlation of pure-fluid properties using QSPR models exist in

literature. Although current QSPR models have been successful in providing reliable structure-based property predictions, they have been limited to estimating properties at a single temperature. Further, little work has been done on QSPR models for mixtures.

In this work, we propose to improve the generalization capabilities of G^E models such as the NRTL and the UNIQUAC models by developing structure-based model parameters using QSPR modeling. Thus, integrated models capable of *a priori* prediction of the phase behavior at various conditions are developed. This work also attempts to overcome the inherent parameter correlation problems in the NRTL and the UNIQUAC models to obtain better model generalizations.

For purposes of comparison, QSPR parameter generalization is also undertaken for the one-parameter Margules model.

3.2 Overview of the Activity Coefficient Models and QSPR modeling

3.2.1 The NRTL Model

The NRTL model was developed by Renon and Prausnitz [2] to improve on the Wilson equation [1]. The model is based on the local composition theory and the Scotts two-liquid solution theory. For binary systems, the activity coefficients are represented as:

$$\ln\gamma_1 = x_2^2\left(\tau_{21}\frac{\exp(-2\alpha_{12}\tau_{21})}{[x_1 + x_2\exp(-\alpha_{12}\tau_{21})]^2} + \tau_{12}\frac{\exp(-\alpha_{12}\tau_{12})}{[x_2 + x_1\exp(-\alpha_{12}\tau_{12})]^2}\right) \tag{3.1}$$

$$\ln\gamma_2 = x_1^2\left(\tau_{12}\frac{\exp(-2\alpha_{12}\tau_{12})}{[x_2 + x_1\exp(-\alpha_{12}\tau_{12})]^2} + \tau_{21}\frac{\exp(-\alpha_{12}\tau_{21})}{[x_1 + x_2\exp(-\alpha_{12}\tau_{21})]^2}\right) \tag{3.2}$$

$$\tau_{12} = \frac{(g_{12} - g_{22})}{RT} = \frac{\Delta g_{12}}{RT} \tag{3.3}$$

$$\tau_{21} = \frac{(g_{21} - g_{11})}{RT} = \frac{\Delta g_{21}}{RT} \tag{3.4}$$

The three adjustable parameters are α_{12}, τ_{12} and τ_{21}. The non-randomness factor α_{12} can often be set *a priori*. The value of α_{12} in this study was fixed at 0.2, since this value was found to work well for liquid-liquid systems, and it has been used in the DECHEMA LLE data collection. The interaction parameters Δg_{12} and Δg_{21} are regressed from experimental data. This model gives accurate representations for VLE and LLE systems and can be extended to multicomponent mixtures using binary parameters. Studies have shown that the interaction parameters Δg_{12} and Δg_{21} are highly correlated when the maximum value of G^E is relatively low [2]. This poses significant problems when dealing with multicomponent predictions and/or attempting model parameter generalization.

3.2.2 The UNIQUAC Model

The UNIQUAC model developed by Abrams and Prausnitz in 1975 [1] is an extension of the Wilson equation wherein the excess Gibbs energy is expressed as the sum of the size and shape dependent combinatorial part and the energy interaction dependent residual part [1, 3]:

$$g^E = g^E_{comb} + g^E_{resid} \tag{3.5}$$

The two parts of the excess Gibbs energy are

$$\frac{g^E_{comb}}{RT} = \sum_i q_i x_i \ln \frac{\phi_i}{x_i} + \frac{Z}{2} \sum_i q_i x_i \ln \frac{\theta_i}{\phi_i} \tag{3.6}$$

and

$$\frac{g^{E}_{resid}}{RT} = -\sum_{i} q_i x_i \ln\left(\sum_{j} \theta_j \tau_{ji}\right) \tag{3.7}$$

where τ_{ji} and τ_{ij} are the interaction parameters between the molecules. The area fraction, ϕ_i is defined as,

$$\phi_i = \frac{x_i r_i}{\sum x_i r_i} \tag{3.8}$$

r_i and x_i are the van der Waals volume and the component mole fraction, respectively. The volume fraction, θ_i is defined as,

$$\theta_i = \frac{x_i q_i}{\sum x_i q_i} \tag{3.9}$$

where q_i is the van der Waals surface area.

The values of the van der Waals surface area (q_i) and the volume (r_i) are obtained from experimental data or the Bondi [13] group contribution method. The interaction parameters are regressed from experimental data. The UNIQUAC model is similar in performance to the NRTL model, except that it has a greater algebraic complexity [1].

3.2.3 The Margules Model

The one-parameter Margules equation is the simplest form of the activity coefficient models available. For a binary system [3],

$$\ln \gamma_1 = \frac{A_{12} x_2^2}{RT} = \hat{A}_{12} x_2^2 \tag{3.10}$$

$$\ln \gamma_2 = \frac{A_{12} x_1^2}{RT} = \hat{A}_{12} x_1^2 \tag{3.11}$$

The Margules model provides accurate representations of many types of liquid solutions [25]. This model, unlike the NRTL and the UNIQUAC is not based on local composition theory.

3.2.4 QSPR Modeling

Computational techniques have improved drastically over the last two decades, along with the revolutionary advances in computing power. They are routinely used to address more complex engineering and design problems in chemical processing. Computationally intensive models are also being used to complement, guide and sometimes replace experimental measurements, thus reducing the amount of time and money spent on research to bring ideas from the lab to practical application.

The QSPR approach is among the computational methods gaining wide use. It is based on the assumption that there exists a relationship between the structure of a substance and its physical and chemical properties. QSPR uses quantum mechanics to define the structure of the molecule in terms of a series of molecular descriptors and then correlates the property in terms of these descriptors. Molecular descriptors are variables which describe various structural characteristics of the molecule and its interactions. They are classified as follows :

Constitutional Descriptors: These are simple descriptors based on the chemical composition of the compound. Example constitutional descriptors include number of atoms, number of bonds, number of rings, and molecular weight.

Topological Descriptors: These descriptors describe the atomic connectivity in the molecule. Example topological descriptors include molecular connectivity indices, substructure counts, molecular distance edge descriptors, kappa indices, and electro topological state indices.

Geometric Descriptors: These descriptors are derived from the three-dimensional structure of the compound. Example geometric descriptors include moments of inertia, solvent-accessible surface area, length-to-breadth ratios, shadow areas, and gravitational index.

Electrostatic Descriptors: These descriptors give the charge distribution of the entire molecule. Example electrostatic descriptors include polarity indices, charged partial surface area, and partial charges.

Quantum Chemical Descriptors: These descriptors are derived from quantum chemical calculations and provide an accurate description of electronic distribution, and they account for the partial charges on fragments of molecules. The descriptors also provide the value of the partial charge of the atoms in the molecule (e.g., dHmin represents the minimum partial charge on a hydrogen atom).

Thermodynamic Descriptors: These descriptors are calculated on the basis of the total partition function (Q) of the molecule and its electronic, translational, rotational, and vibrational components.

The QSPR approach has found applications in the calculation of thermo-physical properties, aqueous solubilities, partition coefficients, and in the design of new chemicals

[14, 15]. This approach has the potential of providing predictions for as-yet unknown or unmeasured compounds based on structural information. The work previously done by this group on aqueous solubility, normal boiling points and saturation properties of pure compounds [16] demonstrates that the QSPR model is an effective tool in correlating and predicting properties from structural information. However, current QSPR studies are limited to the prediction of properties at a single temperature.

Most of the work to date using QSPR models is for pure fluids and little has been done on mixtures. Janowsky and co-workers [17] used the QSPR methodology to model an EOS parameter for carbon dioxide-hydrocarbon mixtures. A similar study was conducted in OSU [18] to generalize the interaction parameters of cubic equations of state for light gas/n-paraffin systems using QSPR modeling. To our knowledge no other work has been published on the use of QSPR models for VLE and LLE predictions of mixtures. In this work, we seek to demonstrate the utility of the QSPR models in estimating the interaction parameters in activity coefficient models from the molecular structure information of the chemical species involved.

3.3 QSPR Methodology

3.3.1 Linear Model

A brief overview of the QSPR methodology is given in Figure 3.1. After a database has been compiled, the names of the individual molecules are stored in EXCEL and 2-D structures are generated using ChemDraw [19]. Then the 3-D structures are generated and the structures are optimized in Chem 3D Ultra [19]. These optimized structures are further optimized and refined in AMPAC 6.0 [20]. The output of AMPAC serves as the input to the QSPR model. The entire data available is split into training and prediction sets. A commercial QSPR package, CODESSA [21], is used for the descriptor

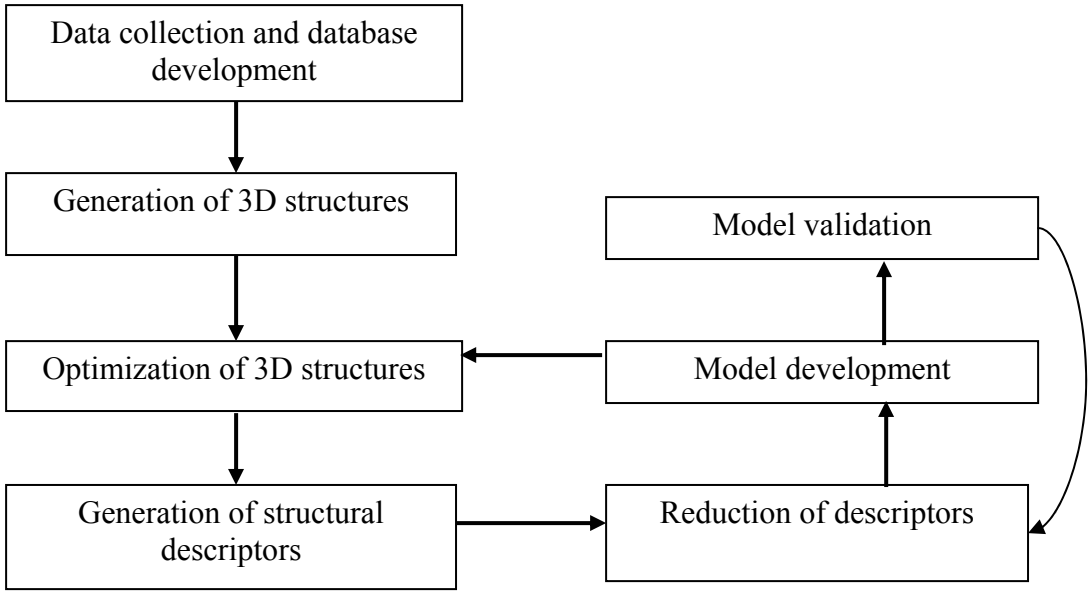

Figure 3.1 Overview of QSPR Methodology

generation. Over 700 molecular descriptors are calculated for each compound. Insignificant descriptors are eliminated by statistical methods available in CODESSA. A multi-linear regression (MLR) analysis is then used to relate the molecular descriptors to

the property of interest, i.e., the model parameters. The generalizations of model parameters thus obtained are used in the selected model to predict the property.

In this study, a multi-linear model was developed relating the molecular descriptors to the property of interest. The general form of the correlation is given as:

$$y = \beta_o + \sum_{i=1}^{N} \beta_i x_i \qquad (3.12)$$

where, y = property of interest, β_o = intercept, N = number of molecular descriptors, β_i = coefficient for descriptor 'i' and x_i = molecular descriptor 'i'. The multi-parameter regression that maximizes the predicting ability is determined using the following strategy:

1. All orthogonal pairs of descriptors i and j are found in a given data set.
2. The property analyzed is treated by using the two-parameter regression with the pairs of descriptors, obtained in Step 1.
3. For each descriptor pair obtained in the previous step, a non-collinear descriptor, k, is added, and the respective three-parameter regression treatment is performed.
4. For each descriptor set chosen in the previous step, an additional non-collinear descriptor scale is added, and the respective (n+1) parameter regression treatment is performed.

The final product of the above steps is a linear relationship between the molecular structure and the property of interest containing n parameters.

3.3.2 Non-Linear Model

CODESSA is used to develop a linear relationship between the descriptors and the parameters. If accurate generalizations are not obtained with a linear model, then the descriptors from the linear model are used as input to develop a non-linear model. A wide range of non-linear architectures are available; often, the network is chosen based on a trial-and-error process. Available literature suggests that a back-propagation network, although it has a simple architecture, is well suited for property prediction models. The number of hidden neurons and hidden layers are again chosen based on a trial-and-error process. As a rule of thumb, the ratio of the number of molecules to the number of adjustable parameters should be greater than two to obtain a reliable non-linear model [22].

Once suitable network architecture has been identified, the next step is to determine the adjustable weights on the network connections. The usual procedure is to initialize randomly these weights multiple times and determine which set of weights provides the lowest training error. A common problem encountered in neural network model development is over training. The root mean square error (RMSE) for the training set usually decreases as the number of training cycles increases; however, the ability of the network to predict eventually decreases. This is called over-fitting, which typically results in larger RMSE for the prediction set than for the training set.

To identify the optimum number of training cycles, where the training and prediction sets exhibit their lowest errors, a procedure known as cross validation (CV) is commonly employed. The entire data are split into training and cross validation sets. The

network is trained using only the training dataset. Periodically, the training is halted and error values for the cross validation set are predicted. Any training beyond the minimum error in the CV set indicates that the network is being over trained. At the onset of an increase in the CV set RMSE, the network has essentially learned all of the general information from the training set and has just started to memorize their individual characteristics. Since the goal of network training is not only to produce small errors in the training set but also to produce reasonable prediction results (referred to as the ability to generalize), the training cycle corresponding to the minimum CV RMSE corresponds to the termination point for training. The model parameters obtained from the non-linear model are then used in the theoretical frameworks to predict the properties considered.

3.4 Database Employed

To develop a robust model and to evaluate the performance of the model, the prime requirement is a reliable database. The database used in this work consists of data sets from three different sources. A low-pressure binary VLE database consisting of 92 systems and totaling 1360 data points was taken from DIPPR [23]. The DIPPR database has been divided into groups according to the polarity of the pure components and the systems are further classified as ideal and non-ideal systems. The second database used was the OSU database, which consisted of 96 binary VLE systems and totaling 3356 data points. The database comprised of systems of aliphatic and aromatic hydrocarbons, water, alcohols, ethers, sulphides and nitrile compounds. The third database, comprising of 144 binary VLE systems and totaling 5051 data points, was taken from the DECHEMA VLE [24] database. The database comprised of systems of aldehydes, ketones, ethers and

aromatic hydrocarbons. These datasets were classified in a similar manner as the DIPPR database. The classification scheme used by Danner et al. [25], as outlined in Table 3.1, was followed in this work, to include a wide variety of systems ranging from nearly ideal to highly non-ideal.

Table 3.1: Classification of database

Systems	Number of systems
Non Polar / Non Polar	39
Non Polar / Weakly Polar	99
Non Polar / Strongly Polar	76
Weakly Polar / Weakly Polar	41
Weakly Polar / Strongly Polar	43
Strongly Polar / Strongly Polar	23
Aqueous	15

The definition of ideality was based on the combinations of the components. According to Danner, in addition to classification of compounds according to polarity and their combinations, the ideal and non-ideal behavior was decided based on the value of the two-suffix Margules constant ($\hat{A}_{12}$). Systems with absolute values of $\hat{A}_{12}$ less than 0.6 are classified as nearly ideal and systems with absolute values of $\hat{A}_{12}$ greater than 0.6 are classified as highly non-ideal systems. According to this classification, the database considered, had 196 nearly ideal systems and 136 systems which approached non-ideal behavior. Figures 3.2–3.15 present example equilibrium phase composition plots and activity coefficient behavior plots of systems from the different classes shown in Table 3.1. As can be observed from Figure 3.2, the toluene/2-pentanone system, involving a Nonpolar/Weakly polar system and the components being reasonably similar in size,

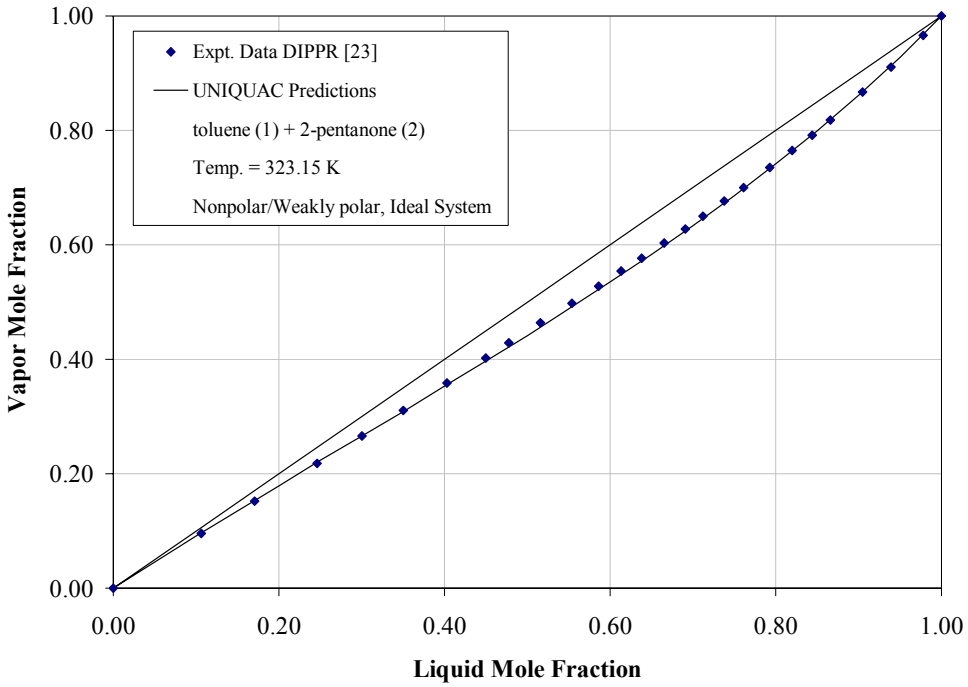

Figure 3.2: Equilibrium phase compositions for toluene (1) + 2-pentanone (2) system

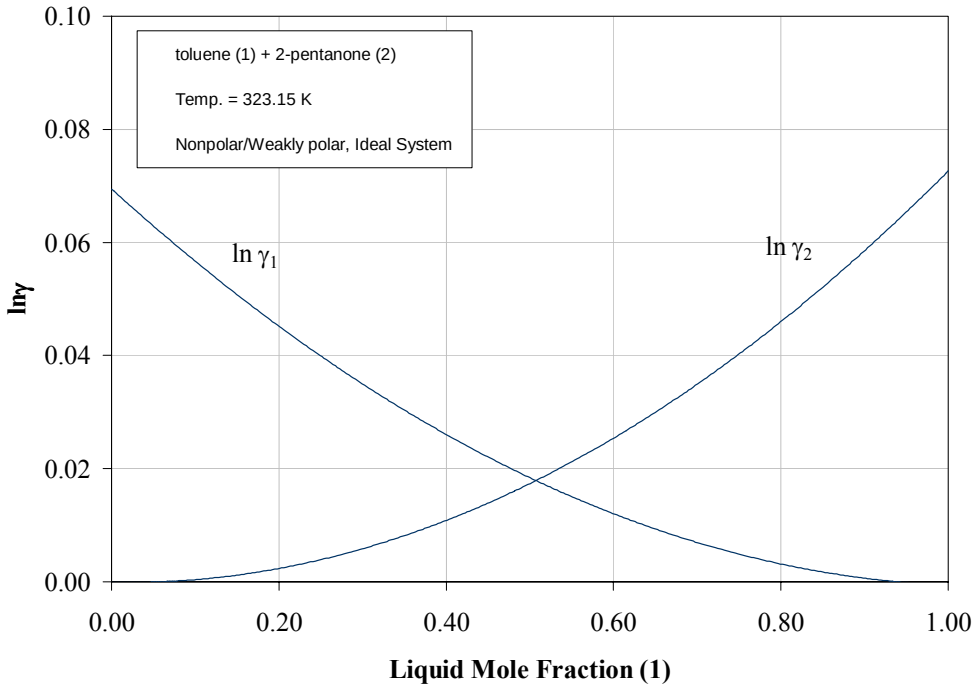

Figure 3.3: Variation of activity coefficients with composition for toluene (1) + 2-pentanone (2) system

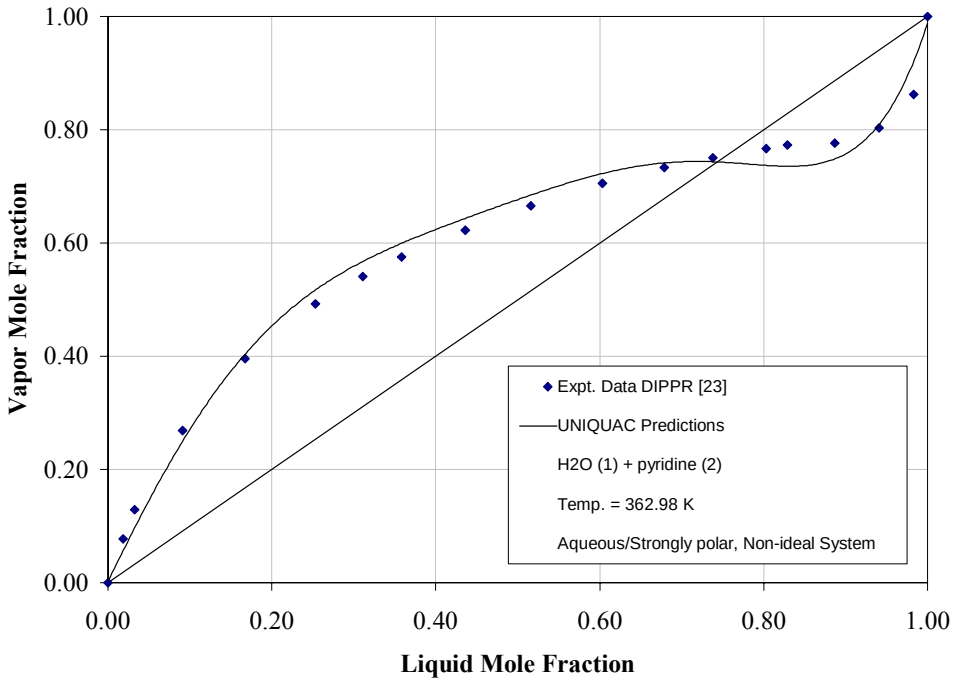

Figure 3.4: Equilibrium phase composition for H_2O (1) + pyridine (2) system

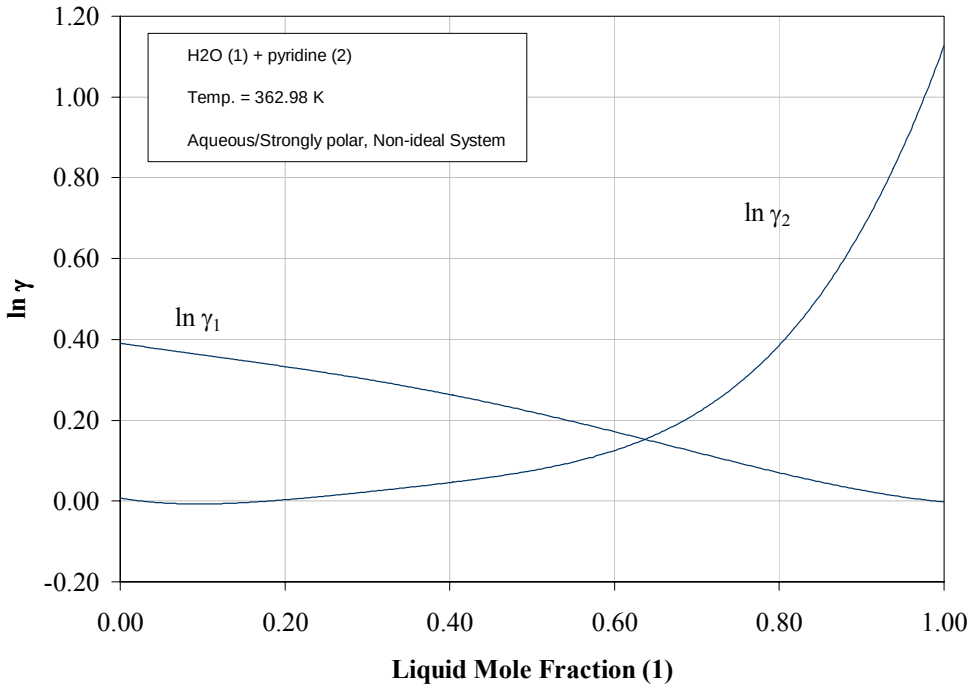

Figure 3.5: Variation of activity coefficients with composition for H_2O (1) + pyridine (2) system

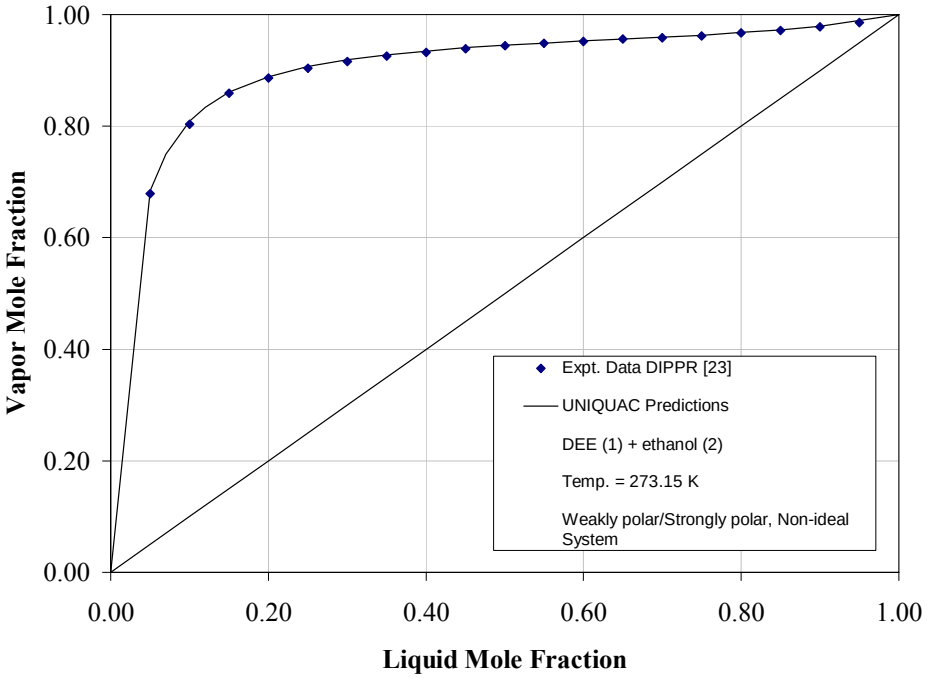

Figure 3.6: Equilibrium phase compositions for DEE (1) + ethanol (2) system

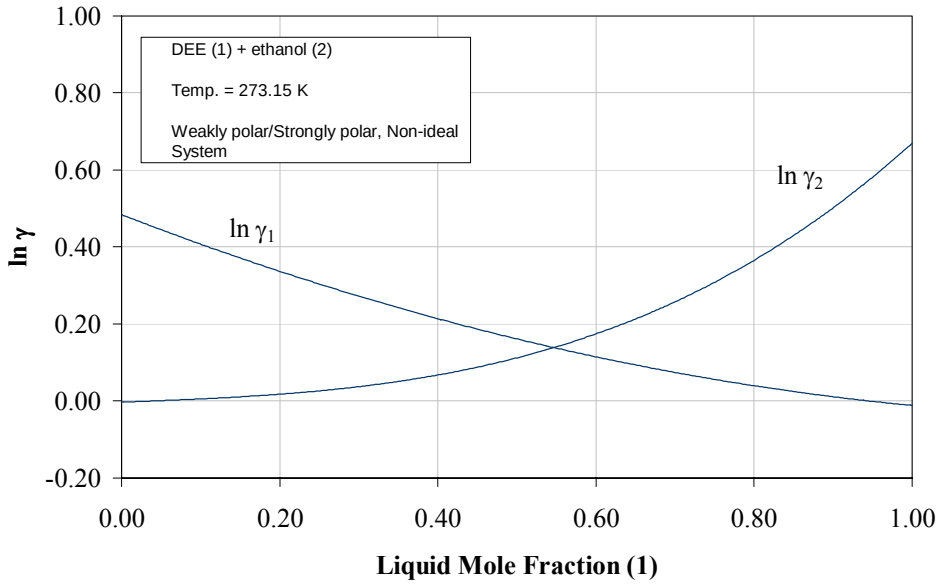

Figure 3.7: Variation of activity coefficients with composition for DEE (1) + ethanol (2) system

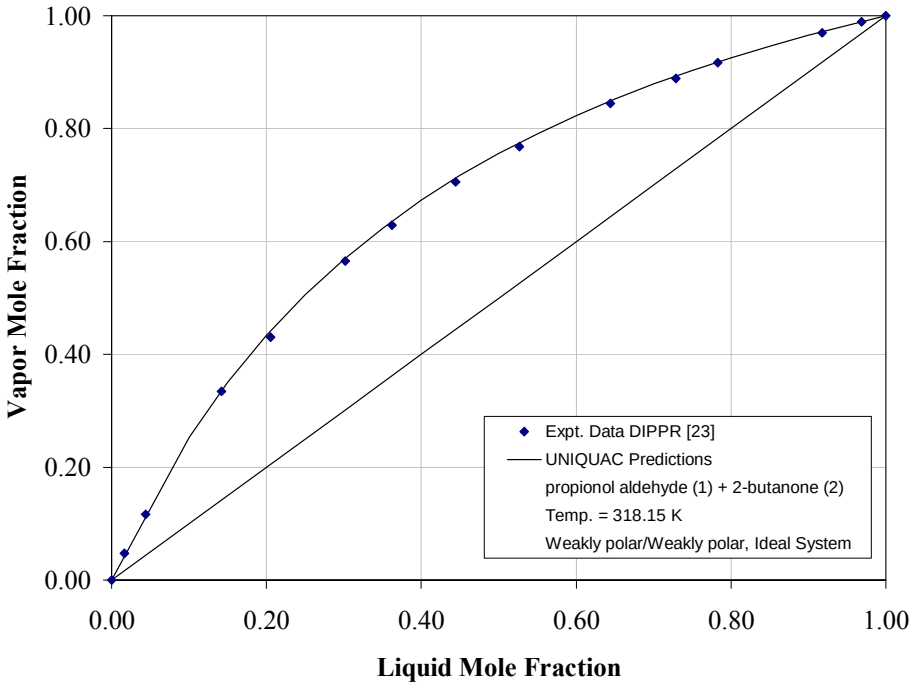

Figure 3.8: Equilibrium phase composition for propianol aldehyde (1) + 2-butanone (2) system

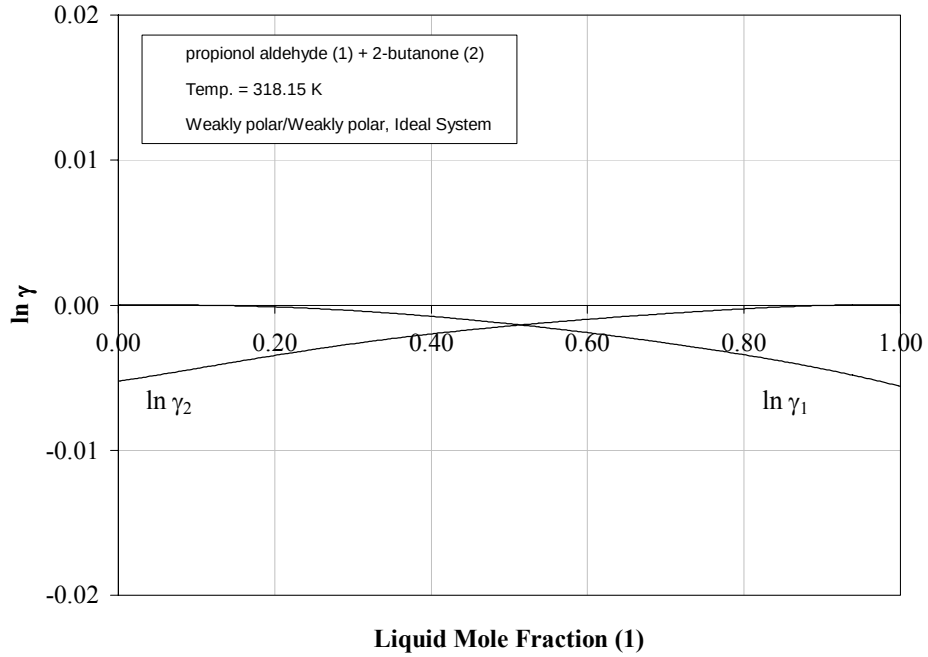

Figure 3.9: Variation of activity coefficients with composition for propionol aldehyde (1) + 2-butanone (2)

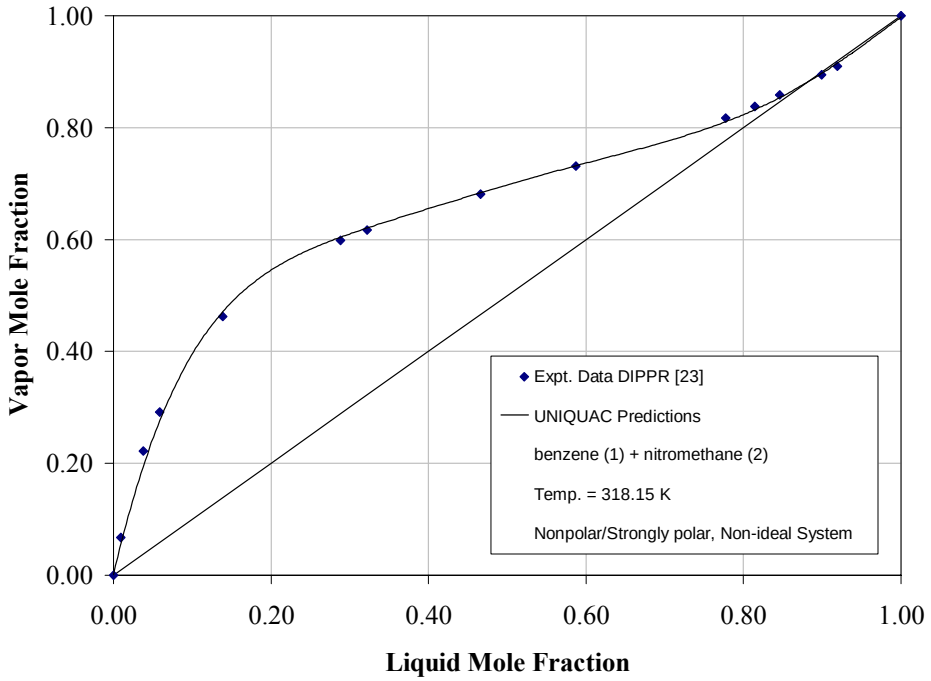

Figure 3.10: Equilibrium phase compositions for benzene (1) + nitromethane (2) system

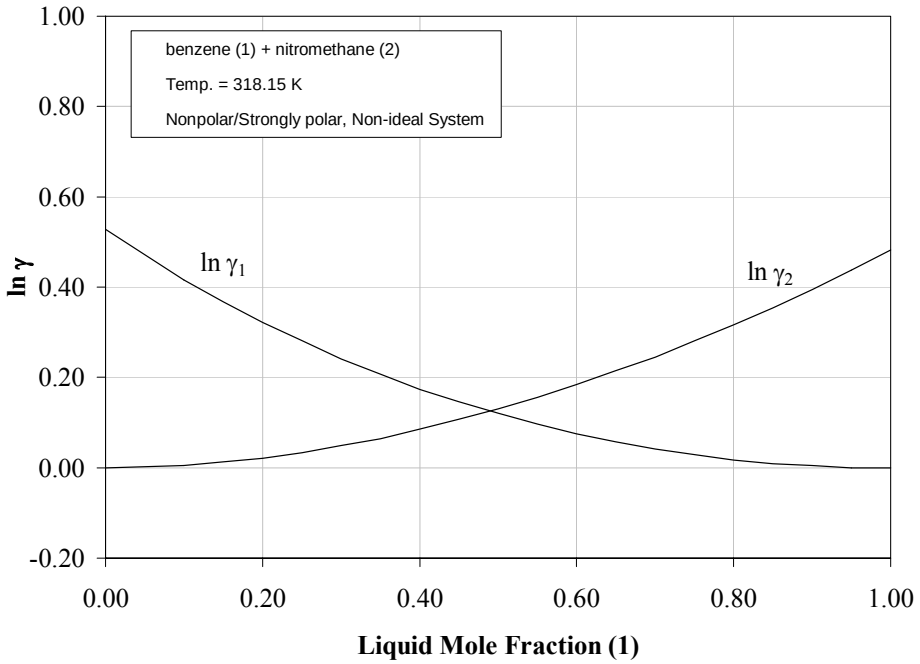

Figure 3.11: Variation of activity coefficients with composition for benzene (1) + nitromethane (2) system

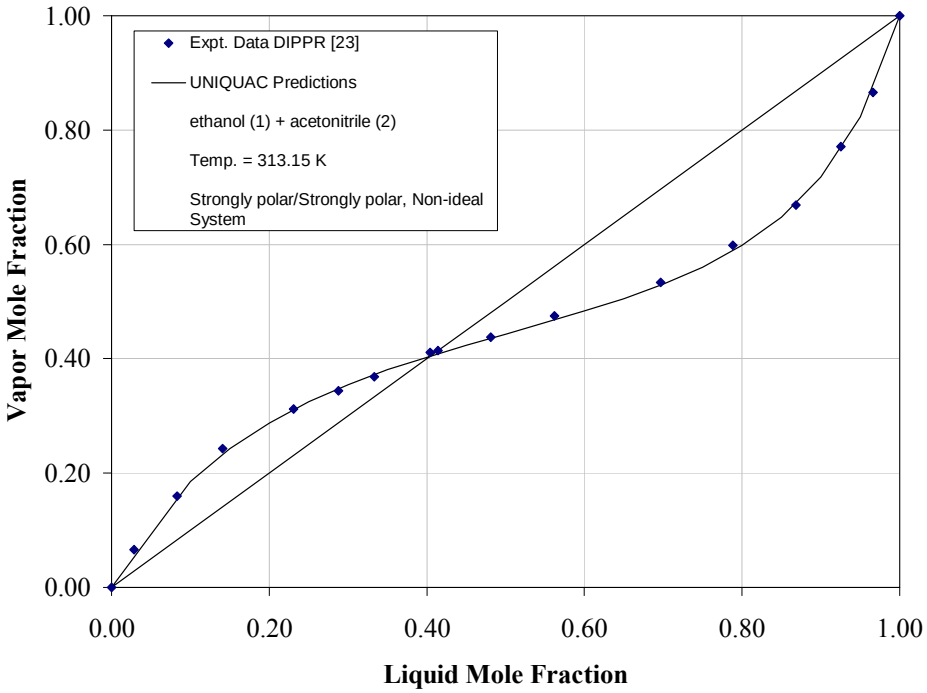

Figure 3.12: Equilibrium phase composition for ethanol (1) + acetonitrile (2) system

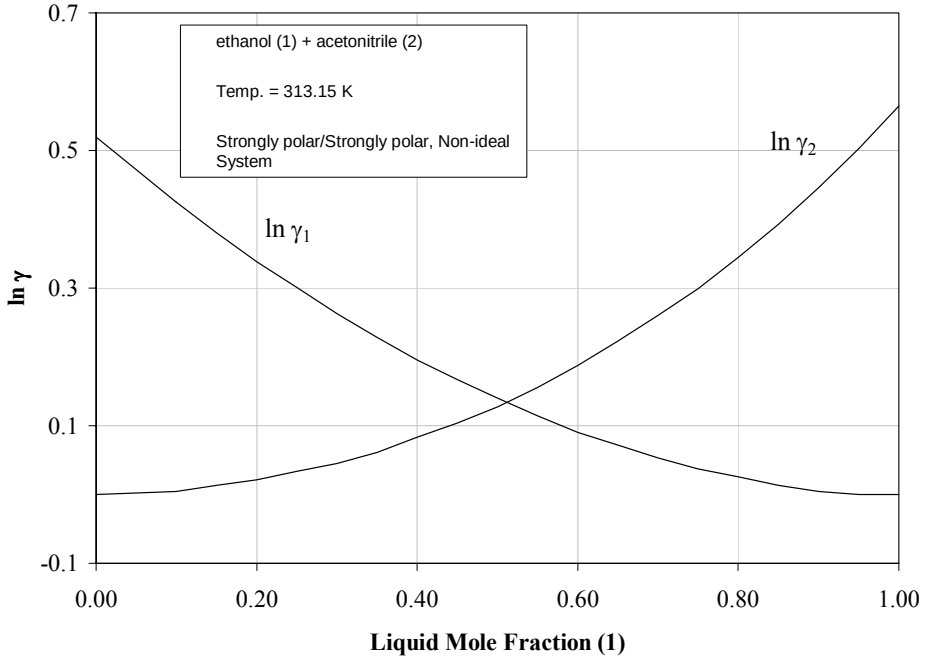

Figure 3.13: Variation of activity coefficients with composition for ethanol (1) + acetonitrile (2) system

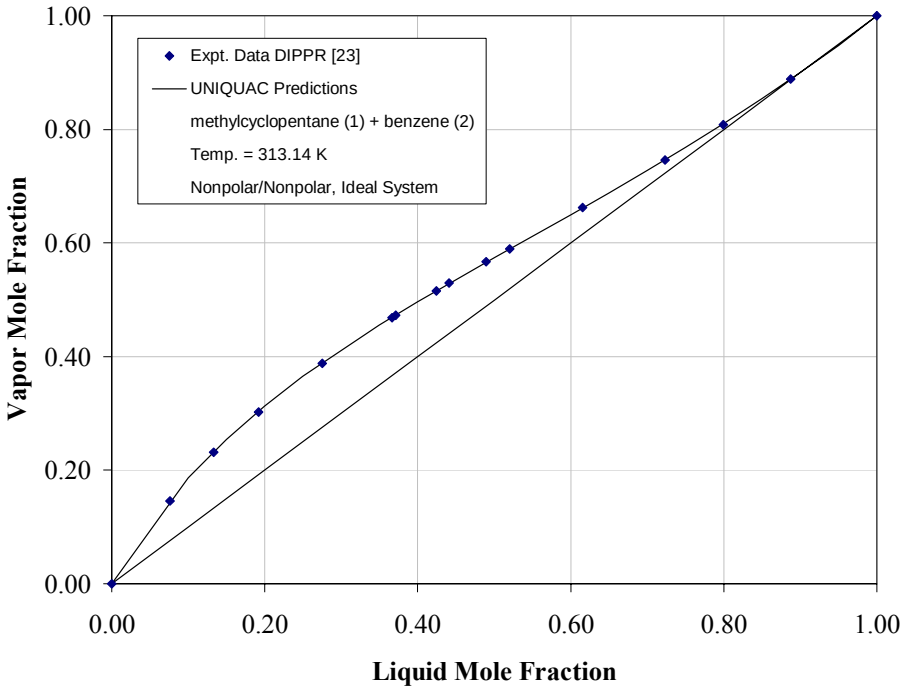

Figure 3.14: Equilibrium phase compositions for methylcyclopentane (1) + benzene (2) system

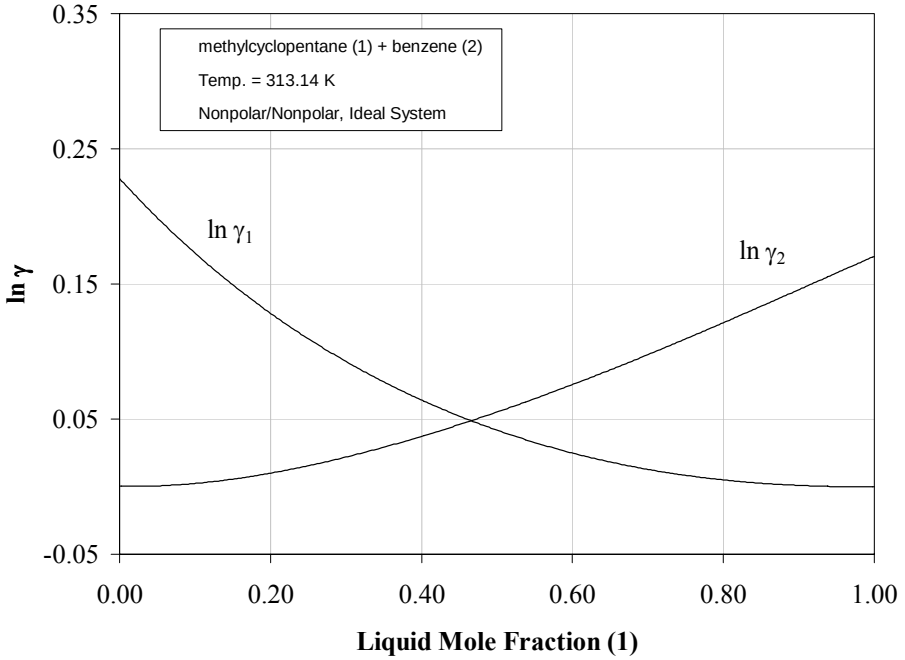

Figure 3.15: Variation of activity coefficients with methylcyclopentane (1) + benzene (2) system

($\hat{A}_{12}$=0.143) exhibits nearly ideal behavior. Similarly, from Figure 3.6, it can be observed that the diethyl ether (DEE)/ethanol system which is a Weakly polar/Strongly polar system, ($\hat{A}_{12}$=1.343) exhibits highly non-ideal behavior. This classification scheme allows for the understanding of the behavior of systems, once the class of the system is determined. The entire data was evenly distributed among the systems and over the entire concentration range. The database was chosen such that there was sufficient representation of the different classes of systems, having a good temperature range and good quality data. The pressure, temperature and composition range of the data used for each system is summarized in Table B.1 of Appendix B. A total of 332 data sets were used for developing and validating the performance of the NRTL-QSPR and the UNIQUAC-QSPR models.

3.5 Methods

The equal-fugacity equilibrium framework used in this study is as follows:

$$\begin{aligned} \hat{f}_i^v &= \hat{f}_i^l \quad i = 1,..n \\ T^v &= T^l \\ P^v &= P^l \end{aligned} \tag{3.13}$$

subject to the constraints of mass balance. For low pressures, which are the focus of this study, Equation (3.11) simplifies to:

$$Py_i = \gamma_i P_i^0 x_i \tag{3.14}$$

where x_i and y_i are the component mole fractions in the liquid and vapor phase, respectively; P_i^0 is the saturation pressure of component 'i' at temperature T and pressure P; and γ_i is the activity coefficient of component 'i'.

The objective function used during parameter regressions, *S*, minimizes the relative error in pressure and the activity coefficients γ_1 and γ_2. The objective function is:

$$S \equiv \sum_{1}^{N}\left(\frac{P^{\exp t} - P^{cal}}{P^{\exp t}}\right)_i + \sum_{1}^{N}\left(\frac{\gamma^{\exp t} - \gamma^{cal}}{\gamma^{\exp t}}\right)_i \tag{3.15}$$

In addition, the qualities of the predictions are assessed for the equilibrium properties temperature (T), pressure (P) and the equilibrium constants K_1 and K_2. The equilibrium constant for component 'i' is defined as:

$$K_i = \frac{y_i}{x_i} = \frac{\gamma_i P_i^0}{P} \tag{3.16}$$

The primary objective of this work was to improve the generalizations of the NRTL and the UNIQUAC activity coefficient models by developing QSPR models to obtain structure-based model parameters while minimizing the effect of parameter correlation of the models. To attain this objective, the entire study was divided into sequential case studies:

Case 1: The ideal gas/ideal solution model combination represents the simplest case that facilitates VLE predictions from pure-component data only.

Case 2: The ideal gas/Margules model combination was used to examine the predictions of one-parameter model that does not involve the local composition concept.

Case 3: The ideal gas/NRTL model combination was used, where two parameters are regressed.

Case 4: The ideal gas/UNIQUAC model combination was used, where two parameters are regressed.

Cases 2Q, 3Q and 4Q: Here, the ideal gas was used for the vapor phase, and the generalized Margules, the NRTL and the UNIQUAC models with structure-based parameters from QSPR modeling were used for the liquid phase activity coefficient.

The model development was initiated with Case 1, wherein predictions were obtained for T, P and K_1 and K_2 for the entire database of 332 binary systems. The next step was to obtain the model regression results for the one-parameter Margules model (Case 2). This was followed by the model regressions of the two-parameter NRTL (Case 3) and the UNIQUAC (Case 4) model. For the NRTL model, the parameters modeled were:

$$\begin{aligned} \Delta_{12} &= g_{12} - g_{11} \\ \Delta_{21} &= g_{21} - g_{22} \end{aligned} \tag{3.17}$$

Similarly, the binary interaction parameters τ_{12} and τ_{21} were the model parameters for the UNIQUAC equation.

Cases 2 through 4 were used to evaluate the correlation abilities of the models considered. They also establish (for the data considered) the ultimate precision which the QSPR generalized models aim to achieve.

The resultant NRTL and UNIQUAC parameters were highly correlated, as shown in Figure 3.16. Since parameter correlation would impede the QSPR models from providing reliable estimates of the parameters from the structure, attempts were made to

overcome this problem. First, the literature recommendation to minimize the absolute value of the regressed parameters was implemented [1]. This failed to reduce the correlation significantly; thus, a sequential parameter regression was undertaken, in which one parameter was fixed at the generalized value, and the other parameter was regressed. The procedure was repeated until the majority of the parameter correlation was eliminated. Subsequently, this approach was used for the two-parameter NRTL and the UNIQUAC model regressions.

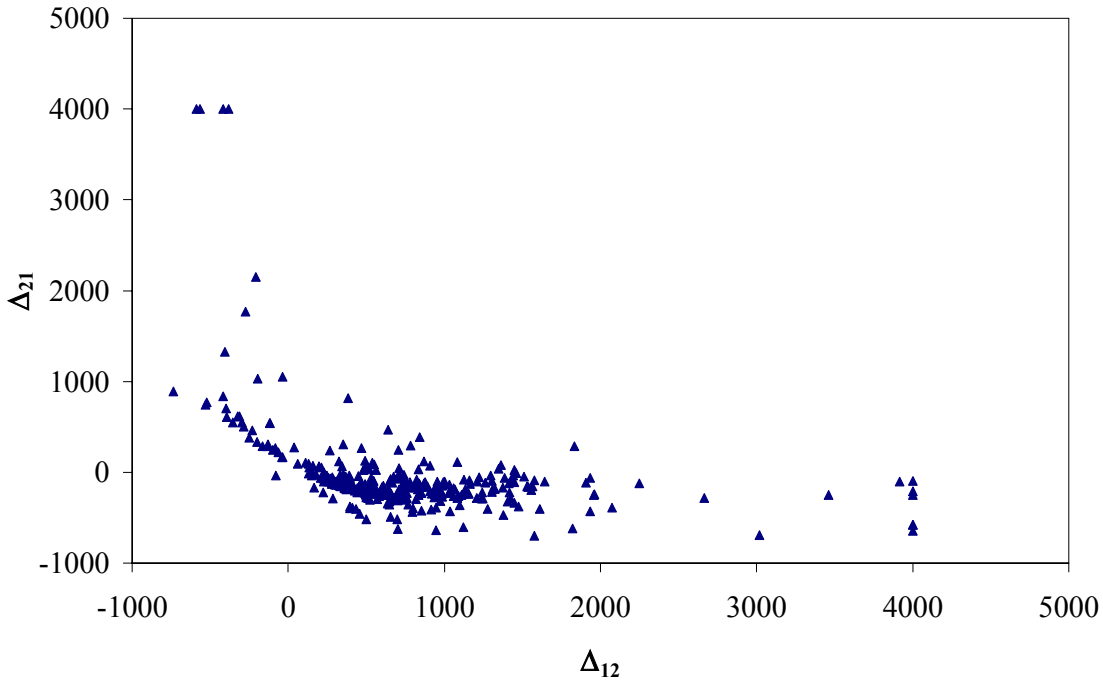

Figure 3.16: Correlation between the NRTL parameters

3.6 Results and Discussion

Table 3.2 presents the results of the model regressions for the four cases discussed. As expected, the ideal gas / ideal solution model (Case 1) performed poorly for

most of the systems. The model gave overall absolute average deviation (AAD) of 1.2%, 11.5%, 10.7% and 16.8% for T, P, K_1 and K_2 predictions, respectively. The one-parameter Margules model (Case 2) gave overall deviations of 0.3%, 3.2%, 3% and 5.4% for T, P, K_1 and K_2 predictions, respectively. Similarly, an overall AAD of around 0.2%, 3%, 3% and 5% in T, P, K_1 and K_2 predictions, respectively, were obtained from the NRTL and the UNIQUAC models (Case 3 and 4). As expected, the performance of the two-parameter models was better than the one-parameter model; however, the amount of improvement observed was not significant.

Table 3.2: Regression results of the two-parameter NRTL model, UNIQUAC model and Margules model

Case	Models (V/L)	Parameters	Property	RMSE	BIAS	%AAD
1	IG/IS	none	T (K)	8.96	3.659	1.3
			P (bar)	0.80	-0.173	11.5
			K (1)	2.98	-0.344	10.7
			K (2)	0.77	-0.111	16.8
2	IG/Marg-1	A_{12} Regressed	T (K)	2.11	0.200	0.3
			P (bar)	0.27	0.007	3.2
			K (1)	1.10	-0.036	3.1
			K (2)	0.35	-0.017	5.5
3	IG/NRTL	Δ_{12} Regressed	T (K)	1.94	0.227	0.2
		Δ_{21} Regressed	P (bar)	0.27	0.003	2.4
			K (1)	0.89	-0.022	2.6
			K (2)	0.24	-0.013	4.9
4	IG/UNIQUAC	τ_{12} Regressed	T (K)	1.86	0.213	0.2
		τ_{21} Regressed	P (bar)	0.20	0.0002	2.4
			K (1)	0.74	-0.010	2.6
			K (2)	0.21	-0.010	4.7

For some systems like toluene/benzaldehyde, acetaldehyde/benzene, benzaldehyde/benzyl acetate and tetrachloroethylene/furfural, all the cases considered yielded large errors in the T and P predictions. Similar results were reported by DECHEMA [24]. The poor quality fits were then attributed to the quality of the experimental data employed.

Cases 2 through 4 established the level of precision for the model representations for the systems considered. The regressed parameters thus obtained from these were then used in the development of the QSPR models (Case 2Q, 3Q and 4Q). This work seeks to produce model generalizations roughly within twice the AAD of the data regressions.

The regressed model parameters from Case 2, 3 and 4 were taken as the input for the linear QSPR model. The entire database was divided into a training set of 221 systems and a prediction set of 111 systems. The heuristic analysis available in the commercial software CODESSA [21] was used to obtain the 25 most significant structural descriptors. These descriptors were further analyzed using a non-linear analysis to obtain the best set of significant molecular descriptors. A three-layer back propagation network with six neurons in the hidden layer was the non-linear network gave the best results for the training and the prediction set. This network was chosen for the final model development. Final sets of 15 molecular descriptors obtained from the non-linear analysis were used in the non-linear QSPR model development. Tables 3.3-3.5 list the molecular descriptors used in the NRTL-QSPR, the UNIQUAC-QSPR and the Margules-QSPR model development. The descriptors listed constitute the descriptors for both the components of the solution.

Table 3.3: Molecular Descriptors used in NRTL-QSPR model development

Coefficient	Molecular Descriptors
Δ_{12}	
33.044	Intercept
-7.017	UMax valency of a C atom
4.093	HACA-1
-1.847	Ucount of H-donors sites
1.868	HOMO-LUMO energy gap
2.667	Max SIGMA-PI bond order
-4.152	UBonding Information content (order 0)
-2.643	UMin net atomic charge for a H atom
4.382	XY Shadow / XY Rectangle
2.312	HOMO-1 energy
-3.715	UFNSA-1 Fractional partial negative surface area
4.062	UMax bond order of a C atom
-3.289	UMin e-e repulsion for a N atom
2.272	exch. Eng. + e-e repulsion for a H-O bond
-2.284	UDPSA-3 Difference in charged partial surface areas
-2.150	LUMO+1 energy
Δ_{21}	
68.773	Intercept
0.706	Moment of inertia A
4.351	UWPSA-2 Weighted positive partial surface area
6.791	UNumber of triple bonds
6.776	Uexch. eng. + e-e repulsion for a H-O bond
-5.294	Max SIGMA-PI bond order
-4.323	UPrincipal moment of inertia B / # of atoms
-2.620	Kier & Hall index (order 0)
-3.301	Polarity parameter / square distance
2.908	UXY Shadow
-4.106	Number of benzene rings
3.611	Relative number of O atoms
-2.955	Number of O atoms
2.307	Max resonance energy for a C-C bond
-2.262	UStructural Information content (order 2)
2.206	Max 1-electron reactive index for a N atom

Table 3.4: Molecular Descriptors used in UNIQUAC-QSPR model development

Coefficient	Molecular Descriptors
τ_{12}	
76.676	Intercept
2.625	RPCS Relative positive charged surface area
-0.687	UHA dependent HDSA-2/TMSA
-1.466	Max e-n attraction for a C-C bond
-6.923	Lowest normal mode vibration frequency
4.582	RNCS Relative negative charged surface area
-3.010	URNCG Relative negative charge
3.088	UMin (>0.1) bond order of a C atom
2.033	UMin electrophilic reactive index for a O atom
-2.397	UMax net atomic charge
2.947	UAvg nucleophilic reactive index for a C atom
2.751	UKier shape index (order 3)
2.171	UMax net atomic charge for a N atom
3.352	Min net atomic charge for a C atom
-2.797	Internal heat (300K)/ # of atoms
2.415	Total hybridization component of the molecular dipole
τ_{21}	
78.289	Intercept
6.764	UHA dependent HDSA-2/SQRT(TMSA)
6.310	UNumber of triple bonds
-3.260	Polarity parameter (Qmax-Qmin)
7.064	LUMO+1 energy
5.434	Total molecular 1-center E-E repulsion
-4.858	Uexch. Eng. + e-e repulsion for a C-C bond
3.666	Average Structural Information content (order 1)
-4.468	UInternal enthalpy (300K) / # of atoms
-3.513	Total hybridization component of the molecular dipole
-2.699	UMin partial charge for a H atom
2.944	Final heat of formation
2.414	UDPSA-3 Difference in charged partial surface areas
2.513	UMin nucleophilic reactive index for a S atom
-2.153	Principal moment of inertia B / # of atoms
2.098	Min resonance energy for a S-S bond

Table 3.5: Molecular Descriptors used in Margules-QSPR model development

Coefficient	Molecular Descriptors
A_{12}	
4.463	Intercept
9.534	RNCS Relative negative charged surface area
-5.208	Max partial charge for a C atom
-4.895	UMax n-n repulsion for a H-N bond
-4.931	UFNSA-1 Fractional Partial negative surface area
-4.712	UMax total interaction for a C-O bond
4.027	UHACA-1
-3.106	UTotal molecular 1-center E-N attraction
0.884	Relative number of triple bonds
-3.494	Min (>0.1) bond order of a H atom
-3.344	Avg nucleoph. reactive index for a S atom
2.427	Max resonance energy for a S-S bond
-1.842	UESP-Max net atomic charge for a H atom
2.159	URelative number of triple bonds
2.528	Average Information content (order 0)
-1.990	Number of benzene rings

Figures 3.17-3.21 show that the NRTL, UNIQUAC and Margules model parameters obtained from the non-linear QSPR models are generally in good agreement with the regressed model parameters for most of the systems. Table 3.6 presents the VLE predictions produced utilizing the structure-based model parameters obtained from the non-linear QSPR models (Case 2Q, 3Q and 4Q). The results produced by the model parameter generalizations indicate that VLE predictions with about twice the average absolute error of the data regressions were obtained for each of the three cases considered.

Table 3.6: Results of the NRTL-QSPR model, UNIQUAC-QSPR model and Margules-QSPR model

Case	Models (V/L)	Parameters	Property	RMSE	BIAS	%AAD
2Q	IG/Margules	A_{12} QSPR	T (K)	4.31	-0.293	0.6
	1-parameter		P (bar)	0.55	0.025	7.0
			K (1)	1.62	-0.001	5.7
			K (2)	0.54	-0.032	9.3
2Q*	IG/Margules	$\hat{A}_{12}$ QSPR	T (K)	4.25	0.400	0.4
	1-parameter		P (bar)	0.51	0.024	5.4
			K (1)	1.07	-0.032	4.7
			K (2)	0.56	-0.010	8.0
3Q	IG/NRTL	Δ_{12} QSPR	T (K)	3.62	-0.232	0.5
	2-parameter	Δ_{12} QSPR	P (bar)	0.36	0.028	5.1
			K (1)	0.84	0.010	4.5
			K (2)	0.32	-0.012	7.5
4Q	IG/UNIQUAC	Δ_{12} QSPR	T (K)	2.95	0.069	0.5
	2-parameter	Δ_{12} QSPR	P (bar)	0.64	0.068	5.3
			K (1)	0.85	-0.029	5.0
			K (2)	0.38	0.003	8.3

* The Margules model with the normalized Margules constant (model not accounting for temperature dependence)

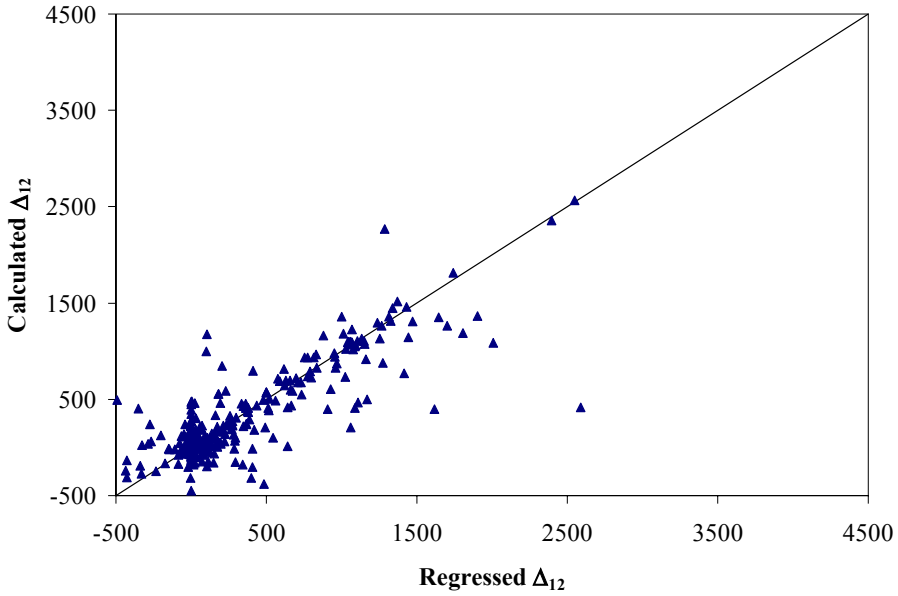

Figure 3.17: Comparision plot of regressed Δ_{12} and calculated Δ_{12} for the two-parameter NRTL model

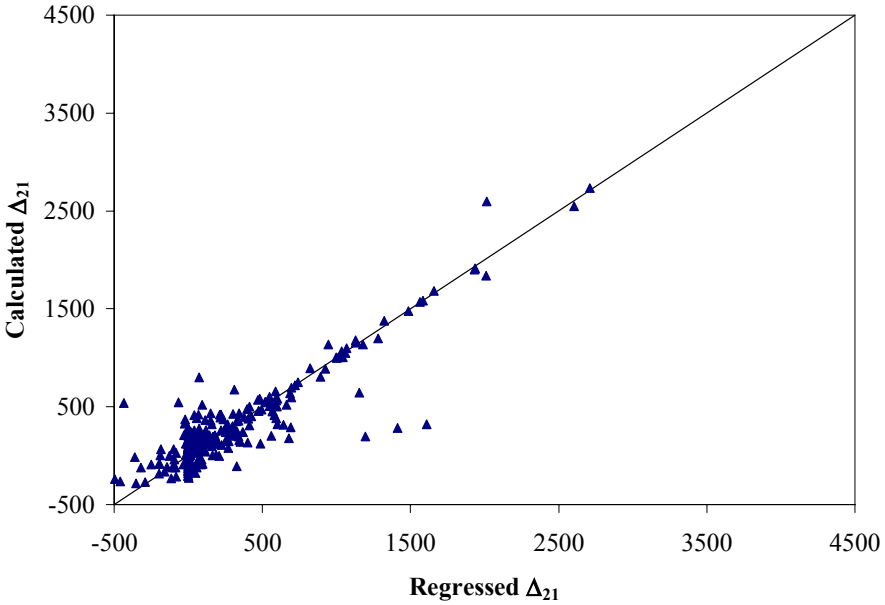

Figure 3.18: Comparision plot of regressed Δ_{21} and calculated Δ_{21} for the two-parameter NRTL model

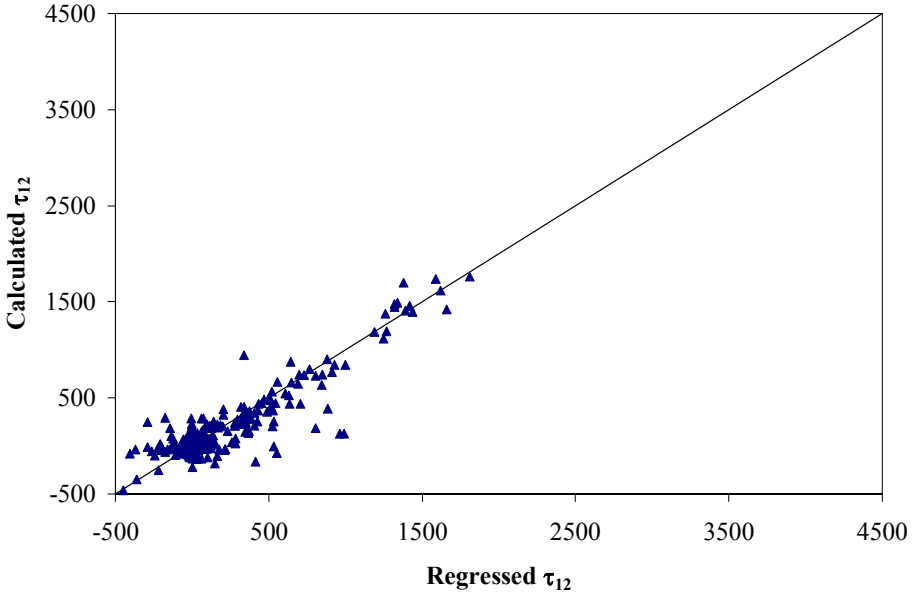

Figure 3.19: Comparision plot of regressed τ_{12} and calculated τ_{12} for the two-parameter UNIQUAC model

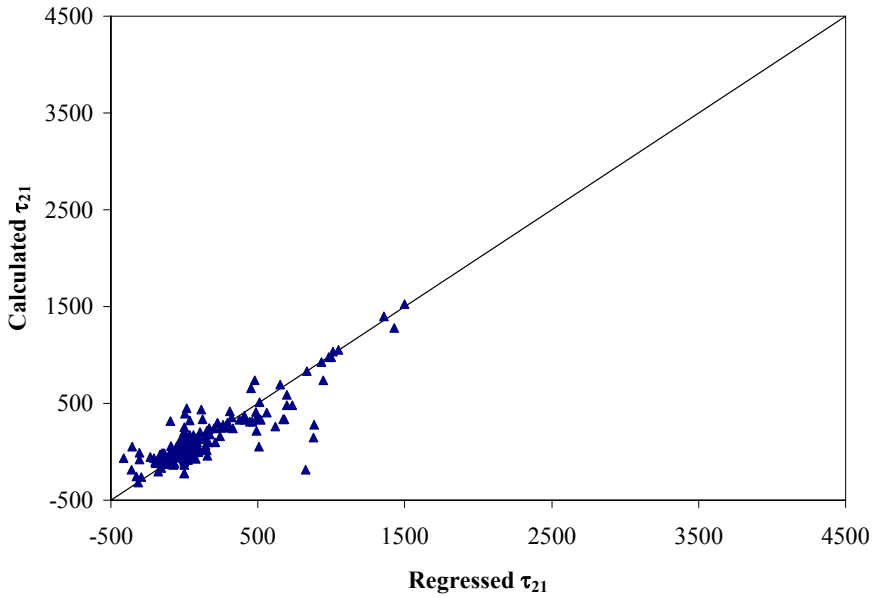

Figure 3.20: Comparision plot of regressed τ_{21} and calculated τ_{21} for the two-parameter UNIQUAC model

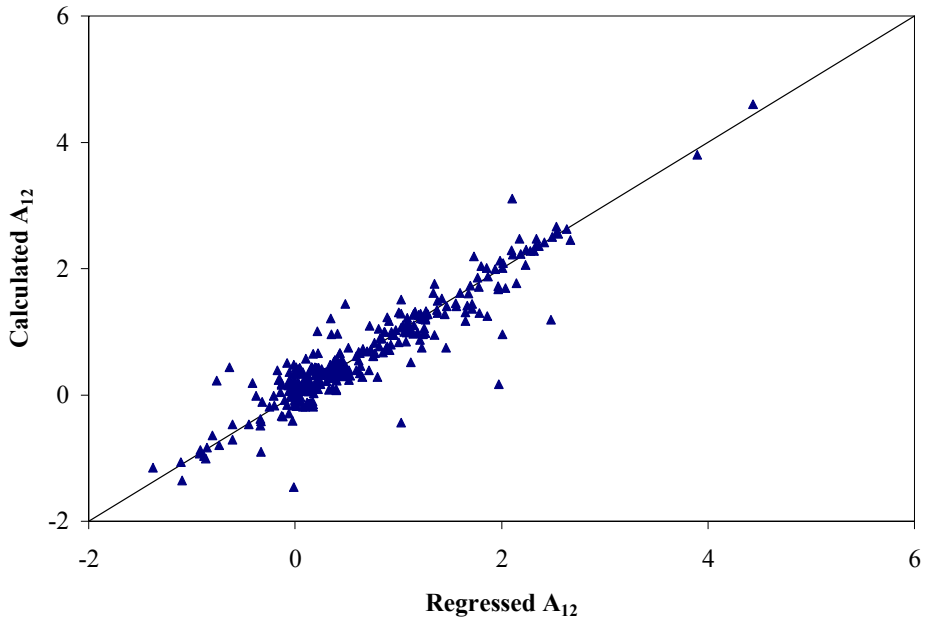

Figure 3.21 : Comparison plot of regressed A_{12} and calculated A_{12} for the one-parameter Margules model

Using the structure-based parameters, T, P, K_1 and K_2 predictions within 0.5%, 5%, 5%, and 8% overall AAD, respectively, are obtained for both Cases 3Q and 4Q. Overall T, P, K_1 and K_2 predictions within 0.6%, 7%, 6%, and 9% AAD were obtained from the one-parameter Margules-QSPR model. These results indicate that the QSPR models yielded comparable structure-based parameters for the one-parameter model. This may be attributed to the minimal amount of correlation that exists between the two regressed parameters of Case 3 and 4, which form the basis for the QSPR models. In addition, the two-parameter model predictions amplify errors associated with two model parameters compared to errors associated with a single parameter in Case 2Q and 2Q*. Interestingly, when the temperature-normalized Margules parameters were generalized (Case 2Q*), the overall quality of fit improved slightly. Additional work would be required to investigate further these prediction results.

The predictions of the NRTL-QSPR and the UNIQUAC-QSPR models were less accurate for some of the aromatic systems and systems with aldehydes. The overall performances of the models were found to be satisfactory. Further, the prediction outliers can be attributed mainly to (a) the quality of the data for some of the systems used, and (b) the lack of a sufficient number of representative systems in the training set.

Figures 3.22 and 3.23, 3.26 and 3.27 present the %AAD distribution of temperature and pressure predictions obtained from Case 3Q and 4Q. For the NRTL-QSPR model, the temperature predictions for 90% of the systems were within 1% AAD, and the pressure predictions for 70% of the systems were within 5% AAD. Similarly, with the UNIQUAC-QSPR model, temperature predictions within 1% AAD for 83% of systems and pressure predictions within 5% AAD for 66% of the systems were obtained. Figures 3.24 and 3.25, 3.28 and 3.29 present the %AAD distribution of equilibrium constants K_1 and K_2 obtained from the Case 3Q and 4Q.

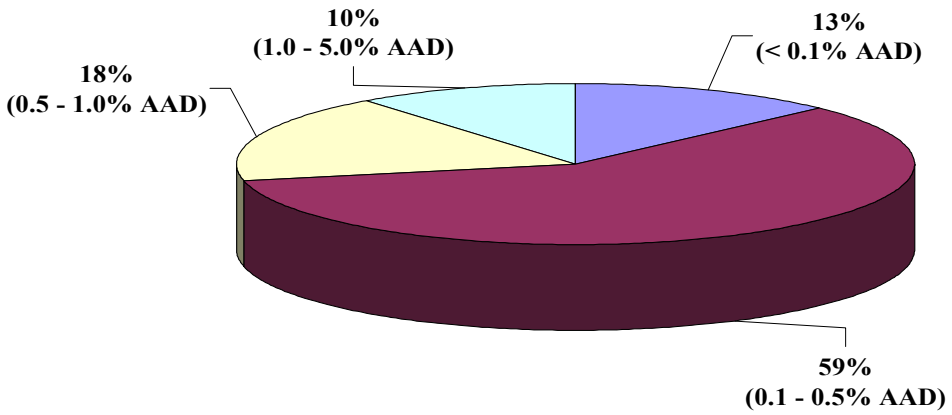

Figure 3.22: %AAD distribution for the temperature predictions from the NRTL-QSPR model

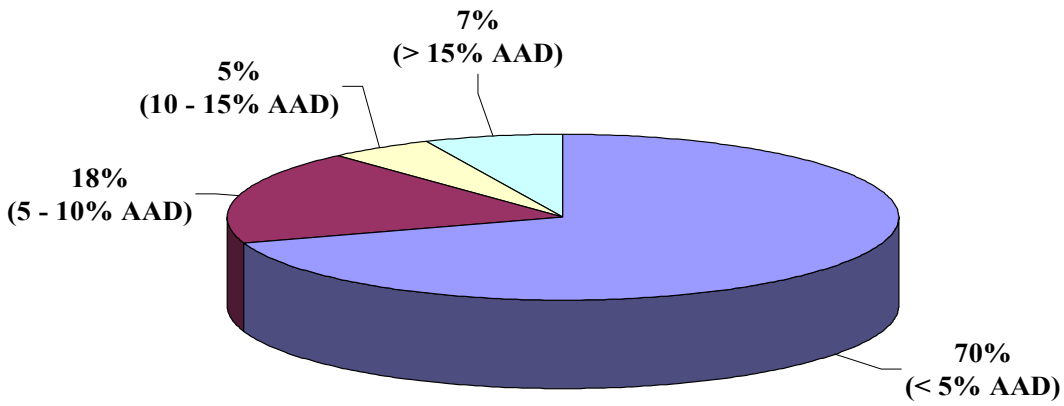

Figure 3.23: %AAD distribution for the pressure predictions from the NRTL-QSPR model

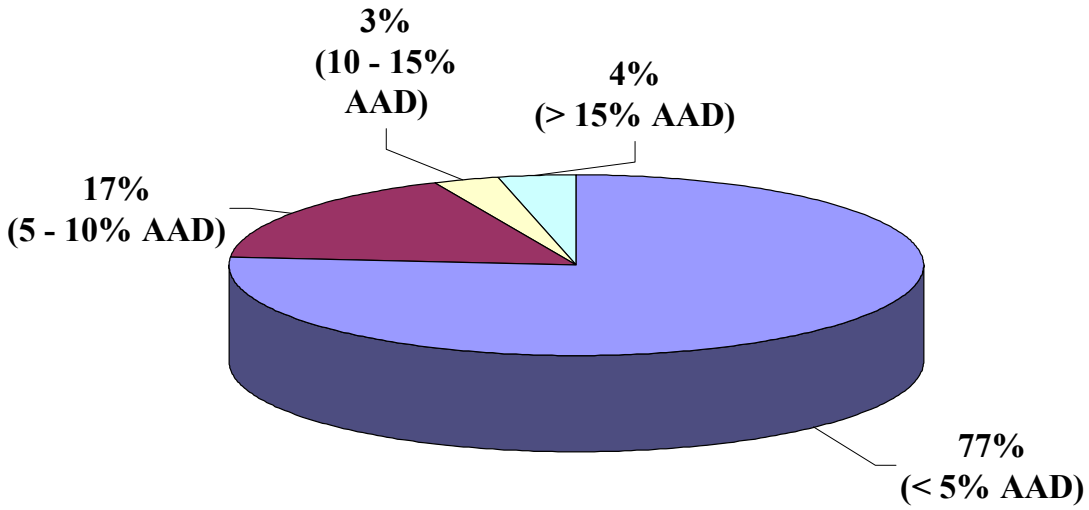

Figure 3.24: %AAD distribution for K_1 predictions from the NRTL-QSPR model

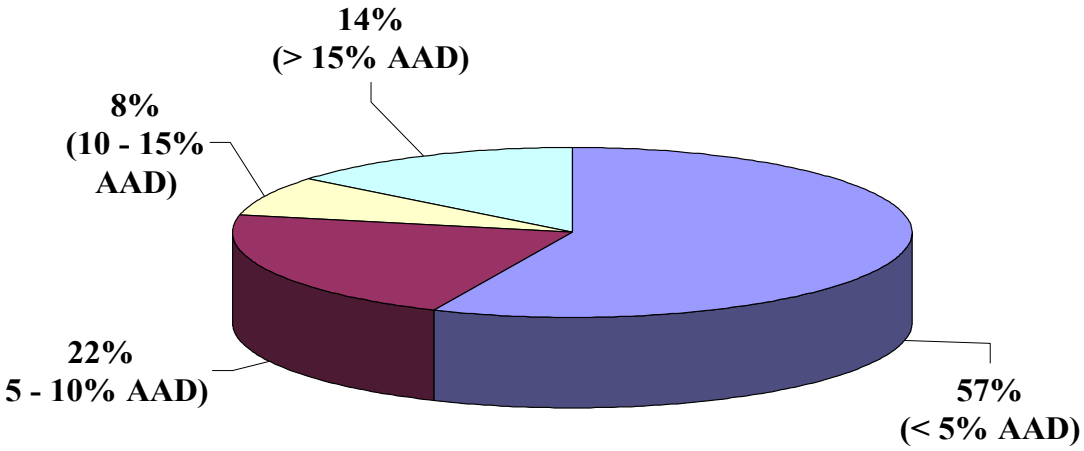

Figure 3.25: %AAD distribution for K_2 predictions from the NRTL-QSPR model

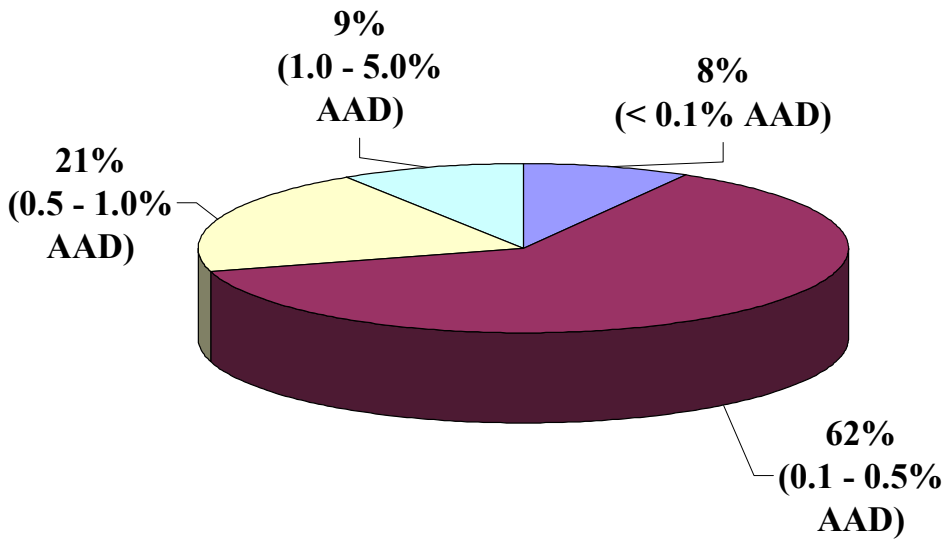

Figure 3.26: %AAD distribution for the temperature predictions from the UNIQUAC-QSPR model

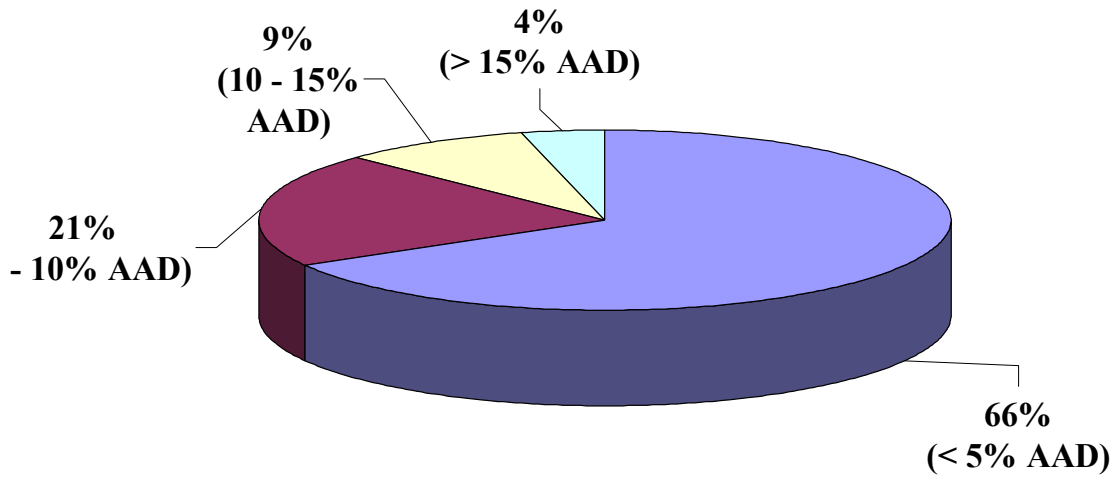

Figure 3.27: %AAD distribution for the pressure predictions from the UNIQUAC-QSPR model

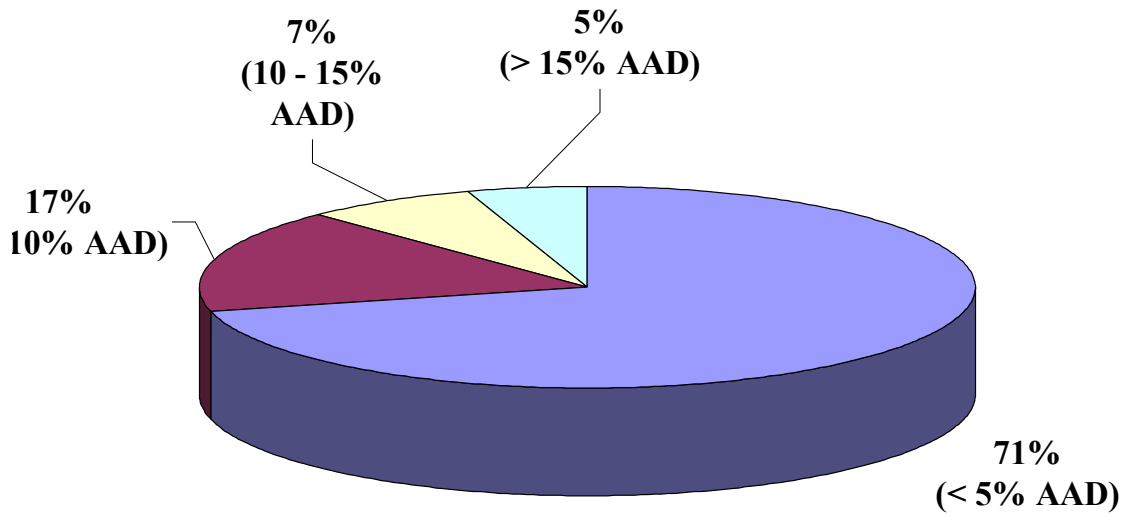

Figure 3.28: %AAD distributions for K_1 predictions from the UNIQUAC-QSPR model

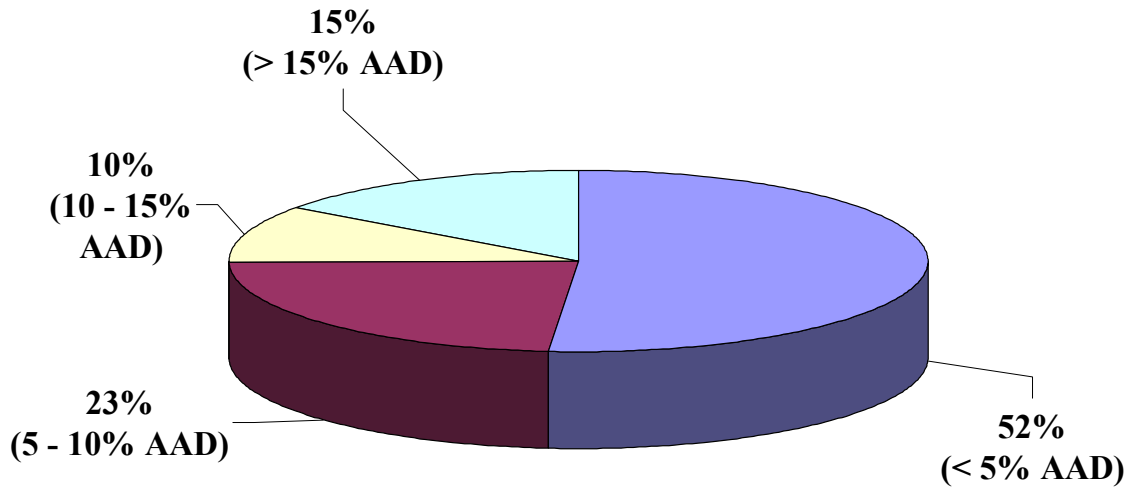

Figure 3.29: %AAD distribution for K_2 predictions from the UNIQUAC-QSPR model

A complete summary of results obtained from Case 3Q and 4Q for the individual systems are presented in Tables B.3 and B.4 of Appendix B. For both the NRTL-QSPR model and the UNIQUAC-QSPR model the overall results obtained were found to be satisfactory. The results for the modified UNIFAC previously obtained by the research group at OSU for a subset of the currently used database (consisting of 96 oxygenate systems) show overall deviations within 2%, 15%, 20% and 20% for the T, P, K_1 and K_2 calculations, respectively. For the same set of 96 systems, using the NRTL-QSPR and the UNIQUAC-QSPR models an overall AAD of 0.46%, 4%, 4% and 7%, respectively was obtained.

The results obtained in this work clearly indicate that combining the activity coefficient models with the QSPR models is an effective method of improving the model

generalizations. However, the QSPR generalized models can be further refined by using a larger database comprising of diverse chemical systems. Also, for the NRTL model the value of α_{12} was fixed at 0.2 to accommodate the LLE calculations. However, once accurate QSPR generalized models are developed for the NRTL interaction parameters, a careful evaluation of the efficacy of modeling α_{12} using QSPR techniques would be viable since the parameter correlation effects would have been eliminated by then.

3.6. Conclusions

The current work demonstrates that the QSPR models have the potential to provide reliable estimates of the interaction parameters for activity coefficient models from structural information only. The integrated NRTL-QSPR and the UNIQUAC-QSPR models produced VLE predictions with about twice the average absolute error of the data regressions. An effective strategy was developed to reduce the correlation between the NRTL and the UNIQUAC model parameters. However, this work is not complete; a larger, reliable database is needed to refine and develop a more accurate model capable of *a priori* predictions of diverse systems in the absence of experimental data.

References

1. Walas, M. S., Phase Equilibrium in Chemical Engineering, Butterworth Publishers, Stoneham, 1985.
2. Renon, H., NRTL: An Empirical Equation or an Inspiring Model for Fluid Mixture Properties?, *Fluid Phase Equilibria*, 24, 87-114 (1985).
3. Prausnitz, J.M., Lichtenthaler, R.N., Azevedo, E.G., Molecular Thermodynamics of Fluid Phase Equilibria, 2nd Ed., Prentice-Hall, 1986.
4. Wilson, G.M., Deal, C.H., Activity Coefficients and Molecular Structure, *Industrial & Engineering Chemistry Fundamentals*, 1, 20 (1960).
5. Prausnitz, J.M., Tavares, F.W., Thermodynamics of Fluid Phase Equilibria for Standard Chemical Engineering Operations, *AIChE Journal*, 50(4), 739-761 (2004).
6. Gmehling, J., Fischer, K., Li, J., Schiller, M., Status and Results of Group Contribution Methods, *Pure & Applied Chemistry*, 65(5), 919-926 (1993).
7. Abildskov, J., Constantinou, L., Gani, R., Towards the Development of a Second-Order Approximation in Activity Coefficient Models Based on Group Contribution, *Fluid Phase Equilibria*, 1, 118 (1996).
8. Putnam, R., Taylor, R., Klamt, A., Eckert, F., Schiller, M., Prediction of Infinite Dilution Activity Coefficients Using COSMOS-RS, *Ind. Eng. Chem. Res*., 42, 3635-3641 (2003).

9. Klamt, A., Jonas, V., Buerger, T., Lohrenz, J. C. W., Refinement and Parameterization of COSMO-RS. *Journal of Physical Chemistry A*, 102, 5074 (1998).
10. Klamt, A., Eckert, F., COSMO-RS: A Novel and Efficient Method for the a priori Prediction of Thermophysical Data of Liquids. *Fluid Phase Equilibria,* 172, 43 (2000).
11. Sum, K. A., Sandler, I. S., Use of *ab initio* Methods to Make Phase Equilibria Predictions Using Activity Coefficient Models, *Fluid Phase Equilibria*, 158-160, 375-380 (1999).
12. Fermeglia, M., Pricl, S., Prediction of Phase Equilibria for Binary Mixtures by Molecular Modeling, *AIChE Journal*, 47(10), 2371-2382 (2001).
13. Bondi, A., Catalog of Molecular Properties, Wiley: New York, 1968.
14. Katrizky, A. R., Lobanov, V. S., Karelson, M., QSPR: The Correlation and Quantitative Prediction of Chemical and Physical Properties from Structure, *Chem. Society Reviews*, 1995.
15. Basak, S. C., Mills, D., Quantitative Structure Property Relationships (QSPRs) for the Estimation of Vapor Pressure: A Hierarchical Approach Using Mathematical Structural Descriptors, *Journal of Chemical Information and Computer Science*, 41, 692-701 (2001).
16. Neely, J. B., Godavarthy, S. S., Robinson Jr., L. R., Gasem, K. A. M., Improved Quantitative Structure Property Relationship Models for Infinite Dilution Activity Coefficients of Aqueous Systems, *Proceedings of the Sixth International Petroleum Environmental Conference*, Albuquerque, November, 2004.

17. Bunz, A. P., Braun, B., Janowsky, R., Quantitative Structure-Property Relationships and Neural Networks: Correlation and Prediction of Physical Properties of Pure Components and Mixtures from Molecular Structure, *Fluid Phase Equilibria*, 158-160, 367-374 (1999).
18. Kasturirangan, A., Cubic Equation-of-State Modeling of Asymmetric Binary Mixtures, M.S. Dissertation, Oklahoma State University, 2004.
19. ChemDraw 8.0, Cambridge Software (2004).
20. AMPAC 6.0, Semichem Inc., 7128 Summit, Shawnee, KS (1997).
21. CODESSA 2.63, Semichem Inc., 7128 Summit, Shawnee, KS (1998).
22. Schneider, G., Wrede, P., Artificial Neural Networks for Computer-based Molecular Design, *Progress in Biophysics & Molecular Biology*, 70, 175-222 (1998).
23. DIPPR Project 801; Physical and Thermodynamic Properties of Pure Chemicals, 2005.
24. Gmehling, J., Onken, U., Arlt, W., Vapor-Liquid Equilibrium Data Collection, *Chemistry Data Series*, Vol. 1-8, DECHEMA (1979).
25. Danner, P. R., Gess, A. M., A Data Base Standard for the Evaluation of Vapor-Liquid-Equilibrium Models, *Fluid Phase Equilibria*, 56, 285-301 (1990).
26. Gasem, K. A. M., The OSU VLE Database, Personal Communication, 2005.

CHAPTER 4

CONCLUSIONS AND RECOMMENDATIONS

This chapter presents a summary of the conclusions and recommendations made based on this work.

4.1 Pure-Fluid Saturation Property Predictions: The SVRC-QSPR Model

The objective in this part of the work was to develop a generalized model capable of *a priori* predictions of pure-fluid saturation properties for a diverse set of organic compounds.

Conclusions

1. Structure-based model parameter generalizations developed using QSPR modeling improved the SVRC vapor pressure, liquid density and vapor density predictions.
2. The SVRC-QSPR model generalizations were within 1% absolute average deviation for the saturation properties considered in this work.
3. The results indicate that integrating a theoretical model with an *ab inito* QSPR model is an effective methodology for generalizing fluid saturation properties over the entire saturation range.

4. The limited database employed in the present work constrained the model generalization efforts. These results, however, constitute a promising initial effort in our quest to develop a robust and effective model based on a larger database.

Recommendations

1. Assemble a larger database of pure-fluid vapor pressures and saturated phase densities, encompassing structurally diverse molecular species.
2. Use a more effective non-linear descriptor reduction method to replace the linear heuristic reduction employed currently.

4.2 Phase Equilibria Modeling: The NRTL-QSPR and UNIQUAC-QSPR Models

The objective here was to obtain *a priori* VLE predictions by improving the generalization abilities of the NRTL and UNIQUAC activity coefficient models. This objective was achieved utilizing structure-based model parameter generalizations.

Conclusions

1. For the data considered, the QSPR model parameter generalizations produced VLE predictions within twice the average absolute error of the data regressions.
2. A sequential model regression and generalization strategy was identified, which reduced considerably the parameter correlation of the NRTL and the UNIQUAC models.

Recommendations

1. Refine the QSPR model further by incorporating structurally diverse chemical systems in the database.

2. Develop a more robust predictive model using a non-linear genetic algorithm for molecular descriptor reduction to replace the heuristic approaches employed currently.

APPENDIX A

THE SVRC-QSPR MODEL: DATABASE DESCRIPTION, PHYSICAL CONSTANTS

Table A.1: Ranges of vapor pressure data used in model development

Compound	Temperature Range, K	Pressure Range, bar	No. of pts.
Methane	90.69 - 190.56	0.116 - 45.992	199
Ethane	127.87 - 305.33	0.010 - 48.718	200
Ethylene	117.61 - 282.35	0.010 - 50.417	200
Propane	161.65 - 369.83	0.010 - 42.472	199
Butane	191.72 - 425.13	0.010 - 37.907	199
Pentane	218.50 - 469.70	0.009 - 33.710	200
Hexane	242.18 - 507.82	0.009 - 30.429	200
Oxygen	60.87 - 154.58	0.009 - 50.428	199
Fluorine	58.02 - 144.41	0.009 - 52.394	199
Nitrogen	63.15 - 126.19	0.125 - 33.958	198
Carbondioxide	216.59 - 304.13	5.179 - 73.773	201
Benzene	278.68 - 562.16	0.047 - 48.982	42
Acetylene	192.15 - 308.33	1.266 - 61.390	27
1,3-Butadiene	164.25 - 425.04	0.0007 - 43.041	45
Carbondisulfide	161.11 - 552.00	0.00001 - 80.408	42
Carbontetrachloride	250.33 - 556.35	0.011 - 45.436	81
Chlorine	172.12 - 416.90	0.013 - 79.800	40
Cyclopentane	179.28 - 511.76	0.00009 - 45.028	35
Propylene	158.04 - 365.57	0.010 - 44.646	201
Isobutane	183.57 - 407.82	0.010 - 36.399	201
Heptane	264.79 - 540.13	0.009 - 27.311	201
Hydrogen	13.95 - 33.19	0.077 - 13.301	199
1-Butene	87.80 - 419.95	1E-09 - 40.391	75
Cumene	177.14 - 631.10	4E-09 - 31.837	62
Cyclohexane	279.69 - 553.58	0.053 - 40.958	66
Cyclohexene	169.67 - 560.40	1E-06 - 43.922	58
1-Decene	206.89 - 616.40	2E-07 - 22.092	88
Ethylbenzene	178.15 - 617.20	4E-08 - 36.088	100
Indene	273.15 - 687.00	0.0002 - 38.492	33
Isobutene	132.81 - 417.90	6E-06 - 39.760	55
Naphthalene	353.33 - 748.35	0.010 - 40.500	90
n-Nonane	219.66 - 594.60	4E-06 - 23.054	65
n-Octane	216.38 - 568.65	2E-05 - 24.890	85
Toluene	178.18 - 591.80	4E-07 - 41.000	80

Table A.1: Ranges of vapor pressure data used in model development (Contd.)

Compound	Temperature Range, K	Pressure Range, bar	No. of pts.
o-Xylene	247.98 - 630.33	0.0002 - 37.424	99
p-Xylene	286.40 - 616.23	0.005 - 35.107	93
Phenanthrene	372.38 - 869.25	0.0003 - 28.965	22
Nitric oxide	110.89 - 180.15	0.266 - 65.156	42
Ammonia	195.50 - 405.40	0.061 - 113.390	201
Water	273.16 - 647.10	0.006 - 220.640	201
Acetone	259.18 - 508.10	0.042 - 47.000	47
Methanol	288.05 - 512.64	0.098 - 80.971	19
Ethanol	292.77 - 513.92	0.057 - 61.484	26
R-22	165.18 - 369.30	0.009 - 49.900	201
R-32	158.91 - 351.26	0.009 - 57.826	201
R-125	172.52 - 339.17	0.029 - 36.179	201
R-123	215.44 - 456.83	0.009 - 36.619	201
R-124	186.10 - 395.43	0.009 - 36.243	201
R-134a	169.85 - 374.21	0.003 - 40.591	201
R-143a	161.34 - 345.86	0.010 - 37.618	201
R-152a	177.75 - 386.41	0.009 - 45.168	201
1-Butanol	184.51 - 563.05	5E-09 - 44.200	55
Chloroform	207.15 - 536.40	0.0005 - 53.700	72
Diethyl ether	156.85 - 466.74	4E-06 - 36.376	50
Ethyl acetate	189.60 - 523.30	1E-05 - 38.502	78
Ethyl mercaptan	125.26 - 499.15	1E-08 - 54.918	43
Ethylamine	190.85 - 456.35	0.001 - 56.276	54
Ethylene glycol	260.15 - 719.70	2E-06 - 77.100	26
Formaldehyde	181.15 - 408.00	0.008 - 65.935	32
Hydrogen chloride	158.97 - 324.65	0.135 - 83.564	25
Cyclopropane	273.00 - 398.30	3.427 - 55.797	201
Methyl acetate	175.15 - 506.55	1E-05 - 46.948	67
Methyl chloride	175.43 - 416.25	0.008 - 66.792	27
Methyl ethyl ketone	211.24 - 536.80	0.0002 - 42.100	54
Methylamine	177.35 - 430.05	0.001 - 74.139	36
Nitric acid	231.55 - 376.10	0.0006 - 2.000	30
Terephthalic acid	700.15 - 1113.00	0.046 - 39.500	21
Diisopropyl ether	187.65 - 500.05	6E-05 - 28.688	22
n-Propyl mercaptan	177.13 - 536.60	1E-05 - 46.300	61

Table A.1: Ranges of vapor pressure data used in model development (Contd.)

Compound	Temperature Range, K	Pressure Range, bar	No. of pts.
1-Butyl acetate	294.15 - 575.40	0.013 - 30.900	113
1,2-Dichloropropane	185.71 - 572.00	6E-06 - 44.195	77
Isopentane	217.19 - 460.43	0.014 - 33.812	94
Glyoxal	288.15 - 495.00	0.208 - 58.800	21
n-Butylamine	259.15 - 531.90	0.013 - 42.000	10
Ethyl formate	273.15 - 508.45	0.096 - 47.376	45
1-Heptanol	315.55 - 632.60	0.001 - 30.580	57
1-Hexanol	243.15 - 610.30	3E-06 - 34.170	43
2-Butanol	293.15 - 536.20	0.017 - 42.020	64
Diphenyl ether	422.04 - 767.15	0.049 - 31.200	29
Isobutylbenzene	225.00 - 650.00	3E-06 - 31.510	36
n-Heptylamine	255.00 - 613.00	0.0001 - 26.600	58
n-Hexylamine	255.00 - 584.00	0.0005 - 30.470	31
2-Methyl propanol	208.15 - 507.00	0.0003 - 41.000	35
Benzaldehyde	192.20 - 695.00	1E-08 - 46.500	20
2-Heptanone	255.00 - 611.40	0.0002 - 29.400	214
n-Octanol	293.15 - 652.50	6E-05 - 27.770	74
Methyl benzoate	298.15 - 693.00	0.0005 - 35.900	52
Cyclohexanol	294.15 - 650.10	0.001 - 42.600	35
Ethylene diamine	294.65 - 593.00	0.013 - 62.900	54
o-Methyl styrene	305.16 - 659.00	0.003 - 34.700	34

Table A.2: Physical constants used in vapor pressure model development

Compound	T_c, K	P_c, bar	T_t, K	P_t, bar	ω	Z_c
Methane	190.56	45.992	90.69	1.17E-01	0.011	0.288
Ethane	305.33	48.718	127.87	1.00E-02	0.099	0.285
Ethylene	282.35	50.417	117.61	1.00E-02	0.089	0.280
Propane	369.83	42.472	161.65	1.00E-02	0.153	0.281
Butane	425.13	37.907	191.72	1.00E-02	0.199	0.274
Pentane	469.70	33.710	218.50	9.56E-03	0.251	0.263
Hexane	507.82	30.429	242.18	9.01E-03	0.299	0.264
Oxygen	154.58	50.428	60.87	9.04E-03	0.025	0.288
Fluorine	144.41	52.394	58.02	8.97E-03	0.054	0.288
Nitrogen	126.19	33.958	63.15	1.25E-01	0.038	0.289
Carbondioxide	304.13	73.773	216.59	5.18E+00	0.239	0.274
Benzene	562.16	48.982	278.68	4.78E-02	0.210	0.266
Acetylene	308.33	61.390	192.15	1.27E+00	0.190	0.271
1,3-Butadiene	425.17	43.041	164.25	6.91E-04	0.195	0.270
Carbondisulfide	552.00	80.408	161.11	1.49E-05	0.109	0.276
Carbontetrachloride	556.35	45.436	250.33	1.12E-02	0.193	0.272
Chlorine	416.90	79.800	172.12	1.37E-02	0.090	0.285
Cyclopentane	511.76	45.028	179.28	9.44E-05	0.196	0.275
Propylene	365.57	44.646	158.04	1.00E-02	0.144	0.274
Isobutane	407.82	36.399	183.57	1.00E-02	0.183	0.283
Heptane	540.13	27.311	264.79	8.92E-03	0.349	0.263
Hydrogen	33.19	13.301	13.95	7.70E-02	0.216	0.305
1-Butene	419.95	40.391	87.80	7.18E-12	0.191	0.277
Cumene	631.10	31.837	177.14	3.80E-09	0.326	0.261
Cyclohexane	553.58	40.958	279.69	5.38E-02	0.212	0.273
Cyclohexene	560.40	43.922	169.67	1.04E-06	0.212	0.272
1-Decene	616.40	22.092	206.89	1.73E-07	0.491	0.280
Ethylbenzene	617.20	36.088	178.15	4.01E-08	0.303	0.263
Indene	687.00	38.492	273.15	1.92E-04	0.334	0.246
Isobutene	417.90	39.760	132.81	6.22E-06	0.194	0.275
Naphthalene	748.35	40.500	353.33	9.85E-03	0.302	0.269
n-Nonane	594.60	23.054	219.66	4.31E-06	0.443	0.252
n-Octane	568.65	24.890	216.38	2.11E-05	0.400	0.256
Toluene	591.80	41.000	178.18	4.23E-07	0.262	0.264

Table A.2: Physical constants used in vapor pressure model development (Contd.)

Compound	T_c, K	P_c, bar	T_t, K	P_t, bar	ω	Z_c
o-Xylene	630.33	37.424	247.98	2.20E-04	0.310	0.263
p-Xylene	616.23	35.107	286.40	5.82E-03	0.321	0.260
Phenanthrene	869.25	28.965	372.38	2.90E-04	0.495	0.222
Nitric oxide	180.15	65.156	110.89	2.67E-01	0.583	0.251
Ammonia	405.40	113.390	195.50	6.09E-02	0.250	0.244
Water	647.10	220.640	273.16	6.12E-03	0.344	0.235
Acetone	508.10	47.000	259.18	4.27E-02	0.304	0.232
Methanol	512.64	80.971	288.05	9.82E-02	0.556	0.224
Ethanol	513.92	61.484	292.77	5.73E-02	0.644	0.240
R-22	369.30	49.900	165.18	9.17E-03	0.219	0.269
R-32	351.26	57.826	158.91	9.24E-03	0.276	0.241
R-125	339.17	36.179	172.52	2.91E-02	0.250	0.270
R-123	456.83	36.619	215.44	9.74E-03	0.281	0.273
R-124	395.43	36.243	186.10	8.94E-03	0.250	0.270
R-134a	374.21	40.591	169.85	3.90E-03	0.237	0.239
R-143a	345.86	37.618	161.34	1.07E-02	0.251	0.253
R-152a	386.41	45.168	177.75	9.19E-03	0.272	0.255
1-Butanol	563.05	44.200	184.51	5.72E-09	0.593	0.260
Chloroform	536.40	53.700	207.15	5.33E-04	0.218	0.293
Diethyl ether	466.74	36.376	156.85	3.95E-06	0.281	0.263
Ethyl acetate	523.30	38.502	189.60	1.43E-05	0.362	0.252
Ethyl mercaptan	499.15	54.918	125.26	1.14E-08	0.191	0.274
Ethylamine	456.35	56.276	190.85	1.33E-03	0.289	0.270
Ethylene glycol	719.70	77.100	260.15	2.48E-06	0.487	0.246
Formaldehyde	408.00	65.935	181.15	8.87E-03	0.253	0.223
Hydrogen chloride	324.65	83.564	158.97	1.35E-01	0.132	0.249
Cyclopropane	398.30	55.797	273.00	3.43E+00	0.131	0.271
Methyl acetate	506.55	46.948	175.15	1.02E-05	0.326	0.254
Methyl chloride	416.25	66.792	175.43	8.71E-03	0.153	0.269
Methyl ethyl ketone	536.80	42.100	211.24	2.67E-04	0.323	0.252
Methylamine	430.05	74.139	177.35	1.33E-03	0.292	0.321
Nitric acid	376.10	2.000	231.55	6.08E-04	0.714	0.231
Terephthalic acid	1113.00	39.500	700.15	4.59E-02	1.059	0.181
Diisopropyl ether	500.05	28.688	187.65	6.86E-05	0.339	0.267
n-Propyl mercaptan	536.60	46.300	177.13	1.00E-05	0.230	0.260

Table A.2: Physical constants used in vapor pressure model development (Contd.)

Compound	T_c, K	P_c, bar	T_t, K	P_t, bar	ω	Z_c
1-Butyl acetate	575.40	30.900	294.15	1.33E-02	0.440	0.250
1,2-Dichloropropane	572.00	44.195	185.71	5.98E-06	0.260	0.260
Isopentane	460.43	33.812	217.19	1.46E-02	0.230	0.270
Glyoxal	495.00	58.800	288.15	2.08E-01	0.410	0.230
n-Butylamine	531.90	42.000	259.15	1.33E-02	0.330	0.290
Ethyl formate	508.45	47.376	273.15	9.66E-02	0.280	0.260
1-Heptanol	632.60	30.580	315.55	1.33E-03	0.570	0.250
1-Hexanol	610.30	34.170	243.15	3.24E-06	0.580	0.260
2-Butanol	536.20	42.020	293.15	1.72E-02	0.580	0.250
Diphenyl ether	767.15	31.200	422.04	4.96E-02	0.440	0.240
Isobutylbenzene	650.00	31.510	225.00	3.11E-06	0.380	0.270
n-Heptylamine	613.00	26.600	255.00	1.30E-04	0.510	0.270
n-Hexylamine	584.00	30.470	255.00	5.40E-04	0.460	0.270
2-Methyl propanol	507.00	41.000	208.15	3.49E-04	0.360	0.260
Benzaldehyde	695.00	46.500	192.20	1.00E-08	0.310	0.260
2-Heptanone	611.40	29.400	255.00	1.80E-04	0.420	0.250
n-Octanol	652.50	27.770	293.15	6.67E-05	0.580	0.250
Methyl benzoate	693.00	35.900	298.15	5.26E-04	0.420	0.270
Cyclohexanol	650.10	42.600	294.15	1.33E-03	0.370	0.250
Ethylene diamine	593.00	62.900	294.65	1.33E-02	0.470	0.340
o-Methyl styrene	659.00	34.700	305.16	3.87E-03	0.340	0.260

Table A.3: Ranges of liquid density data used in model development

Compound	Temperature Range, K	Density Range, kg/m^3	No. of pts.
R22	115.73 - 369.30	1721.300 - 523.840	201
R32	136.34 - 351.25	1429.300 - 424.000	201
R123	166.00 - 456.83	1771.000 - 550.000	201
R125	172.52 - 339.17	1690.700 - 573.580	201
R124	120.00 - 395.42	1852.800 - 560.000	201
R134a	169.85 - 374.21	1591.100 - 511.900	201
R152a	154.56 - 386.41	1192.900 - 368.000	201
R143a	161.34 - 345.86	1330.500 - 431.000	201
Methane	90.69 - 190.56	451.480 - 162.660	201
Ethane	90.35 - 305.33	651.450 - 206.580	201
Ethylene	103.99 - 282.35	654.600 - 214.240	201
Propane	85.48 - 369.82	733.560 - 218.500	201
Propylene	100.00 - 365.57	754.840 - 223.390	199
Butane	134.87 - 425.13	735.350 - 227.840	201
Isobutane	113.56 - 407.82	740.390 - 224.360	201
Pentane	143.47 - 469.70	762.350 - 232.000	201
Hexane	177.83 - 507.60	761.740 - 232.278	198
Heptane	182.55 - 540.13	776.130 - 232.000	189
Oxygen	54.36 - 154.58	1306.100 - 436.140	201
Fluorine	53.48 - 144.41	1706.700 - 592.860	186
Nitrogen	63.15 - 126.19	867.220 - 313.300	201
Ammonia	195.50 - 405.40	732.900 - 225.000	201
Water	273.16 - 647.13	999.760 - 322.000	47
Carbondioxide	216.59 - 304.13	1178.500 - 467.600	201
Hydrogen	13.96 - 33.19	76.903 - 30.120	186
Acetic acid	293.15 - 591.95	1049.520 - 334.178	43
Benzene	278.70 - 562.05	894.014 - 305.138	124
Ethanol	223.15 - 514.00	848.913 - 274.220	56
Methanol	176.15 - 512.50	904.609 - 273.863	46
Acetone	329.25 - 508.15	750.000 - 273.000	9
1,3-Butadiene	164.20 - 425.00	763.827 - 244.753	88
Carbondisulfide	243.15 - 552.00	1338.510 - 475.879	16
Carbontetrachloride	253.15 - 556.35	1668.960 - 559.904	51
Cyclopentane	193.15 - 511.76	820.993 - 269.747	30
1-Butene	195.04 - 419.60	705.383 - 233.781	49

Table A.3: Ranges of liquid density data used in model development (Contd.)

Compound	Temperature Range, K	Density Range, kg/m^3	No. of pts.
Cumene	177.14 - 631.10	960.001 - 279.999	43
Cyclohexane	280.15 - 553.58	790.602 - 273.653	23
Cyclohexene	243.15 - 560.40	856.940 - 282.344	47
1-Decene	273.15 - 615.00	756.400 - 215.798	18
Ethylbenzene	183.10 - 617.20	963.603 - 283.991	82
Indene	273.15 - 687.00	1010.000 - 315.142	17
Isobutene	203.15 - 417.90	694.779 - 234.759	55
Naphthalene	333.15 - 748.40	992.605 - 310.348	17
n-Nonane	223.15 - 594.60	772.510 - 234.047	47
n-Octane	333.15 - 568.80	669.747 - 232.176	24
Toluene	178.00 - 591.80	971.160 - 291.583	101
o-Xylene	248.00 - 630.33	917.803 - 287.994	63
p-Xylene	288.15 - 616.23	864.878 - 280.124	72
Phenanthrene	372.38 - 873.00	1069.000 - 321.720	14
1-Butanol	186.15 - 563.05	891.178 - 269.537	39
Chloroform	209.00 - 536.40	1644.530 - 499.694	61
Diethyl ether	273.15 - 466.74	736.202 - 264.724	31
Ethyl acetate	273.15 - 523.30	925.380 - 308.063	28
Ethyl mercaptan	273.15 - 499.15	862.380 - 300.915	19
Ethylamine	200.50 - 456.40	785.413 - 247.715	14
Ethylene glycol	260.15 - 719.70	1137.020 - 324.875	92
Hydrogen chloride	183.62 - 324.65	1201.880 - 450.687	15
Cyclopropane	153.15 - 536.80	916.989 - 275.665	63
Methyl acetate	198.06 - 506.85	1052.660 - 325.197	26
Methyl chloride	175.44 - 416.25	1131.980 - 363.480	41
Methylamine	190.57 - 430.05	777.863 - 201.678	14
Diisopropyl ether	293.15 - 500.30	728.133 - 264.707	6
o-Methyl styrene	273.00 - 659.00	928.504 - 290.358	16
Ethylene diamine	273.15 - 593.00	914.095 - 291.747	18
Ethyl formate	273.15 - 508.45	948.742 - 323.487	50
1-Heptanol	253.15 - 633.00	852.977 - 267.126	26
1-Hexanol	253.15 - 611.00	848.736 - 268.162	19
n-Octanol	253.15 - 652.50	857.004 - 265.775	38
Diphenyl ether	303.15 - 766.80	1066.110 - 338.384	8
Methyl benzoate	273.15 - 692.00	1107.676 - 343.813	16

Table A.3: Ranges of liquid density data used in model development (Contd.)

Compound	Temperature Range, K	Density Range, kg/m^3	No. of pts.
n-Heptylamine	273.15 - 613.00	790.916 - 244.621	13
n-Hexylamine	253.15 - 584.00	796.992 - 242.081	17
Benzaldehyde	290.75 - 695.00	1049.262 - 327.537	24
2-Heptanone	253.15 - 611.50	851.321 - 263.100	19
n-Propyl mercaptan	283.15 - 536.60	850.022 - 299.845	19
1-Butyl acetate	273.15 - 579.00	901.634 - 290.400	33
Isopentane	149.87 - 460.98	753.174 - 236.099	59
n-Butylamine	293.15 - 531.90	741.420 - 235.925	9
2-Butanol	293.15 - 536.20	806.574 - 275.545	14

Table A.4: Physical constants used in liquid density model development

Compound	T_c, K	ρ_c, kg/m^3	T_t, K	ρ_t, kg/m^3	ω	Z_c
R22	369.30	523.840	115.73	1.72E+03	0.219	0.269
R32	351.25	424.000	136.34	1.43E+03	0.276	0.241
R123	456.83	550.000	166.00	1.77E+03	0.281	0.273
R125	339.17	573.580	172.52	1.69E+03	0.250	0.270
R124	395.42	560.000	120.00	1.85E+03	0.250	0.270
R134a	374.21	511.900	169.85	1.59E+03	0.237	0.239
R152a	386.41	368.000	154.56	1.19E+03	0.272	0.255
R143a	345.86	431.000	161.34	1.33E+03	0.251	0.253
Methane	190.56	162.660	90.69	4.51E+02	0.011	0.288
Ethane	305.33	206.580	90.35	6.51E+02	0.099	0.285
Ethylene	282.35	214.240	103.99	6.55E+02	0.089	0.280
Propane	369.82	218.500	85.48	7.34E+02	0.153	0.281
Propylene	365.57	223.390	100.00	7.55E+02	0.144	0.274
Butane	425.13	227.840	134.87	7.35E+02	0.199	0.274
Isobutane	407.82	224.360	113.56	7.40E+02	0.183	0.283
Pentane	469.70	232.000	143.47	7.62E+02	0.251	0.263
Hexane	507.60	232.279	177.83	7.62E+02	0.299	0.264
Heptane	540.13	232.000	182.55	7.76E+02	0.349	0.263
Oxygen	154.58	436.140	54.36	1.31E+03	0.025	0.288
Fluorine	144.41	592.860	53.48	1.71E+03	0.054	0.288
Nitrogen	126.19	313.300	63.15	8.67E+02	0.038	0.289
Ammonia	405.40	225.000	195.50	7.33E+02	0.250	0.244
Water	647.13	322.000	273.16	1.00E+03	0.344	0.235
Carbondioxide	304.13	467.600	216.59	1.18E+03	0.239	0.274
Hydrogen	33.19	30.120	13.96	7.69E+01	-0.216	0.305
Acetic acid	591.95	334.179	293.15	1.05E+00	0.447	0.201
Benzene	562.05	305.138	278.70	9.00E-01	0.212	0.271
Ethanol	514.00	274.220	223.15	8.06E-01	0.644	0.240
Methanol	512.50	273.863	176.15	8.10E-01	0.556	0.224
Acetone	508.15	273.000	329.25	7.50E+02	0.304	0.232
1,3-Butadiene	425.00	244.753	164.20	7.64E+02	0.195	0.270
Carbondisulfide	552.00	475.879	243.15	1.34E+03	0.109	0.276
Carbontetrachloride	556.35	559.905	253.15	1.67E+03	0.193	0.272
Cyclopentane	511.76	269.747	193.15	8.21E+02	0.196	0.275
1-Butene	419.60	233.781	195.04	7.05E+02	0.191	0.277

Table A.4: Physical constants used in liquid density model development (Contd.)

Compound	T_c, K	ρ_c, kg/m^3	T_t, K	ρ_t, kg/m^3	ω	Z_c
Cumene	631.10	279.999	177.14	9.60E+02	0.326	0.261
Cyclohexane	553.58	273.653	280.15	7.91E+02	0.212	0.273
Cyclohexene	560.40	282.344	243.15	8.57E+02	0.212	0.272
1-Decene	615.00	215.798	273.15	7.56E+02	0.491	0.250
Ethylbenzene	617.20	283.991	183.10	9.64E+02	0.303	0.263
Indene	687.00	315.142	273.15	1.01E+03	0.334	0.246
Isobutene	417.90	234.759	203.15	6.95E+02	0.194	0.275
Naphthalene	748.40	310.348	333.15	9.93E+02	0.302	0.269
n-Nonane	594.60	234.047	223.15	7.73E+02	0.443	0.252
n-Octane	568.80	232.176	333.15	6.70E+02	0.400	0.256
Toluene	591.80	291.583	178.00	9.71E+02	0.262	0.264
o-Xylene	630.33	287.994	248.00	9.18E+02	0.310	0.263
p-Xylene	616.23	280.124	288.15	8.65E+02	0.321	0.260
Phenanthrene	873.00	321.720	372.38	1.07E+03	0.495	0.222
1-Butanol	563.05	269.537	186.15	8.91E+02	0.593	0.260
Chloroform	536.40	499.694	209.00	1.64E+03	0.218	0.293
Diethyl ether	466.74	264.724	273.15	7.36E+02	0.281	0.263
Ethyl acetate	523.30	308.063	273.15	9.25E+02	0.362	0.252
Ethyl mercaptan	499.15	300.915	273.15	8.62E+02	0.191	0.274
Ethylamine	456.40	247.715	200.50	7.85E+02	0.289	0.270
Ethylene glycol	719.70	324.876	260.15	1.14E+03	0.487	0.246
Hydrogen chloride	324.65	450.687	183.62	1.20E+03	0.132	0.249
Cyclopropane	536.80	275.665	153.15	8.17E+02	0.620	0.252
Methyl acetate	506.85	325.197	198.06	1.05E+03	0.326	0.254
Methyl chloride	416.25	363.480	175.44	1.13E+03	0.153	0.269
Methylamine	430.05	201.679	190.57	7.78E+02	0.292	0.321
Diisopropyl ether	500.30	264.707	293.15	7.28E+02	0.339	0.267
o-Methyl styrene	659.00	290.358	273.00	9.29E+02	0.340	0.260
Ethylene diamine	593.00	291.747	273.15	9.14E+02	0.470	0.340
Ethyl formate	508.45	323.487	273.15	9.48E+02	0.280	0.260
1-Heptanol	633.00	267.126	253.15	8.53E+02	0.570	0.250
1-Hexanol	611.00	268.162	253.15	8.49E+02	0.580	0.260
n-Octanol	652.50	265.775	253.15	8.57E+02	0.580	0.250
Diphenyl ether	766.80	338.384	303.15	1.07E+03	0.440	0.240
Methyl benzoate	692.00	343.813	273.15	1.11E+03	0.420	0.270

Table A.4: Physical constants used in liquid density model development (Contd.)

Compound	T_c, K	ρ_c, kg/m^3	T_t, K	ρ_t, kg/m^3	ω	Z_c
n-Heptylamine	613.00	244.621	273.15	7.91E+02	0.510	0.270
n-Hexylamine	584.00	242.081	253.15	7.97E+02	0.460	0.270
Benzaldehyde	695.00	327.537	290.75	1.05E+03	0.310	0.260
2-Heptanone	611.50	263.100	253.15	8.51E+02	0.420	0.250
n-Propyl mercaptan	536.60	299.845	283.15	8.50E+02	0.230	0.260
1-Butyl acetate	579.00	290.400	273.15	9.02E+02	0.440	0.250
Isopentane	460.98	236.100	149.87	7.53E+02	0.230	0.270
n-Butylamine	531.90	235.925	293.15	7.41E+02	0.330	0.290
2-Butanol	536.20	275.545	293.15	8.07E+02	0.577	0.250

Table A.5: Ranges of vapor density data used in model development

Compound	Temperature Range, K	Density Range, kg/m^3	No. of pts.
R-22	149.96 - 369.30	0.010 - 523.400	201
R-32	148.16 - 351.25	0.010 - 424.000	201
R-123	192.17 - 456.83	0.010 - 550.000	201
R-125	172.52 - 339.17	0.244 - 573.580	201
R-124	166.82 - 395.43	0.011 - 560.000	201
R-134a	169.85 - 374.21	0.028 - 511.900	201
R-152a	163.83 - 386.41	0.010 - 368.000	201
R-143a	161.34 - 345.86	0.067 - 431.000	201
Methane	90.69 - 190.56	0.250 - 162.660	201
Ethane	120.45 - 305.33	0.011 - 206.580	201
Ethylene	110.23 - 282.35	0.010 - 214.240	201
Propane	150.88 - 369.82	0.011 - 218.500	201
Propylene	147.80 - 365.57	0.011 - 223.390	201
Butane	178.41 - 425.12	0.011 - 227.840	201
Isobutane	169.47 - 407.82	0.010 - 224.360	201
Pentane	202.19 - 469.70	0.010 - 232.000	201
Hexane	224.03 - 507.82	0.010 - 233.180	201
Heptane	245.13 - 540.13	0.010 - 232.000	201
Oxygen	54.36 - 154.58	0.010 - 436.140	201
Fluorine	53.48 - 144.41	0.020 - 592.860	201
Nitrogen	63.15 - 126.19	0.674 - 313.300	201
Ammonia	195.50 - 405.40	0.064 - 225.000	201
Water	284.30 - 647.10	0.010 - 322.000	201
Carbondioxide	216.59 - 304.13	13.761 - 467.600	201
Hydrogen	13.95 - 33.19	0.136 - 30.120	199
Benzene	298.09 - 561.70	0.398 - 276.367	62
Carbonmonoxide	68.13 - 132.80	0.769 - 303.920	191

Table A.6: Physical constants used in vapor density model development

Compound	T_c, K	ρ_c, kg/m^3	T_t, K	ρ_t, kg/m^3	ω	Z_c
R-22	369.30	523.840	149.96	1.08E-02	0.183	0.276
R-32	351.25	424.000	148.16	1.09E-02	0.276	0.241
R-123	456.83	550.000	192.17	1.08E-02	0.281	0.273
R-125	339.17	573.580	172.52	2.45E-01	0.250	0.270
R-124	395.43	560.000	166.82	1.12E-02	0.250	0.270
R-134a	374.21	511.900	169.85	2.82E-02	0.237	0.239
R-152a	386.41	368.000	163.83	1.00E-02	0.272	0.255
R-143a	345.86	431.000	161.34	6.75E-02	0.251	0.253
Methane	190.56	162.660	90.69	2.51E-01	0.011	0.288
Ethane	305.33	206.580	120.45	1.13E-02	0.099	0.285
Ethylene	282.35	214.240	110.23	1.05E-02	0.089	0.280
Propane	369.82	218.500	150.88	1.10E-02	0.153	0.281
Propylene	365.57	223.390	147.80	1.10E-02	0.144	0.274
Butane	425.12	227.840	178.41	1.14E-02	0.199	0.274
Isobutane	407.82	224.360	169.47	1.04E-02	0.183	0.283
Pentane	469.70	232.000	202.19	1.04E-02	0.251	0.263
Hexane	507.82	233.180	224.03	1.02E-02	0.299	0.264
Heptane	540.13	232.000	245.13	1.05E-02	0.349	0.263
Oxygen	154.58	436.140	54.36	1.04E-02	0.025	0.288
Fluorine	144.41	592.860	53.48	2.04E-02	0.054	0.288
Nitrogen	126.19	313.300	63.15	6.74E-01	0.038	0.289
Ammonia	405.40	225.000	195.50	6.41E-02	0.250	0.244
Water	647.10	322.000	284.30	1.01E-02	0.344	0.235
Carbondioxide	304.13	467.600	216.59	1.38E+01	0.239	0.274
Hydrogen	33.19	30.120	13.96	1.36E-01	-0.216	0.305
Benzene	561.70	276.367	298.10	3.98E-01	0.212	0.271
Carbonmonoxide	132.80	303.920	68.13	7.69E-01	0.066	0.295

APPENDIX B

THE NRTL-QSPR AND THE UNIQUAC-QSPR MODEL: DATABASE DESCRIPTION, PHYSICAL CONSTANTS AND MODEL RESULTS

Table B.1: Alias names of compounds

Compound No.	Alias	Compound
1	MEO	methanol
2	TBA	teritiary butyl alcohol
3	MTBE	methyl teritiary butyl ether
4	NC4	butane
5	IC5	isopentane
6	MCYC6	methyl cyclohexane
7	ETH	ethanol
8	ETBE	ethyl teritiary butyl ether
9	TAME	teritiary amyl methyl ether
10	TOH	teritiary amyl alcohol
12	NC5	n-pentane
13	H2O	water
14	NC7	n-heptane
15	DEE	diethyl ether
16	1C7-	1-heptene
17	IC5-	isopentene
18	ACTN	acetonitrile
19	13BD	1,3-butadiene
20	IC4-	isobutene
21	PPN	propionitrile
22	2M2B	2-methyl 2-butene
23	IC4	isobutane
24	DISB	diisobutylene
25	C2B-	cis, 2-butene
26	T2B-	trans, 2-butene
27	2M1B	2-methyl 1-butene
28	DMDS	dimethyl disulfide
29	MEM	methyl mercaptan
30	DMS	dimethyl sulfide
31	TOL	toluene
32	ETHBENZ	ethylbenzene
33	PXYL	p-xylene
34	CYC6	cyclohexane
35	BENZ	benzene
36	CYC5	cyclopentane

Table B.1: Alias names of compounds (Contd.)

Compound No.	Alias	Compound
37	TETCHMETH	tetrachloromethane
38	4M2P	4-methyl 2-pentanone
39	2PENT	2-pentanone
40	ACETONE	acetone
41	2BUTANONE	2-butanone
42	THIOPHENE	thiophene
43	DIPE	diisopropyl ether
44	3PENTANONE	3-pentanone
45	FURF	furfural
46	12DICHMETH	1,2-dichloromethane
47	DIETHAMINE	diethylamine
48	TRIETHAMINE	triethylamine
49	ACRYL	acrylonitrile
50	NITROBENZ	nitrobenzene
51	BUTYLCH	butylchloride
52	CHLOROFORM	chloroform
53	NITROMETH	nitromethane
54	TBUT	teritiary butanol
55	2PROP	2-propanol
56	ETHIOD	ethyl iodide
57	PYRD	pyridine
58	1BUT	1-butanol
59	1PROP	1-propanol
60	VIACETATE	vinyl acetate
61	PROPACETATE	propyl acetate
62	METHACETATE	methyl acetate
63	DME	dimethyl ether
64	METHIOD	methyl iodide
65	DICHMETH	dichloromethane
66	2M1P	2-methyl 1-propanol
67	12DICHETH	1,2-dichloroethane
68	PROPOX	propylene oxide
69	NC10	n-decane
70	BENZALD	benzaldehyde
71	BENZACETATE	benzyl acetate
72	ETHACETATE	ethyl acetate

Table B.1: Alias names of compounds (Contd.)

Compound No.	Alias	Compound
73	112TRICHETH	1,1,2-trichloroethane
74	CYCHEXANONE	cyclohexanone
75	NC8	n-octane
76	HFBENZ	hexafluorobenzene
77	14DIOX	1,4-dioxane
78	PROPANAL	propionic aldehyde
79	BUTYRALD	butyraldehyde
80	METHAMINE	methylamine
81	BROMOBENZ	bromobenzene
82	NITROETH	nitroethane
83	ETHDIAMINE	ethylenediamine
84	4 HEPTANONE	4-heptanone
85	TETCHETHY	tetrachloroethylene
86	CS2	carbondisulfide
87	BUTAMINE	butylamine
88	ACETALD	acetaldehyde
89	3HEXANONE	3-hexanone
90	23DMETHBUT	2,3-dimethylbutane
91	C13P	cis, 1,3-pentadiene
92	T13P	trans, 1,3-pentadiene

Table B.2: Ranges of VLE data used in the NRTL-QSPR and the UNIQUAC-QSPR model development

System No.	System	Temperature Range, K	Pressure Range, bar	First component mole fraction range		Reference
				Liquid	Vapor	
1	MTBE + MEO	298.15 - 417.85	0.170 - 10.000	0.000 - 1.000	0.000 - 1.000	1, 2, 3, 4, 5, 6
2	MTBE + TBA	324.65 - 355.75	1.010 - 1.010	0.000 - 1.000	0.000 - 1.000	3, 7
3	DME + MTBE	298.15 - 348.15	0.340 - 19.800	0.000 - 1.000	0.000 - 1.000	15
4	MTBE + NC4	273.15 - 373.15	0.110 - 15.180	0.000 - 1.000	0.000 - 1.000	8
5	MTBE + IC5	288.15 - 421.95	0.220 - 18.350	0.000 - 1.000	0.000 - 1.000	8
6	MTBE + MCYC6	266.15 - 333.15	0.010 - 0.510	0.000 - 0.271	0.000 - 0.702	44
7	IC4- + MTBE	323.15 - 353.15	0.850 - 12.240	0.000 - 1.000	0.000 - 1.000	8, 12
8	ETBE + ETH	343.15 - 363.15	0.940 - 2.420	0.057 - 0.884	0.161 - 0.795	8
9	TBA + ETBE	323.15 - 423.15	0.240 - 8.680	0.000 - 1.000	0.000 - 1.000	8
10	IC5 + ETBE	293.15 - 303.15	0.130 - 1.090	0.000 - 1.000	0.000 - 1.000	47
11	MCYC6 + ETBE	323.15 - 443.15	0.190 - 10.130	0.000 - 1.000	0.000 - 1.000	8
12	IC4- + ETBE	323.15 - 373.15	0.460 - 18.380	0.000 - 1.000	0.000 - 1.000	8
13	MEO + TAME	289.25 - 448.15	0.130 - 24.850	0.000 - 1.000	0.000 - 1.000	9, 10, 11
14	TAME + TOH	363.15 - 393.15	0.650 - 1.890	0.000 - 0.045	0.000 - 1.000	13
15	TOH + TAME	363.15 - 393.15	1.110 - 2.490	0.000 - 0.065	0.000 - 0.000	13
16	TAME + NC5	343.15 - 383.15	0.600 - 7.380	0.000 - 1.000	0.000 - 1.000	13
17	TAME + MCYC6	293.15 - 333.15	0.050 - 0.420	0.000 - 1.000	0.000 - 1.000	45
18	DME + MEO	273.15 - 293.15	0.040 - 5.210	0.000 - 1.000	0.000 - 1.000	39
19	DEE + H2O	298.15 - 308.15	0.030 - 1.050	0.000 - 1.000	0.000 - 1.000	28, 29
20	MEO + ETH	298.15 - 351.90	0.080 - 1.020	0.000 - 1.000	0.000 - 1.000	36, 37, 38
21	NC4 + MEO	273.15 - 373.15	0.040 - 17.180	0.000 - 1.000	0.000 - 1.000	14, 15

Table B.2: Ranges of VLE data used in the NRTL-QSPR and the UNIQUAC-QSPR model development (Contd.)

System No.	System	Temperature Range, K	Pressure Range, bar	First component mole fraction range		Reference
				Liquid	Vapor	
22	MEO + NC7	331.95 - 371.55	1.010 - 1.010	0.000 - 1.000	0.000 - 1.000	32, 33, 34
23	IC4 + MEO	273.15 - 423.15	0.040 - 46.790	0.000 - 1.000	0.000 - 1.000	40, 7
24	NC5 + MEO	303.31 - 335.37	1.000 - 1.010	0.001 - 1.000	0.050 - 1.000	33, 35
25	NC5- + MEO	299.45 - 337.85	1.010 - 1.010	0.000 - 1.000	0.000 - 1.000	41
26	IC5- + MEO	306.20 - 337.85	1.010 - 1.010	0.000 - 1.000	0.000 - 1.000	41
27	ISOPRENE + MEO	303.15 - 337.85	0.990 - 1.010	0.000 - 1.000	0.000 - 1.000	16, 17
28	ISOPRENE + DEE	303.35 - 307.75	1.010 - 1.010	0.000 - 0.400	0.001 - 0.467	46
29	MEO + 1C7-	331.75 - 366.75	1.010 - 1.010	0.000 - 1.000	0.000 - 1.000	31
30	MEO + H2O	307.11 - 373.15	0.270 - 1.010	0.000 - 1.000	0.000 - 1.000	18, 19
31	NC4 + ETH	298.45 - 345.65	0.080 - 8.810	0.000 - 1.000	0.000 - 1.000	20
32	ETH + H2O	298.15 - 373.15	0.030 - 1.010	0.000 - 1.000	0.000 - 1.000	21, 22, 42, 43
33	NC6 + TBA	313.15 - 355.57	0.140 - 1.010	0.000 - 1.000	0.000 - 1.000	23, 24
34	TBA + NC7	313.15 - 348.15	0.120 - 0.880	0.000 - 1.000	0.000 - 1.000	24, 25
35	NC8 + TBA	313.15 - 313.15	0.040 - 0.140	0.000 - 1.000	0.000 - 0.000	24
36	TBA + IC5	303.15 - 373.15	0.080 - 7.230	0.000 - 1.000	0.000 - 1.000	8
37	TBA + IC5-	303.15 - 373.15	0.080 - 5.700	0.000 - 1.000	0.000 - 1.000	8
38	ISOPRENE + TBA	307.25 - 355.70	1.010 - 1.010	0.000 - 1.000	0.000 - 1.000	8
39	TBA + H2O	298.15 - 373.15	0.030 - 1.010	0.000 - 1.000	0.000 - 1.000	26, 27
40	TOH + NC5	343.15 - 383.15	0.270 - 7.370	0.000 - 1.000	0.000 - 1.000	13
41	MTB + ACTN	313.15 - 313.15	0.230 - 0.610	0.000 - 1.000	0.000 - 1.000	49
42	MTB + 13BD	273.15 - 323.15	0.110 - 5.620	0.000 - 1.000	0.000 - 1.000	48

Table B.2: Ranges of VLE data used in the NRTL-QSPR and the UNIQUAC-QSPR model development (Contd.)

System No.	System	Temperature Range, K	Pressure Range, bar	First component mole fraction range		Reference
				Liquid	Vapor	
43	MEO + TBA	298.15 - 355.55	0.060 - 1.010	0.000 - 1.000	0.000 - 1.000	26, 50, 51, 52, 53
44	MEO + IC4-	323.15 - 323.15	0.550 - 6.310	0.000 - 1.000	0.000 - 1.000	12
45	MEO + ACTN	298.15 - 354.75	0.130 - 1.010	0.000 - 1.000	0.000 - 1.000	54, 55, 56, 57, 58
46	MEO + PPN	337.85 - 370.50	1.010 - 1.010	0.000 - 1.000	0.000 - 1.000	57
47	ETH + TBA	313.15 - 355.75	0.140 - 1.010	0.000 - 1.000	0.000 - 1.000	59, 60
48	TOH + H2O	360.35 - 375.05	1.010 - 1.010	0.099 - 1.000	0.381 - 1.000	61
49	NC4 + TBA	333.15 - 433.15	3.650 - 38.890	0.084 - 0.930	0.303 - 0.981	62
50	NC4 + NC5	298.15 - 298.15	0.730 - 1.080	0.017 - 0.187	0.000 - 0.594	63
51	NC5 + ETH	293.15 - 422.60	0.060 - 19.630	0.000 - 1.000	0.000 - 1.000	64, 65, 65
52	NC5 + 2M2B	273.15 - 298.15	0.210 - 0.680	0.000 - 1.000	0.000 - 0.000	67
53	NC5 + ACTN	333.15 - 363.15	0.490 - 5.570	0.000 - 1.000	0.000 - 0.000	68, 69
54	IC4 + NC4	273.15 - 273.15	1.040 - 1.570	0.000 - 1.000	0.000 - 1.000	70
55	IC4- + NC4	277.59 - 344.26	1.220 - 10.090	0.000 - 1.000	0.000 - 0.000	71
56	IC4- + IC4	277.59 - 344.26	1.550 - 11.130	0.000 - 1.000	0.000 - 0.000	71
57	1C4- + NC4	310.93 - 410.93	3.550 - 34.890	0.000 - 1.000	0.000 - 1.000	72, 73
58	1C4- + IC4	277.62 - 344.36	1.620 - 10.890	0.251 - 0.753	0.000 - 0.000	74
59	1C4- + 13BD	277.61 - 344.38	1.460 - 9.880	0.000 - 1.000	0.000 - 1.000	72, 74
60	C2B- + NC4	278.15 - 358.15	1.140 - 11.210	0.106 - 0.735	0.000 - 0.000	76
61	T2B- + NC4	278.15 - 358.15	1.220 - 11.300	0.099 - 0.751	0.000 - 0.000	76
62	2M1B + MEO	300.53 - 317.85	1.010 - 1.010	0.050 - 0.890	0.536 - 0.837	30, 41
63	2M1B + NC5	273.15 - 298.15	0.250 - 0.810	0.000 - 1.000	0.000 - 0.000	67

Table B.2: Ranges of VLE data used in the NRTL-QSPR and the UNIQUAC-QSPR model development (Contd.)

System No.	System	Temperature Range, K	Pressure Range, bar	First component mole fraction range		Reference
				Liquid	Vapor	
64	2M1B + 2M2B	273.15 - 308.80	0.210 - 0.990	0.000 - 1.000	0.000 - 0.629	67, 77
65	2M2B + MEO	305.80 - 337.85	1.010 - 1.010	0.000 - 1.000	0.000 - 1.000	30, 33
66	2M2B + ETH	309.95 - 351.83	1.010 - 1.010	0.000 - 1.000	0.000 - 0.000	78
67	2M2B + ACTN	309.25 - 416.96	1.010 - 5.230	0.000 - 1.000	0.000 - 1.000	79, 80
68	ACTN + ETH	293.15 - 393.15	0.060 - 4.490	0.000 - 1.000	0.000 - 1.000	57, 81, 82, 83, 84, 85
69	ACTN + TBA	333.15 - 355.55	0.390 - 1.010	0.000 - 1.000	0.000 - 1.000	86, 87
70	ACTN + NC4	425.40 - 545.50	37.970 - 48.300	0.000 - 1.000	0.000 - 1.000	88
71	ACTN + DISB	313.15 - 313.15	0.120 - 0.320	0.000 - 1.000	0.000 - 0.000	89
72	ACTN + H2O	323.15 - 333.15	0.120 - 0.560	0.000 - 1.000	0.000 - 1.000	81, 82
73	PPN + NC5	467.70 - 553.70	36.30 - 45.700	0.100 - 0.958	0.000 - 0.000	90
74	PPN + H2O	359.15 - 371.05	1.010 - 1.010	0.001 - 0.975	0.073 - 0.871	91
75	13BD + MEO	323.15 - 323.15	0.550 - 5.820	0.000 - 1.000	0.000 - 1.000	12
76	13BD + NC4	310.93 - 338.71	3.550 - 8.360	0.000 - 1.000	0.000 - 1.000	72
77	13BD + IC4	277.54 - 344.04	1.630 - 10.990	0.247 - 0.747	0.000 - 0.000	74
78	13BD + C2B-	278.15 - 338.15	1.100 - 7.830	0.088 - 0.749	0.000 - 0.000	76
79	13BD + T2B-	278.15 - 338.15	1.200 - 8.190	0.052 - 0.951	0.000 - 0.000	76
80	13BD + ACTN	304.71 - 330.18	0.730 - 6.390	0.056 - 0.913	0.000 - 0.000	109
81	C13P + MEO	311.15 - 337.85	1.010 - 1.010	0.000 - 1.000	0.000 - 1.000	33
82	T13P + MEO	309.63 - 337.85	1.010 - 1.010	0.000 - 1.000	0.000 - 1.000	30, 33
83	T13P + ACTN	303.15 - 313.15	0.360 - 0.950	0.100 - 0.900	0.000 - 0.000	93
84	TBA + 2M1B	303.15 - 373.15	0.080 - 7.230	0.000 - 1.000	0.000 - 1.000	94

Table B.2: Ranges of VLE data used in the NRTL-QSPR and the UNIQUAC-QSPR model development (Contd.)

System No.	System	Temperature Range, K	Pressure Range, bar	First component mole fraction range		Reference
				Liquid	Vapor	
85	TBA + 2M2B	303.15 - 373.15	0.080 - 5.700	0.000 - 1.000	0.000 - 1.000	94
86	DME + MEO	273.15 - 293.15	0.040 - 5.210	0.000 - 1.000	0.000 - 1.000	39
87	MEO + H2O	307.11 - 373.15	0.270 - 1.010	0.000 - 1.000	0.000 - 1.000	18, 19
88	MEM + MEO	269.15 - 288.15	0.030 - 1.430	0.000 - 1.000	0.000 - 0.000	39
89	DMS + MEO	263.15 - 288.15	0.020 - 0.460	0.000 - 1.000	0.000 - 0.000	83
90	H2S + MEO	298.15 - 348.15	0.170 - 58.000	0.000 - 1.000	0.000 - 1.000	75
91	MEO + DMDS	310.95 - 335.95	0.070 - 0.960	0.000 - 1.000	0.000 - 1.000	65
92	MEM + H2O	323.06 - 372.65	0.120 - 5.020	0.000 - 0.008	0.000 - 0.000	95
93	DMDS + MEM	273.15 - 373.15	0.010 - 14.450	0.000 - 1.000	0.000 - 1.000	96
94	H2S + MEM	305.35 - 321.35	22.770 - 25.930	0.775 - 0.991	0.949 - 0.999	16
95	H2S + DMS	313.71 - 313.71	5.370 - 16.210	0.221 - 0.619	0.813 - 0.962	4
96	MEM + DMS	263.15 - 368.23	0.170 - 12.420	0.082 - 0.950	0.000 - 0.982	4, 15
97	BENZ + TOL	353.25 - 383.76	1.010 - 1.010	0.000 - 1.000	0.000 - 1.000	97
98	NC7 + ETHBENZ	327.76 - 327.76	0.060 - 0.230	0.000 - 1.000	0.000 - 1.000	97
99	NC8 + ETHBENZ	398.85 - 409.35	1.010 - 1.010	0.000 - 1.000	0.000 - 1.000	97
100	1C7- + TOL	328.15 - 328.15	0.150 - 0.270	0.000 - 1.000	0.000 - 1.000	97
101	NC7 + PXYL	313.11 - 313.11	0.030 - 0.120	0.000 - 1.000	0.000 - 1.000	97
102	BENZ + CYC6	313.15 - 313.15	0.240 - 0.270	0.000 - 1.000	0.000 - 1.000	97
103	MCYC5 + BENZ	313.14 - 313.14	0.240 - 0.340	0.000 - 1.000	0.000 - 1.000	97
104	CYC6 + TOL	298.15 - 298.15	0.040 - 0.130	0.000 - 1.000	0.000 - 1.000	97
105	ISOPRENE + 2M2B	307.22 - 311.72	1.010 - 1.010	0.000 - 1.000	0.000 - 1.000	97

Table B.2: Ranges of VLE data used in the NRTL-QSPR and the UNIQUAC-QSPR model development (Contd.)

System No.	System	Temperature Range, K	Pressure Range, bar	First component mole fraction range		Reference
				Liquid	Vapor	
106	HFBENZ + TOL	303.15 - 303.15	0.050 - 0.140	0.000 - 1.000	0.000 - 1.000	97
107	TETCHMETH + BENZ	349.68 - 353.18	1.010 - 1.010	0.000 - 1.000	0.000 - 1.000	97
108	CS2 + CYC6	298.15 - 298.15	0.130 - 0.480	0.000 - 1.000	0.000 - 1.000	97
109	CS2 + CYC5	288.15 - 288.15	0.280 - 0.340	0.000 - 1.000	0.000 - 1.000	97
110	CS2 + TETCHMETH	298.15 - 298.15	0.160 - 0.470	0.031 - 0.962	0.105 - 0.984	97
111	HFBENZ + PXYL	313.15 - 313.15	0.030 - 0.220	0.000 - 1.000	0.000 - 1.000	97
112	HFBENZ + CYC6	303.15 - 303.15	0.140 - 0.210	0.000 - 1.000	0.000 - 1.000	97
113	TOL + 4M2P	323.15 - 323.15	0.090 - 0.120	0.000 - 1.000	0.000 - 1.000	97
114	TOL + 2PENT	323.15 - 323.15	0.120 - 0.160	0.000 - 1.000	0.000 - 1.000	97
115	BENZ + ACETONE	329.33 - 353.25	1.010 - 1.010	0.000 - 1.000	0.000 - 1.000	97
116	BENZ + 2BUTANONE	389.65 - 392.75	3.080 - 3.080	0.100 - 0.900	0.109 - 0.885	97
117	BENZ + THIOPHENE	328.15 - 328.15	0.380 - 0.440	0.000 - 1.000	0.000 - 1.000	97
118	HFBENZ + DIPE	298.13 - 298.13	0.110 - 0.200	0.000 - 1.000	0.000 - 1.000	97
119	TETCHMETH + 2BUTANONE	346.85 - 352.70	1.010 - 1.010	0.000 - 1.000	0.000 - 1.000	97
120	CYC6 + 2BUTANONE	344.75 - 353.95	1.010 - 1.010	0.000 - 1.000	0.000 - 1.000	97
121	NC7 + THIOPHENE	328.15 - 328.15	0.230 - 0.390	0.000 - 1.000	0.000 - 1.000	97
122	NC7 + 3PENTANONE	353.15 - 353.15	0.500 - 0.670	0.000 - 1.000	0.000 - 1.000	97
123	NC7 + 2BUTANONE	350.15 - 371.45	1.010 - 1.010	0.000 - 1.000	0.000 - 1.000	97
124	NC10 + ACETONE	333.15 - 333.15	0.020 - 1.150	0.000 - 1.000	0.000 - 1.000	97
125	TETCHMETH + FURF	350.15 - 434.85	1.010 - 1.010	0.000 - 1.000	0.000 - 1.000	97
126	TETCHMETH + ACETONE	304.35 - 321.92	0.400 - 0.400	0.000 - 1.000	0.000 - 1.000	97

Table B.2: Ranges of VLE data used in the NRTL-QSPR and the UNIQUAC-QSPR model development (Contd.)

System No.	System	Temperature Range, K	Pressure Range, bar	First component mole fraction range		Reference
				Liquid	Vapor	
127	BENZ + 12DICHMETH	353.25 - 356.62	1.010 - 1.010	0.000 - 1.000	0.000 - 1.000	97
128	TOL + 12DICHMETH	356.60 - 383.76	1.010 - 1.010	0.000 - 1.000	0.000 - 1.000	97
129	BENZ + DIETHAMINE	328.15 - 328.15	0.440 - 1.000	0.000 - 1.000	0.000 - 1.000	97
130	BENZ + TRIETHAMINE	353.15 - 353.15	0.760 - 1.010	0.000 - 1.000	0.000 - 1.000	97
131	ETHBENZ + ACRYL	282.95 - 330.85	0.070 - 0.070	0.000 - 1.000	0.000 - 1.000	97
132	TOL + NITROBENZ	373.15 - 373.15	0.030 - 0.750	0.000 - 1.000	0.000 - 1.000	97
133	NC7 + BUTYLCH	323.15 - 323.15	0.190 - 0.390	0.000 - 1.000	0.000 - 1.000	97
134	CYC5 + CHLOROFORM	298.15 - 298.15	0.260 - 0.420	0.000 - 1.000	0.000 - 1.000	97
135	NC7 + TRIETHAMINE	333.15 - 333.15	0.280 - 0.390	0.000 - 1.000	0.000 - 1.000	97
136	23DMETHBUT + CHLOROFORM	328.65 - 333.95	1.010 - 1.010	0.000 - 1.000	0.000 - 1.000	97
137	ETHBENZ + NITROBENZ	373.15 - 373.15	0.030 - 0.340	0.000 - 1.000	0.000 - 1.000	97
138	BENZ + NITROMETH	318.15 - 318.15	0.130 - 0.300	0.000 - 1.000	0.000 - 1.000	97
139	BENZ + TBUT	318.15 - 318.15	0.180 - 0.340	0.000 - 1.000	0.000 - 1.000	97
140	BENZ + ETH	324.35 - 335.65	0.530 - 0.530	0.000 - 1.000	0.000 - 1.000	97
141	BENZ + 2PROP	344.28 - 355.53	1.010 - 1.010	0.000 - 1.000	0.000 - 1.000	97
142	NC7 + ETHIOD	323.15 - 323.15	0.190 - 0.470	0.000 - 1.000	0.000 - 1.000	97
143	CYC6 + PYRD	353.15 - 388.45	1.010 - 1.010	0.000 - 1.000	0.000 - 1.000	97
144	NC8 + PYRD	353.15 - 353.15	0.230 - 0.390	0.000 - 1.000	0.000 - 1.000	97
145	NC8 + MEO	335.85 - 398.75	1.010 - 1.010	0.000 - 1.000	0.000 - 1.000	97
146	CYC6 + ETH	308.15 - 308.15	0.140 - 0.300	0.000 - 1.000	0.000 - 1.000	97
147	NC5 + 1BUT	303.15 - 303.15	0.010 - 0.820	0.000 - 1.000	0.000 - 1.000	97

Table B.2: Ranges of VLE data used in the NRTL-QSPR and the UNIQUAC-QSPR model development (Contd.)

System No.	System	Temperature Range, K	Pressure Range, bar	First component mole fraction range		Reference
				Liquid	Vapor	
148	TETCHETHY + ETH	350.85 - 394.25	1.010 - 1.010	0.000 - 1.000	0.000 - 1.000	97
149	HFBENZ + 1PROP	288.15 - 288.15	0.020 - 0.080	0.000 - 1.000	0.000 - 1.000	97
150	HFBENZ + MEO	288.15 - 288.15	0.070 - 0.150	0.000 - 1.000	0.000 - 1.000	97
151	PROPANAL + ACETONE	321.13 - 329.35	1.010 - 1.010	0.000 - 1.000	0.000 - 1.000	97
152	PROPANAL + 2BUTANONE	318.15 - 318.15	0.300 - 0.910	0.000 - 1.000	0.000 - 1.000	97
153	ACETONE + VIACETATE	329.45 - 345.80	1.010 - 1.010	0.000 - 1.000	0.000 - 1.000	97
154	ACETALD + PROPACETATE	330.85 - 372.15	1.010 - 1.010	0.020 - 0.960	0.090 - 0.990	97
155	ACETALD + VIACETATE	293.50 - 345.71	1.010 - 1.010	0.000 - 1.000	0.000 - 1.000	97
156	ACETALD + METHACETATE	293.50 - 330.05	1.010 - 1.010	0.000 - 1.000	0.000 - 1.000	97
157	DEE + ACETONE	303.15 - 303.15	0.380 - 0.860	0.000 - 1.000	0.000 - 1.000	97
158	ACETALD + DEE	292.80 - 307.80	1.010 - 1.010	0.000 - 1.000	0.000 - 1.000	97
159	DEE + METHIOD	308.15 - 308.15	0.780 - 1.030	0.000 - 1.000	0.000 - 1.000	97
160	DEE + DICHMETH	307.10 - 313.35	0.990 - 0.990	0.000 - 1.000	0.000 - 1.000	97
161	14DIOX + 2PROP	355.65 - 372.65	1.010 - 1.010	0.036 - 0.955	0.033 - 0.900	97
162	EPE + CHLOROFORM	316.05 - 322.20	0.530 - 0.530	0.000 - 1.000	0.000 - 1.000	97
163	DEE + CHLOROFORM	310.45 - 333.45	1.000 - 1.000	0.056 - 0.87	0.064 - 0.972	97
164	ACETONE + CHLOROFORM	308.15 - 308.15	0.340 - 0.460	0.000 - 1.000	0.000 - 1.000	97
165	PROPACETATE + 1PROP	361.21 - 367.14	0.800 - 0.800	0.000 - 1.000	0.000 - 1.000	97
166	ETHACETATE + 2PROP	333.15 - 333.15	0.420 - 0.580	0.045 - 0.922	0.1254 - 0.9	97
167	DEE + ETH	273.15 - 273.15	0.050 - 0.240	0.050 - 0.950	0.679 - 0.986	97
168	FURF + ETH	338.15 - 338.15	0.070 - 0.560	0.020 - 0.980	0.005 - 0.351	97

Table B.2: Ranges of VLE data used in the NRTL-QSPR and the UNIQUAC-QSPR model development (Contd.)

System No.	System	Temperature Range, K	Pressure Range, bar	First component mole fraction range		Reference
				Liquid	Vapor	
169	ACETONE + MEO	328.15 - 328.15	0.690 - 1.000	0.000 - 1.000	0.000 - 1.000	97
170	14DIOX + MEO	308.15 - 308.15	0.080 - 0.280	0.000 - 1.000	0.000 - 1.000	97
171	ETH + TRIETHAMINE	308.00 - 308.00	0.140 - 0.160	0.000 - 1.000	0.000 - 1.000	97
172	TBUT + 1BUT	312.57 - 343.06	0.130 - 0.130	0.000 - 1.000	0.000 - 1.000	97
173	1PROP + 2M1P	343.15 - 343.15	0.210 - 0.330	0.000 - 1.000	0.000 - 1.000	97
174	ETH + 2PROP	351.61 - 355.54	1.010 - 1.010	0.000 - 1.000	0.000 - 1.000	97
175	MEO + 2M1P	323.15 - 323.15	0.070 - 0.560	0.000 - 1.000	0.000 - 1.000	97
176	ETH + 2M1P	333.15 - 333.15	0.130 - 0.470	0.000 - 1.000	0.000 - 1.000	97
177	BUTAMINE + 1BUT	313.15 - 313.15	0.030 - 0.250	0.000 - 1.000	0.000 - 1.000	97
178	DIETHAMINE + ETH	313.15 - 313.15	0.190 - 0.570	0.000 - 1.000	0.000 - 1.000	97
179	ETH + ACTN	313.15 - 313.15	0.180 - 0.280	0.000 - 1.000	0.000 - 1.000	97
180	BUTAMINE + 1PROP	318.15 - 318.15	0.090 - 0.310	0.000 - 1.000	0.000 - 1.000	97
181	BROMOBENZ + CYC6	383.15 - 383.15	0.170 - 0.280	0.000 - 1.000	0.000 - 1.000	97
182	12DICHETH + 2M1P	323.15 - 323.15	0.070 - 0.310	0.000 - 1.000	0.000 - 1.000	97
183	MEO + 12DICHETH	313.15 - 313.15	0.200 - 0.440	0.000 - 1.000	0.000 - 1.000	97
184	H2O + DIETHAMINE	311.50 - 311.50	0.070 - 0.540	0.000 - 1.000	0.000 - 1.000	97
185	H2O + PYRD	362.98 - 362.98	0.460 - 0.870	0.000 - 1.000	0.000 - 1.000	97
186	H2O + MEO	337.65 - 373.15	1.010 - 1.010	0.000 - 1.000	0.000 - 1.000	97
187	H2O + 2PROP	308.93 - 323.86	0.130 - 0.130	0.000 - 1.000	0.000 - 1.000	97
188	H2O + ETH	351.27 - 369.25	1.010 - 1.010	0.105 - 0.985	0.105 - 0.8575	97
189	ACETALD + PROPOX	293.15 - 308.15	1.010 - 1.010	0.000 - 1.000	0.000 - 1.000	98

Table B.2: Ranges of VLE data used in the NRTL-QSPR and the UNIQUAC-QSPR model development (Contd.)

System No.	System	Temperature Range, K	Pressure Range, bar	First component mole fraction range		Reference
				Liquid	Vapor	
190	ACETALD + BENZ	293.95 - 353.25	1.010 - 1.010	0.000 - 1.000	0.000 - 1.000	98
191	PROPANAL + CYC6	318.15 - 318.15	0.300 - 0.920	0.000 - 1.000	0.000 - 1.031	98
192	CHLOROFORM + FURF	336.05 - 424.35	1.010 - 1.010	0.040 - 0.929	0.296 - 0.999	98
193	1C4- + FURF	310.95 - 324.85	1.010 - 5.270	0.032 - 0.312	0.984 - 0.999	98
194	TOL + FURF	384.45 - 426.45	1.010 - 1.010	0.027 - 0.953	0.2507 - 0.983	98
195	ETHBENZ + FURF	405.45 - 427.65	0.960 - 0.960	0.035 - 0.979	0.1383 - 0.974	98
196	PXYL + FURF	407.35 - 428.95	0.960 - 0.960	0.022 - 0.962	0.096 - 0.954	98
197	NC5 + ACETONE	238.15 - 322.30	0.010 - 1.010	0.000 - 1.000	0.000 - 1.000	98
198	FURF + NC10	420.35 - 437.55	1.010 - 1.010	0.074 - 0.978	0.300 - 0.865	98
199	TOL + BENZALD	327.55 - 370.05	0.130 - 0.130	0.100 - 0.900	0.553 - 0.985	98
200	BENZALD + BENZACETATE	392.55 - 414.85	0.130 - 0.130	0.082 - 0.830	0.255 - 0.974	98
201	ACETONE + TETCHMETH	304.35 - 349.85	0.400 - 1.010	0.000 - 1.000	0.000 - 1.000	98
202	CS2 + ACETONE	273.15 - 308.32	0.090 - 0.890	0.000 - 1.000	0.000 - 0.903	98
203	ACETONE +ACTN	318.15 - 318.15	0.300 - 0.640	0.052 - 0.896	0.120 - 0.951	98
204	ACETONE + 12DICHETH	329.26 - 356.56	1.000 - 1.010	0.000 - 1.000	0.000 - 1.000	98
205	ACETONE + ETHIOD	293.15 - 293.15	0.190 - 0.270	0.090 - 0.950	0.000 - 0.000	98
206	METHACETATE + ACETONE	328.55 - 329.45	1.010 - 1.010	0.105 - 0.933	0.125 - 0.912	98
207	ACETONE + METHACETATE	293.15 - 329.65	0.230 - 1.010	0.027 - 0.965	0.033 - 0.964	98
208	ACETONE + 2BUTANONE	330.05 - 395.15	1.010 - 3.450	0.019 - 0.950	0.037 - 0.972	98
209	ACETONE + ETHACETATE	329.75 - 348.45	1.010 - 1.010	0.046 - 0.980	0.102 - 0.989	98
210	DEE + ACETONE	293.15 - 293.15	0.250 - 0.580	0.000 - 1.000	0.000 - 0.000	98

Table B.2: Ranges of VLE data used in the NRTL-QSPR and the UNIQUAC-QSPR model development (Contd.)

System No.	System	Temperature Range, K	Pressure Range, bar	First component mole fraction range		Reference
				Liquid	Vapor	
211	ACETONE + PYRD	329.25 - 388.45	1.010 - 1.010	0.000 - 1.000	0.000 - 1.000	98
212	ISOPRENE + ACETONE	307.05 - 329.55	1.010 - 1.010	0.000 - 1.000	0.000 - 1.000	98
213	2M2B + ACETONE	308.75 - 317.90	1.010 - 1.010	0.139 - 0.906	0.384 - 0.866	98
214	2MB + ACETONE	298.73 - 317.50	1.010 - 1.010	0.059 - 0.952	0.371 - 0.92	98
215	ACETONE + PROPACETATE	330.85 - 372.15	1.010 - 1.010	0.020 - 0.960	0.090 - 0.990	98
216	ACETONE + 112TRICHETH	330.45 - 385.15	1.010 - 1.010	0.022 - 0.919	0.080 - 0.991	98
217	CYC6 + 4M2P	338.40 - 383.95	0.530 - 1.010	0.055 - 0.965	0.172 - 0.97	98
218	BENZ + 4M2P	338.50 - 385.85	0.430 - 1.010	0.042 - 0.968	0.118 - 0.99	98
219	CHLOROFORM + 4M2P	335.00 - 386.60	1.010 - 1.010	0.045 - 0.977	0.094 - 0.999	98
220	CYC6 + CYCHEXANONE	323.15 - 348.15	0.100 - 0.830	0.065 - 0.96	0.662 - 0.990	98
221	NC7 + 3PENTANONE	338.15 - 368.15	0.290 - 1.070	0.000 - 1.000	0.000 - 1.000	98
222	3PENTANONE + 4M2P	375.67 - 387.55	1.010 - 1.010	0.126 - 0.951	0.161 - 0.972	98
223	ETHACETATE + 3PENTANONE	350.25 - 374.85	1.010 - 1.010	0.000 - 1.000	0.000 - 1.000	98
224	METHACETATE + 3PENTANONE	329.85 - 374.85	1.010 - 1.010	0.000 - 1.000	0.000 - 1.000	98
225	2BUTANONE + ETHBENZ	298.15 - 348.15	0.010 - 0.840	0.000 - 1.000	0.000 - 0.988	98
226	2BUTANONE + NC8	338.15 - 338.15	0.220 - 0.610	0.058 - 0.97	0.472 - 0.968	98
227	2BUTANONE + NC7	323.15 - 371.45	0.280 - 1.010	0.000 - 1.000	0.000 - 1.000	98
228	2BUTANONE + TOL	323.15 - 383.75	0.120 - 1.010	0.000 - 1.000	0.000 - 1.000	98
229	2BUTANONE + BENZ	323.15 - 421.95	0.360 - 5.650	0.000 - 1.000	0.000 - 1.000	98
230	BENZ + 2BUTANONE	313.15 - 333.15	0.240 - 0.550	0.000 - 0.919	0.069 - 0.908	98
231	2M2B + 2BUTANONE	311.69 - 352.65	1.010 - 1.010	0.000 - 1.000	0.000 - 0.000	98

Table B.2: Ranges of VLE data used in the NRTL-QSPR and the UNIQUAC-QSPR model development (Contd.)

System No.	System	Temperature Range, K	Pressure Range, bar	First component mole fraction range		Reference
				Liquid	Vapor	
232	ETHACETATE + 2BUTANONE	349.78 - 353.10	1.010 - 1.010	0.000 - 1.000	0.000 - 1.000	98
233	CHLOROFORM + 2BUTANONE	336.05 - 352.85	1.010 - 1.010	0.035 - 0.935	0.033 - 0.981	98
234	TETCHMETH + 2BUTANONE	323.15 - 323.15	0.360 - 0.460	0.000 - 1.000	0.000 - 1.000	98
235	ACETONE + NC10	313.15 - 333.15	0.020 - 1.150	0.000 - 1.000	0.000 - 1.000	98
236	DEE + BENZ	273.15 - 353.45	0.040 - 1.020	0.000 - 1.000	0.000 - 0.000	98
237	DEE + HFBENZ	298.13 - 298.13	0.110 - 0.710	0.000 - 0.996	0.000 - 0.999	98
238	DEE + ETHACETATE	273.15 - 303.15	0.030 - 0.870	0.000 - 1.000	0.000 - 0.000	98
239	14DIOX + NC8	353.15 - 353.15	0.250 - 0.530	0.021 - 0.981	0.098 - 0.967	98
240	14DIOX + TOL	335.27 - 382.70	0.270 - 1.010	0.000 - 1.000	0.000 - 1.000	98
241	NC7 + 14DIOX	353.15 - 353.15	0.530 - 0.720	0.017 - 0.977	0.063 - 0.951	98
242	BENZ + 14DIOX	298.15 - 373.21	0.050 - 1.010	0.000 - 1.000	0.000 - 1.000	98
243	DIETHAMINE + 14DIOX	328.45 - 374.55	1.010 - 1.010	0.000 - 1.000	0.000 - 1.000	98
244	ETHACETATE + 14DIOX	350.05 - 374.55	1.010 - 1.010	0.000 - 1.000	0.000 - 1.000	98
245	CS2 + 14DIOX	293.15 - 293.15	0.030 - 0.400	0.000 - 1.000	0.000 - 0.000	98
246	TETCHMETH + 14DIOX	298.15 - 313.15	0.050 - 0.280	0.000 - 1.000	0.000 - 0.000	98
247	DIPE + ETHBENZ	323.15 - 343.15	0.080 - 1.000	0.048 - 0.950	0.345 - 0.993	98
248	DIPE + TOL	323.15 - 343.15	0.150 - 1.000	0.044 - 0.892	0.163 - 0.965	98
249	DIPE + BENZ	323.15 - 353.25	0.360 - 1.070	0.000 - 1.000	0.000 - 1.000	98
250	DIPE + HFBENZ	298.13 - 298.13	0.110 - 0.20	0.000 - 1.000	0.000 - 1.000	98
251	CHLOROFORM + DIPE	303.50 - 343.75	0.330 - 1.01	0.000 - 1.000	0.000 - 1.000	98
252	DIPE + NC7	342.35 - 388.85	1.010 - 2.210	0.197 - 0.932	0.360 - 0.972	98

Table B.2: Ranges of VLE data used in the NRTL-QSPR and the UNIQUAC-QSPR model development (Contd.)

System No.	System	Temperature Range, K	Pressure Range, bar	First component mole fraction range		Reference
				Liquid	Vapor	
253	ACETALD + DEE	292.80 - 304.30	1.010 - 1.010	0.058 - 0.926	0.155 - 0.904	98
254	PROPANAL + METHACETATE	303.16 - 313.13	0.360 - 0.760	0.000 - 1.000	0.000 - 1.000	98
255	PROPANAL + ETHACETATE	303.16 - 313.15	0.160 - 0.760	0.000 - 1.000	0.000 - 1.000	98
256	PROPANAL + BENZ	313.15 - 313.15	0.240 - 0.760	0.000 - 1.000	0.000 - 1.000	98
257	NC5 + PROPANAL	313.15 - 313.15	0.760 - 1.360	0.000 - 1.000	0.000 - 1.000	98
258	ISOPRENE + BUTYRALD	307.25 - 337.35	1.010 - 1.010	0.100 - 1.000	0.000 - 0.000	98
259	DICHMETH + FURF	312.30 - 434.95	1.010 - 1.010	0.000 - 1.000	0.000 - 1.000	98
260	12DICHETH + FURF	356.65 - 434.95	1.010 - 1.010	0.000 - 1.000	0.000 - 1.000	98
261	ACETONE + FURF	329.25 - 434.85	1.010 - 1.010	0.000 - 1.000	0.000 - 1.000	98
262	ETHACETATE + FURF	350.35 - 434.85	1.010 - 1.010	0.000 - 1.000	0.000 - 1.000	98
263	NC4 + FURF	310.95 - 324.85	1.020 - 4.630	0.022 - 0.179	0.984 - 0.998	98
264	4M2P + FURF	368.09 - 368.09	0.110 - 0.530	0.000 - 1.000	0.000 - 1.000	98
265	TETCHETHY + FURF	393.80 - 434.95	1.010 - 1.010	0.000 - 1.000	0.000 - 1.000	98
266	ETHBENZ + BENZALD	348.15 - 368.15	0.030 - 0.290	0.000 - 1.000	0.000 - 1.000	98
267	DEE + TETCHMETH	298.15 - 308.15	0.150 - 1.040	0.000 - 1.000	0.000 - 1.000	98
268	DEE + CYC6	298.15 - 298.15	0.130 - 0.710	0.000 - 1.000	0.000 - 0.000	98
269	DEE + TOL	273.15 - 383.45	0.010 - 1.010	0.001 - 0.989	0.021 - 0.997	98
270	2MB + DEE	300.95 - 307.75	1.010 - 1.010	0.000 - 0.98	0.001 - 0.981	98
271	MTBE + TETCHMETH	313.15 - 313.15	0.280 - 0.600	0.000 - 1.000	0.000 - 1.000	98
272	MTBE + CHLOROFORM	313.15 - 313.15	0.400 - 0.600	0.000 - 1.000	0.000 - 1.000	98
273	MTBE + METHACETATE	323.35 - 373.17	0.940 - 4.050	0.000 - 1.000	0.000 - 1.000	98

Table B.2: Ranges of VLE data used in the NRTL-QSPR and the UNIQUAC-QSPR model development (Contd.)

System No.	System	Temperature Range, K	Pressure Range, bar	First component mole fraction range		Reference
				Liquid	Vapor	
274	MTBE + ETHACETATE	353.15 - 373.17	1.110 - 3.640	0.000 - 1.000	0.000 - 1.000	98
275	MTBE + BENZ	313.15 - 363.05	0.240 - 2.790	0.000 - 1.000	0.000 - 1.000	98
276	MTBE + CYC6	313.15 - 313.15	0.250 - 0.600	0.000 - 1.000	0.000 - 0.000	98
277	MTBE + DIPE	325.75 - 339.12	0.940 - 0.940	0.000 - 1.000	0.000 - 1.000	98
278	MTBE + TOL	325.60 - 381.04	0.300 - 1.010	0.000 - 1.000	0.000 - 1.000	98
279	MTBE + NC7	298.15 - 366.45	0.060 - 0.940	0.000 - 1.000	0.000 - 1.000	98
280	DICHMETH + MTBE	308.15 - 308.15	0.500 - 0.850	0.000 - 1.000	0.000 - 1.000	98
281	NC4 + MTBE	273.15 - 322.89	0.110 - 4.600	0.000 - 1.000	0.000 - 0.000	98
282	ISOPRENE +MTBE	307.23 - 328.15	1.010 - 1.010	0.000 - 1.000	0.000 - 0.000	98
283	2M2B + MTBE	311.75 - 328.15	1.010 - 1.010	0.000 - 1.000	0.000 - 0.000	98
284	2MB + MTBE	288.15 - 322.90	0.220 - 1.950	0.000 - 1.000	0.000 - 0.000	98
285	2MB + ETBE	293.15 - 322.90	0.130 - 1.960	0.000 - 1.000	0.000 - 1.000	98
286	ETBE + TOL	293.15 - 333.15	0.030 - 0.660	0.000 - 1.000	0.000 - 1.000	98
287	ETBE + NC8	323.15 - 323.15	0.070 - 0.470	0.000 - 1.000	0.000 - 0.000	98
288	DME + METHAMINE	273.15 - 273.15	1.340 - 2.680	0.000 - 1.000	0.000 - 0.000	98
289	DME + NC4	282.96 - 297.86	1.470 - 5.790	0.000 - 1.000	0.000 - 1.000	98
290	DME + MTBE	298.15 - 298.15	0.340 - 5.910	0.000 - 1.000	0.000 - 1.000	98
291	CHLOROFORM + BENZ	273.15 - 373.15	0.040 - 3.240	0.000 - 1.000	0.000 - 1.000	98
292	CS2 + BENZ	273.15 - 353.15	0.040 - 2.710	0.000 - 1.000	0.000 - 0.990	98
293	BUTAMINE + BENZ	323.15 - 343.15	0.360 - 0.810	0.000 - 1.000	0.000 - 1.000	98
294	DIETHAMINE + BENZ	308.15 - 353.25	0.200 - 1.010	0.000 - 1.000	0.000 - 1.000	98

Table B.2: Ranges of VLE data used in the NRTL-QSPR and the UNIQUAC-QSPR model development (Contd.)

System No.	System	Temperature Range, K	Pressure Range, bar	First component mole fraction range		Reference
				Liquid	Vapor	
295	BENZ + ACTN	293.15 - 364.25	0.040 - 1.010	0.015 - 0.991	0.000 - 0.972	98
296	BENZ + PYRD	293.15 - 382.70	0.020 - 1.010	0.000 - 1.000	0 .000- 0.960	98
297	BENZ + HFBENZ	273.58 - 353.60	0.140 - 1.010	0.000 - 1.000	0.000 - 1.000	98
298	BENZ + BROMOBENZ	303.15 - 353.15	0.010 - 1.010	0.000 - 1.000	0.000 - 1.000	98
299	BENZ + NITROBENZ	298.15 - 343.15	0.010 - 0.700	0.000 - 1.000	0.000 - 1.000	98
300	BENZ + ETHBENZ	353.53 - 409.33	1.010 - 1.010	0.000 - 1.000	0.000 - 1.000	98
301	BENZ + PXYL	356.75 - 402.15	1.010 - 1.010	0.086 - 0.886	0.285 - 0.979	98
302	TOL + NITROETH	318.15 - 318.15	0.080 - 0.110	0.000 - 1.000	0.000 - 0.000	98
303	TOL + ETHDIAMINE	376.15 - 386.45	1.010 - 1.010	0.027 - 0.96	0.095 - 0.909	98
304	TOL + PYRD	293.15 - 388.32	0.020 - 1.010	0.000 - 1.000	0.000 - 0.928	98
305	CHLOROFORM + TOL	334.48 - 382.07	0.990 - 1.010	0.000 - 1.000	0.000 - 1.000	98
306	CS2 + TOL	283.15 - 363.15	0.020 - 3.480	0.000 - 1.000	0.000 - 0.000	98
307	ACTN + TOL	313.15 - 381.45	0.100 - 1.010	0.000 - 2.492	0.000 - 0.972	98
308	12DICHETH + TOL	303.15 - 383.76	0.050 - 1.010	0.000 - 1.000	0.000 - 1.000	98
309	TETCHMETH + ETHBENZ	303.15 - 407.25	0.020 - 1.020	0.000 - 1.0003	0.000 - 0.996	98
310	ACTN + ETHBENZ	354.90 - 405.90	1.010 - 1.010	0.010 - 0.970	0.115 - 0.978	98
311	DIETHAMINE + ETHBENZ	308.15 - 308.15	0.020 - 0.480	0.000 - 1.000	0.000 - 1.000	98
312	TETCHMETH + PXYL	273.15 - 409.55	0.000 - 1.010	0.000 - 1.000	0.000 - 0.997	98
313	ACTN + PXYL	354.96 - 408.65	1.010 - 1.010	0.010 - 0.9775	0.095 - 0.982	98
314	12DICHETH + PXYL	303.15 - 303.15	0.020 - 0.130	0.000 - 1.000	0.000 - 0.000	98
315	ACETALD + TOL	293.95 - 383.95	1.010 - 1.010	0.000 - 1.000	0.000 - 1.000	98

Table B.2: Ranges of VLE data used in the NRTL-QSPR and the UNIQUAC-QSPR model development (Contd.)

System No.	System	Temperature Range, K	Pressure Range, bar	First component mole fraction range		Reference
				Liquid	Vapor	
316	BUTYRAL + TOL	349.85 - 378.35	1.010 - 1.010	0.083 - 0.917	0.197 - 0.956	98
317	2M1B + ACETONE	303.25 - 329.55	1.010 - 1.010	0.000 - 1.000	0.000 - 0.000	98
318	PROPOX + ACETONE	307.40 - 329.65	1.010 - 1.010	0.000 - 1.000	0.000 - 1.000	98
319	3HEXANONE + 4 HEPTANONE	396.55 - 417.25	1.010 - 1.010	0.000 - 1.000	0.000 - 1.000	98
320	TOL + CYCHEXANONE	383.55 - 427.95	1.010 - 1.010	0.000 - 1.000	0.000 - 1.000	98
321	NC6 + 3 PENTANONE	338.15 - 338.15	0.460 - 0.920	0.126 - 0.937	0.430 - 0.951	98
322	3PENATANONE + 4HEPTANONE	374.55 - 417.25	1.010 - 1.010	0.000 - 1.000	0.000 - 1.000	98
323	NC6 + 2BUTANONE	333.15 - 338.15	0.670 - 1.030	0.055 - 0.961	0.175 - 0.917	98
324	NC6 + 14DIOX	341.95 - 358.05	0.610 - 1.430	0.030 - 0.977	0.198 - 0.977	98
325	ACETALD + ACETONE	293.35 - 348.15	0.300 - 5.400	0.000 - 1.000	0.000 - 1.000	98
326	PROPOX + PROPANAL	307.93 - 319.90	1.000 - 1.000	0.036 - 0.942	0.053 - 0.964	98
327	METHACETATE + BUTYRAL	313.15 - 323.15	0.290 - 0.790	0.000 - 1.000	0.000 - 1.000	98
328	BUTYRAL + PROPACETATE	323.15 - 333.15	0.150 - 0.620	0.000 - 1.000	0.000 - 1.000	98
329	BUTYRAL + BENZ	313.15 - 393.15	0.240 - 3.140	0.000 - 1.000	0.000 - 1.000	98
330	BUTYRAL + NC7	298.15 - 343.15	0.060 - 0.890	0.000 - 1.000	0.000 - 1.000	98
331	13BD + MTBE	273.15 - 323.15	0.100 - 5.550	0.000 - 1.000	0.000 - 1.000	98
332	ETBE + NC7	353.55 - 366.93	0.570 - 2.210	0.000 - 1.000	0.000 - 1.000	98

Table B.3: Physical constants used in the NRTL-QSPR and the UNIQUAC-QSPR model development

Compound No.	Compound	T_C, K	P_C, bar	ω	Mol. Wt.
1	MEO	513.10	80.94	0.532	32.04
2	TBA	506.20	39.72	0.582	74.12
3	MTBE	497.10	34.30	0.259	88.15
4	NC4	425.10	37.84	0.193	58.12
5	IC5	460.40	33.81	0.228	72.15
6	MCYC6	572.20	34.72	0.242	98.19
7	ETH	516.10	63.80	0.607	46.07
8	ETBE	513.50	29.49	0.288	102.20
9	TAME	533.80	30.42	0.301	102.20
10	TOH	545.00	39.52	0.476	88.15
12	NC5	469.60	33.65	0.249	72.15
13	H2O	647.10	220.60	0.345	18.01
14	NC7	539.20	27.40	0.350	100.20
15	DEE	466.80	36.06	0.267	74.12
16	1C7-	533.30	28.27	0.347	98.19
17	IC5-	470.40	34.47	0.271	70.13
18	ACTN	548.00	48.33	0.301	41.05
19	13BD	425.40	43.30	0.194	54.09
20	IC4-	417.90	39.99	0.209	56.11
21	PPN	564.40	41.80	0.325	55.08
22	2M2B	470.40	34.47	0.271	70.13
23	IC4	407.80	36.40	0.177	58.12
24	DISB	560.10	26.45	0.212	112.20
25	C2B-	435.60	42.06	0.208	56.11
26	T2B-	428.60	41.02	0.219	56.11
27	2M1B	465.40	34.47	0.228	70.13
28	DMDS	605.70	53.64	0.256	94.20
29	MEM	469.90	72.33	0.167	48.11
30	DMS	503.00	55.30	0.197	62.13
31	TOL	591.80	41.00	0.264	92.14
32	ETHBENZ	617.20	36.00	0.302	106.20
33	PXYL	616.20	35.10	0.320	106.20
34	CYC6	553.50	40.70	0.212	84.16
35	BENZ	562.20	48.90	0.212	78.11

Table B.3: Physical constants used in the NRTL-QSPR and the UNIQUAC-QSPR model development (Contd.)

Compound No.	Compound	T_C, K	P_C, bar	ω	Mol. Wt.
36	CYC5	511.70	45.10	0.196	70.14
37	TETCHMETH	556.40	45.60	0.193	153.80
38	4M2P	571.40	32.70	0.356	100.20
39	2PENT	564.00	38.91	0.343	86.13
40	ACETONE	508.10	47.00	0.304	58.08
41	2BUTANONE	535.50	41.50	0.324	72.11
42	THIOPHENE	579.40	56.90	0.196	84.14
43	DIPE	500.30	28.80	0.331	102.20
44	3PENTANONE	561.00	37.40	0.345	86.13
45	FURF	670.00	58.90	0.383	96.09
46	12DICHMETH	566.00	53.70	0.278	98.96
47	DIETHAMINE	496.50	37.10	0.291	73.14
48	TRIETHAMINE	535.00	30.30	0.320	101.20
49	ACRYL	536.00	45.60	0.350	53.06
50	NITROBENZ	732.10	44.00	0.449	123.20
51	BUTYLCH	542.00	36.80	0.274	92.57
52	CHLOROFORM	536.40	53.70	0.218	119.40
53	NITROMETH	588.00	63.10	0.310	61.04
54	TBUT	506.20	39.70	0.612	74.12
55	2PROP	508.30	47.64	0.665	60.10
56	ETHIOD	554.10	59.90	0.214	156.00
57	PYRD	620.00	56.30	0.243	79.10
58	1BUT	563.00	44.13	0.593	74.12
59	1PROP	536.80	51.70	0.623	60.10
60	VIACETATE	525.00	43.50	0.340	86.09
61	PROPACETATE	549.40	33.60	0.398	102.10
62	METHACETATE	506.80	46.90	0.326	74.08
63	DME	400.00	53.70	0.205	46.07
64	METHIOD	528.00	65.90	0.197	141.90
65	DICHMETH	510.00	63.00	0.199	84.93
66	2M1P	547.80	42.95	0.592	74.12
67	12DICHETH	566.00	53.70	0.278	98.96
68	PROPOX	482.30	49.20	0.268	58.08
69	NC10	617.90	21.00	0.490	142.30

Table B.3: Physical constants used in the NRTL-QSPR and the UNIQUAC-QSPR model development (Contd.)

Compound No.	Compound	T_C, K	P_C, bar	ω	Mol. Wt.
70	BENZALD	694.80	45.40	0.316	106.10
71	BENZACETATE	699.00	31.80	0.473	150.20
72	ETHACETATE	523.20	38.30	0.362	88.11
73	112TRICHETH	602.00	44.80	0.259	133.40
74	CYCHEXANONE	629.00	39.00	0.299	98.15
75	NC8	568.80	24.90	0.398	114.20
76	HFBENZ	516.70	33.00	0.396	186.10
77	14DIOX	587.10	52.08	0.279	88.11
78	PROPANAL	515.30	63.30	0.313	58.08
79	BUTYRALD	545.40	53.80	0.352	72.11
80	METHAMINE	430.10	74.14	0.281	31.06
81	BROMOBENZ	670.00	45.20	0.251	157.10
82	NITROETH	593.00	51.60	0.380	75.07
83	ETHDIAMINE	593.00	62.90	0.510	60.10
84	4 HEPTANONE	600.00	29.10	0.412	114.20
85	TETCHETHY	620.25	44.90	0.214	165.83
86	CS2	552.00	79.00	0.109	76.13
87	BUTAMINE	524.15	42.00	0.329	73.14
88	ACETALD	497.10	34.30	0.259	88.15
89	3HEXANONE	582.80	33.20	0.378	100.16
90	23DMETHBUT	500.00	31.30	0.247	86.18
91	C13P	499.150	40.13	0.1882	68.12
92	T13P	496.000	39.92	0.1864	68.12

Table B.4: Results of the UNIQUAC-QSPR model

System No.	System	% AAD			
		T, K	P, bar	K_1	K_2
1	MTBE + MEO	0.20	2.29	6.40	4.66
2	MTBE + TBA	0.65	6.99	6.19	12.87
3	DME + MTBE	0.71	6.09	2.32	20.07
4	MTBE + NC4	0.38	3.09	10.89	4.36
5	MTBE + IC5	0.97	9.52	13.80	16.23
6	MTBE + MCYC6	0.34	4.87	4.05	4.56
7	IC4- + MTBE	0.34	2.90	1.89	9.93
8	ETBE + ETH	1.33	14.23	12.62	13.44
9	TBA + ETBE	0.90	10.04	12.38	9.19
10	IC5 + ETBE	0.58	6.36	4.13	8.15
11	MCYC6 + ETBE	0.10	0.98	4.78	2.71
12	IC4- + ETBE	0.42	3.50	1.99	18.89
13	MEO + TAME	0.20	2.23	3.00	3.58
14	TAME + TOH	0.07	0.88	0.00	0.00
15	TOH + TAME	0.07	0.69	0.00	0.00
16	TAME + NC5	0.78	6.85	0.00	0.00
17	TAME + MCYC6	0.26	3.44	4.45	6.85
18	DME + MEO	0.35	3.40	1.94	28.27
19	DEE + H2O	0.56	5.86	0.00	0.00
20	MEO + ETH	0.13	1.99	0.43	0.85
21	NC4 + MEO	0.76	6.96	3.50	15.89
22	MEO + NC7	0.23	2.87	2.11	6.12
23	IC4 + MEO	0.60	4.98	7.89	31.14
24	NC5 + MEO	0.81	8.95	9.28	14.85
25	NC5- + MEO	0.26	2.92	2.71	10.06
26	IC5- + MEO	0.27	2.99	1.77	6.00
27	ISOPRENE + MEO	0.44	5.18	4.92	10.12
28	ISOPRENE + DEE	0.43	4.51	20.17	4.51
29	MEO + 1C7-	0.21	2.64	2.48	5.28
30	MEO + H2O	0.20	2.99	0.48	0.70
31	NC4 + ETH	0.55	4.60	0.00	0.00
32	ETH + H2O	0.14	2.13	4.73	2.23
33	NC6 + TBA	0.23	2.91	5.05	3.75
34	TBA + NC7	0.34	4.86	2.98	5.54

Table B.4: Results of the UNIQUAC-QSPR model (Contd.)

System No.	System	% AAD			
		T, K	P, bar	K_1	K_2
35	NC8 + TBA	0.45	8.17	0.00	0.00
36	TBA + IC5	1.71	20.20	27.30	11.22
37	TBA + IC5-	0.25	2.66	7.23	3.67
38	ISOPRENE + TBA	0.74	7.84	3.20	10.50
39	TBA + H2O	1.34	19.03	18.25	24.56
40	TOH + NC5	0.34	3.15	0.00	0.00
41	MTB + ACTN	0.20	2.37	3.84	5.47
42	MTB + 13BD	0.26	2.95	5.42	1.52
43	MEO + TBA	0.23	3.76	3.45	5.55
44	MEO + IC4-	0.48	4.06	6.95	0.56
45	MEO + ACTN	0.16	2.19	1.56	2.62
46	MEO + PPN	0.17	2.13	1.45	4.42
47	ETH + TBA	0.09	1.44	0.23	0.85
48	TOH + H2O	0.41	5.32	12.57	11.08
49	NC4 + TBA	0.90	7.33	10.69	22.39
50	NC4 + NC5	0.35	3.76	4.00	3.46
51	NC5 + ETH	0.77	7.48	3.55	13.61
52	NC5 + 2M2B	0.43	5.23	0.00	0.00
53	NC5 + ACTN	0.45	4.09	0.00	0.00
54	IC4 + NC4	0.38	3.87	9.79	4.98
55	IC4- + NC4	0.17	1.48	0.00	0.00
56	IC4- + IC4	0.33	2.82	0.00	0.00
57	1C4- + NC4	0.17	1.35	2.52	1.66
58	1C4- + IC4	0.11	0.96	0.00	0.00
59	1C4- + 13BD	0.07	0.62	0.47	0.28
60	C2B- + NC4	1.00	7.70	0.00	0.00
61	T2B- + NC4	0.32	2.86	0.00	0.00
62	2M1B + MEO	0.16	1.78	2.74	9.08
63	2M1B + NC5	0.17	2.02	0.00	0.00
64	2M1B + 2M2B	0.09	1.03	0.39	0.40
65	2M2B + MEO	0.21	2.36	3.16	7.56
66	2M2B + ETH	0.62	6.54	0.00	0.00
67	2M2B + ACTN	0.34	3.25	2.20	5.13
68	ACTN + ETH	0.27	3.53	2.59	3.93

Table B.4: Results of the UNIQUAC-QSPR model (Contd.)

System No.	System	% AAD			
		T, K	P, bar	K_1	K_2
69	ACTN + TBA	0.76	10.56	10.66	24.12
70	ACTN + NC4	0.29	2.06	12.97	1.22
71	ACTN + DISB	0.17	2.19	0.00	0.00
72	ACTN + H2O	0.20	2.63	1.58	3.21
73	PPN + NC5	1.33	8.81	0.00	0.00
74	PPN + H2O	0.18	2.10	7.30	5.81
75	13BD + MEO	0.24	2.02	0.44	5.34
76	13BD + NC4	0.09	0.78	0.79	0.63
77	13BD + IC4	0.50	4.21	0.00	0.00
78	13BD + C2B-	1.68	12.74	0.00	0.00
79	13BD + T2B-	0.18	1.64	0.00	0.00
80	13BD + ACTN	0.40	3.31	0.00	0.00
81	C13P + MEO	0.19	2.26	3.61	6.62
82	T13P + MEO	0.15	1.73	2.75	6.81
83	T13P + ACTN	0.16	1.81	0.00	0.00
84	TBA + 2M1B	0.66	6.52	13.47	3.48
85	TBA + 2M2B	0.36	4.00	9.52	5.55
86	DME + MEO	0.35	3.40	1.94	28.27
87	MEO + H2O	0.20	2.99	0.48	0.70
88	MEM + MEO	0.47	5.77	0.00	0.00
89	DMS + MEO	2.10	36.48	0.00	0.00
90	H2S + MEO	0.98	7.09	1.49	32.40
91	MEO + DMDS	0.09	1.25	0.72	3.63
92	MEM + H2O	1.18	8.20	0.00	0.00
93	DMDS + MEM	0.52	5.16	17.54	3.43
94	H2S + MEM	1.34	10.22	1.07	99.99
95	H2S + DMS	0.29	2.18	2.04	24.80
96	MEM + DMS	0.20	2.25	0.07	2.07
97	BENZ + TOL	0.19	1.98	1.97	3.04
98	NC7 + ETHBENZ	0.75	9.51	3.84	10.15
99	NC8 + ETHBENZ	0.37	4.02	5.29	6.13
100	1C7- + TOL	0.30	3.82	4.62	6.50
101	NC7 + PXYL	0.43	5.90	2.14	6.47
102	BENZ + CYC6	0.21	2.66	2.75	4.03
103	MCYC5 + BENZ	0.25	3.20	3.58	3.11

Table B.4: Results of the UNIQUAC-QSPR model (Contd.)

System No.	System	% AAD			
		T, K	P, bar	K_1	K_2
104	CYC6 + TOL	0.16	2.12	1.78	4.56
105	ISOPRENE + 2M2B	0.24	2.55	2.82	3.09
106	HFBENZ + TOL	0.22	3.16	3.47	5.29
107	TETCHMETH + BENZ	0.08	0.87	1.73	1.88
108	CS2 + CYC6	0.35	4.09	2.60	6.64
109	CS2 + CYC5	0.54	6.12	8.16	8.24
110	CS2 + TETCHMETH	0.04	0.46	1.08	1.27
111	HFBENZ + PXYL	0.19	2.79	1.40	5.20
112	HFBENZ + CYC6	0.26	3.52	3.96	3.54
113	TOL + 4M2P	0.33	4.60	3.41	4.53
114	TOL + 2PENT	0.03	0.41	0.61	1.07
115	BENZ + ACETONE	0.44	5.12	14.15	7.08
116	BENZ + 2BUTANONE	0.07	0.69	2.90	4.56
117	BENZ + THIOPHENE	0.12	1.45	0.79	0.41
118	HFBENZ + DIPE	0.87	12.79	19.27	17.05
119	TETCHMETH + 2BUTANONE	0.05	0.50	1.79	1.90
120	CYC6 + 2BUTANONE	0.10	1.14	2.37	2.11
121	NC7 + THIOPHENE	0.10	1.32	3.89	2.47
122	NC7 + 3PENTANONE	0.32	3.68	4.53	6.52
123	NC7 + 2BUTANONE	0.70	7.41	12.19	11.95
124	NC10 + ACETONE	0.20	2.24	6.50	0.07
125	TETCHMETH + FURF	1.55	14.05	2.93	43.89
126	TETCHMETH + ACETONE	0.10	1.22	3.05	1.52
127	BENZ + 12DICHMETH	0.23	2.60	3.02	3.53
128	TOL + 12DICHMETH	0.07	0.72	1.07	0.68
129	BENZ + DIETHAMINE	0.11	1.26	1.38	2.80
130	BENZ + TRIETHAMINE	0.37	3.98	4.86	4.61
131	ETHBENZ + ACRYL	0.94	14.66	16.87	6.13
132	TOL + NITROBENZ	0.12	1.46	0.30	5.93
133	NC7 + BUTYLCH	0.35	4.45	6.39	6.10
134	CYC5 + CHLOROFORM	0.30	3.53	3.12	5.07
135	NC7 + TRIETHAMINE	0.32	3.85	4.89	3.04
136	23DMETHBUT + CHLOROFORM	0.05	0.54	1.67	1.75
137	ETHBENZ + NITROBENZ	0.33	4.23	1.02	6.63
138	BENZ + NITROMETH	0.10	1.27	0.95	1.72

Table B.4: Results of the UNIQUAC-QSPR model (Contd.)

System No.	System	% AAD			
		T, K	P, bar	K_1	K_2
139	BENZ + TBUT	0.40	5.41	4.88	6.79
140	BENZ + ETH	0.07	0.90	1.32	1.92
141	BENZ + 2PROP	0.17	2.10	3.77	2.73
142	NC7 + ETHIOD	0.11	1.30	3.98	1.49
143	CYC6 + PYRD	0.06	0.68	0.76	3.68
144	NC8 + PYRD	0.10	1.31	1.92	1.35
145	NC8 + MEO	0.32	4.22	10.23	1.27
146	CYC6 + ETH	0.11	1.54	2.56	4.00
147	NC5 + 1BUT	0.40	4.36	0.61	9.03
148	TETCHETHY + ETH	0.13	1.66	3.66	1.00
149	HFBENZ + 1PROP	0.43	6.67	0.54	2.64
150	HFBENZ + MEO	0.11	1.71	4.91	3.85
151	PROPANAL + ACETONE	0.23	2.57	4.65	2.50
152	PROPANAL + 2BUTANONE	0.24	2.92	4.76	4.10
153	ACETONE + VIACETATE	0.08	0.87	1.31	1.90
154	ACETALD + PROPACETATE	0.38	4.08	5.26	6.28
155	ACETALD + VIACETATE	0.09	0.96	1.86	3.48
156	ACETALD + METHACETATE	0.68	7.61	9.14	16.16
157	DEE + ACETONE	0.50	5.52	7.46	9.58
158	ACETALD + DEE	0.12	1.24	0.84	1.96
159	DEE + METHIOD	0.04	0.48	0.89	1.26
160	DEE + DICHMETH	0.20	2.26	2.54	1.98
161	14DIOX + 2PROP	0.51	6.66	9.67	10.03
162	EPE + CHLOROFORM	0.12	1.47	3.41	2.66
163	DEE + CHLOROFORM	0.76	7.80	14.42	14.43
164	ACETONE + CHLOROFORM	0.17	2.11	3.13	4.19
165	PROPACETATE + 1PROP	0.07	0.95	1.51	1.01
166	ETHACETATE + 2PROP	0.19	2.56	4.94	4.38
167	DEE + ETH	0.36	5.00	1.39	10.12
168	FURF + ETH	0.57	7.57	25.90	4.35
169	ACETONE + MEO	0.10	1.20	2.47	2.22
170	14DIOX + MEO	0.12	1.80	2.53	1.57
171	ETH + TRIETHAMINE	0.37	5.85	4.67	8.13
172	TBUT + 1BUT	0.21	3.75	1.93	6.90
173	1PROP + 2M1P	0.04	0.62	2.81	2.96

Table B.4: Results of the UNIQUAC-QSPR model (Contd.)

System No.	System	% AAD			
		T, K	P, bar	K_1	K_2
174	ETH + 2PROP	0.08	1.10	2.06	2.13
175	MEO + 2M1P	0.72	10.05	2.53	8.74
176	ETH + 2M1P	0.15	2.31	0.42	1.19
177	BUTAMINE + 1BUT	0.25	3.99	4.64	6.96
178	DIETHAMINE + ETH	0.62	9.30	17.26	11.68
179	ETH + ACTN	0.51	6.91	8.75	7.74
180	BUTAMINE + 1PROP	0.81	13.71	25.81	19.27
181	BROMOBENZ + CYC6	0.20	2.81	2.75	4.17
182	12DICHETH + 2M1P	0.80	10.43	3.91	13.73
183	MEO + 12DICHETH	0.22	3.06	1.06	2.75
184	H2O + DIETHAMINE	2.75	53.02	61.00	10.04
185	H2O + PYRD	0.27	3.46	5.00	4.91
186	H2O + MEO	0.13	1.72	3.36	0.68
187	H2O + 2PROP	0.22	3.54	6.69	5.00
188	H2O + ETH	0.52	6.86	8.48	9.25
189	ACETALD + PROPOX	2.90	26.12	50.71	25.11
190	ACETALD + BENZ	1.60	19.00	6.76	25.13
191	PROPANAL + CYC6	0.24	2.71	5.91	5.99
192	CHLOROFORM + FURF	1.18	13.38	9.42	47.88
193	1C4- + FURF	1.29	9.19	0.12	38.77
194	TOL + FURF	0.54	6.19	4.59	15.11
195	ETHBENZ + FURF	0.29	3.25	3.97	6.39
196	PXYL + FURF	0.24	2.67	2.67	3.33
197	NC5 + ACETONE	0.96	11.32	5.90	12.00
198	FURF + NC10	1.22	13.28	11.61	18.73
199	TOL + BENZALD	0.19	2.58	1.18	17.11
200	BENZALD + BENZACETATE	1.00	12.59	17.10	35.50
201	ACETONE + TETCHMETH	0.42	4.66	7.39	13.73
202	CS2 + ACETONE	1.96	19.96	14.96	14.75
203	ACETONE +ACTN	0.45	5.65	6.79	6.41
204	ACETONE + 12DICHETH	0.49	5.62	7.07	12.83
205	ACETONE + ETHIOD	0.42	5.26	0.00	0.00
206	METHACETATE + ACETONE	0.29	3.35	2.76	2.78
207	ACETONE + METHACETATE	0.07	0.92	1.71	1.33
208	ACETONE + 2BUTANONE	0.19	2.06	5.62	8.44

Table B.4: Results of the UNIQUAC-QSPR model (Contd.)

System No.	System	% AAD			
		T, K	P, bar	K_1	K_2
209	ACETONE + ETHACETATE	0.26	2.85	4.12	4.07
210	DEE + ACETONE	0.10	1.16	0.00	0.00
211	ACETONE + PYRD	0.17	1.84	1.51	17.15
212	ISOPRENE + ACETONE	0.42	4.66	4.56	9.58
213	2M2B + ACETONE	0.42	4.75	6.20	8.97
214	2MB + ACETONE	0.45	4.65	2.30	6.11
215	ACETONE + PROPACETATE	0.38	4.08	5.28	6.32
216	ACETONE + 112TRICHETH	0.42	4.52	5.25	14.73
217	CYC6 + 4M2P	0.28	3.18	4.64	15.09
218	BENZ + 4M2P	0.15	1.76	3.21	7.45
219	CHLOROFORM + 4M2P	0.64	7.17	15.66	28.44
220	CYC6 + CYCHEXANONE	0.33	3.88	0.99	9.20
221	NC7 + 3PENTANONE	0.31	3.54	4.56	6.90
222	3PENTANONE + 4M2P	0.08	0.88	0.82	1.96
223	ETHACETATE + 3PENTANONE	0.06	0.69	4.10	5.10
224	METHACETATE + 3PENTANONE	0.38	4.13	7.20	4.27
225	2BUTANONE + ETHBENZ	0.19	2.72	1.05	4.71
226	2BUTANONE + NC8	0.26	3.05	2.85	12.71
227	2BUTANONE + NC7	0.41	4.53	9.11	9.89
228	2BUTANONE + TOL	0.21	2.63	2.12	3.66
229	2BUTANONE + BENZ	0.55	5.82	9.27	6.64
230	BENZ + 2BUTANONE	0.25	3.17	4.20	5.52
231	2M2B + 2BUTANONE	0.24	2.58	0.00	0.00
232	ETHACETATE + 2BUTANONE	0.16	1.80	4.77	5.98
233	CHLOROFORM + 2BUTANONE	0.80	9.25	13.07	18.98
234	TETCHMETH + 2BUTANONE	0.12	1.47	1.71	2.16
235	ACETONE + NC10	1.17	11.53	0.27	27.28
236	DEE + BENZ	0.23	2.86	0.00	0.00
237	DEE + HFBENZ	0.01	0.12	0.65	4.56
238	DEE + ETHACETATE	0.60	8.24	0.00	0.00
239	14DIOX + NC8	1.17	13.06	14.46	28.57
240	14DIOX + TOL	0.52	6.03	5.14	5.43
241	NC7 + 14DIOX	0.34	4.07	11.95	9.12
242	BENZ + 14DIOX	0.15	1.98	0.62	2.54
243	DIETHAMINE + 14DIOX	0.36	3.81	1.77	2.85

Table B.4: Results of the UNIQUAC-QSPR model (Contd.)

System No.	System	% AAD			
		T, K	P, bar	K_1	K_2
244	ETHACETATE + 14DIOX	0.04	0.47	1.76	1.40
245	CS2 + 14DIOX	0.58	7.41	0.00	0.00
246	TETCHMETH + 14DIOX	0.44	6.26	0.00	0.00
247	DIPE + ETHBENZ	1.14	12.94	6.65	23.18
248	DIPE + TOL	0.53	6.15	3.45	7.33
249	DIPE + BENZ	0.12	1.38	4.43	2.78
250	DIPE + HFBENZ	0.14	1.90	1.67	2.35
251	CHLOROFORM + DIPE	0.15	1.78	5.99	4.38
252	DIPE + NC7	0.31	3.39	3.31	6.40
253	ACETALD + DEE	0.10	1.11	1.01	2.36
254	PROPANAL + METHACETATE	0.14	1.68	3.28	2.62
255	PROPANAL + ETHACETATE	0.09	1.16	3.53	4.81
256	PROPANAL + BENZ	0.56	7.17	11.09	12.70
257	NC5 + PROPANAL	0.34	3.56	3.57	3.50
258	ISOPRENE + BUTYRALD	1.49	17.67	0.00	0.00
259	DICHMETH + FURF	3.95	48.06	11.26	42.94
260	12DICHETH + FURF	0.90	10.24	8.05	16.29
261	ACETONE + FURF	0.13	1.46	0.65	34.16
262	ETHACETATE + FURF	0.21	2.26	0.96	16.86
263	NC4 + FURF	5.46	31.93	0.59	99.99
264	4M2P + FURF	0.81	9.82	9.50	12.31
265	TETCHETHY + FURF	0.15	1.73	1.66	3.19
266	ETHBENZ + BENZALD	0.59	7.80	3.06	9.79
267	DEE + TETCHMETH	0.35	4.02	3.10	6.31
268	DEE + CYC6	0.40	4.90	0.00	0.00
269	DEE + TOL	1.35	14.46	5.39	21.70
270	2MB + DEE	0.18	1.93	6.34	6.94
271	MTBE + TETCHMETH	0.47	5.70	6.05	5.73
272	MTBE + CHLOROFORM	0.91	11.83	23.36	14.78
273	MTBE + METHACETATE	0.20	2.06	2.09	3.21
274	MTBE + ETHACETATE	0.13	1.32	1.89	3.38
275	MTBE + BENZ	0.37	4.14	1.67	0.85
276	MTBE + CYC6	1.00	12.70	0.00	0.00
277	MTBE + DIPE	0.33	3.60	5.13	7.96
278	MTBE + TOL	0.13	1.43	0.84	6.96

Table B.4: Results of the UNIQUAC-QSPR model (Contd.)

System No.	System	% AAD			
		T, K	P, bar	K_1	K_2
279	MTBE + NC7	0.11	1.35	0.26	1.44
280	DICHMETH + MTBE	0.19	2.17	1.72	7.56
281	NC4 + MTBE	0.93	9.08	0.00	0.00
282	ISOPRENE +MTBE	0.10	1.07	0.00	0.00
283	2M2B + MTBE	0.18	1.91	0.00	0.00
284	2MB + MTBE	0.28	2.98	0.00	0.00
285	2MB + ETBE	0.65	6.89	2.01	4.41
286	ETBE + TOL	0.79	11.83	2.39	2.23
287	ETBE + NC8	0.47	6.07	0.00	0.00
288	DME + METHAMINE	0.14	1.47	0.00	0.00
289	DME + NC4	1.51	12.58	9.75	22.50
290	DME + MTBE	0.53	4.84	2.28	17.98
291	CHLOROFORM + BENZ	0.42	4.23	1.98	2.63
292	CS2 + BENZ	0.41	4.89	2.51	3.20
293	BUTAMINE + BENZ	0.99	11.04	19.38	26.63
294	DIETHAMINE + BENZ	0.75	8.11	10.59	18.67
295	BENZ + ACTN	1.64	22.98	18.80	23.47
296	BENZ + PYRD	0.31	4.02	0.76	1.62
297	BENZ + HFBENZ	0.69	4.42	2.78	3.51
298	BENZ + BROMOBENZ	0.50	6.40	5.17	15.81
299	BENZ + NITROBENZ	0.34	4.65	0.34	40.41
300	BENZ + ETHBENZ	0.32	3.24	4.06	13.54
301	BENZ + PXYL	0.32	3.28	1.52	6.10
302	TOL + NITROETH	0.79	10.48	0.00	0.00
303	TOL + ETHDIAMINE	0.89	10.00	10.22	10.19
304	TOL + PYRD	0.28	3.87	0.19	0.21
305	CHLOROFORM + TOL	0.21	2.22	4.21	6.57
306	CS2 + TOL	0.89	10.37	0.00	0.00
307	ACTN + TOL	0.66	8.22	3.10	10.16
308	12DICHETH + TOL	0.24	2.86	5.20	3.24
309	TETCHMETH + ETHBENZ	0.31	3.78	0.84	2.73
310	ACTN + ETHBENZ	1.70	20.26	18.31	33.22
311	DIETHAMINE + ETHBENZ	0.23	3.02	1.11	11.48
312	TETCHMETH + PXYL	0.42	5.87	2.27	4.37
313	ACTN + PXYL	0.88	9.95	11.26	29.25

Table B.4: Results of the UNIQUAC-QSPR model (Contd.)

System No.	System	% AAD			
		T, K	P, bar	K_1	K_2
314	12DICHETH + PXYL	0.20	2.90	0.00	0.00
315	ACETALD + TOL	3.62	48.59	10.61	46.29
316	BUTYRAL + TOL	0.33	3.62	9.90	14.34
317	2M1B + ACETONE	0.21	2.28	0.00	0.00
318	PROPOX + ACETONE	0.19	2.06	2.61	8.22
319	3HEXANONE + 4 HEPTANONE	0.50	6.30	7.50	11.86
320	TOL + CYCHEXANONE	0.22	2.35	3.10	3.52
321	NC6 + 3 PENTANONE	0.51	5.45	1.93	5.44
322	3PENATANONE + 4HEPTANONE	0.25	2.95	3.53	21.24
323	NC6 + 2BUTANONE	0.78	8.31	8.28	10.71
324	NC6 + 14DIOX	0.15	1.69	4.03	3.79
325	ACETALD + ACETONE	0.88	10.20	7.75	15.49
326	PROPOX + PROPANAL	0.24	2.67	3.65	5.02
327	METHACETATE + BUTYRAL	0.71	9.29	7.90	11.71
328	BUTYRAL + PROPACETATE	0.24	3.07	2.05	4.70
329	BUTYRAL + BENZ	0.38	4.39	5.34	4.47
330	BUTYRAL + NC7	0.24	3.10	1.17	3.66
331	13BD + MTBE	0.33	3.61	0.93	6.11
332	ETBE + NC7	0.47	4.63	2.47	6.05

Table B.5: Results of the NRTL-QSPR model

System No.	System	% AAD			
		T, K	P, bar	K_1	K_2
1	MTBE + MEO	0.83	10.21	18.27	13.66
2	MTBE + TBA	0.87	11.04	10.26	10.95
3	DME + MTBE	0.71	6.00	1.35	15.66
4	MTBE + NC4	0.52	4.54	9.71	5.42
5	MTBE + IC5	0.15	1.31	5.37	5.42
6	MTBE + MCYC6	0.63	9.13	6.40	6.95
7	IC4- + MTBE	0.66	5.97	3.51	8.92
8	ETBE + ETH	1.43	15.38	11.07	10.47
9	TBA + ETBE	0.37	4.52	5.59	3.12
10	IC5 + ETBE	0.16	1.88	1.42	4.41
11	MCYC6 + ETBE	0.16	1.76	6.38	2.89
12	IC4- + ETBE	0.88	7.67	3.13	16.02
13	MEO + TAME	0.29	3.71	3.45	6.14
14	TAME + TOH	0.16	2.01	0.00	0.00
15	TOH + TAME	0.05	0.51	0.00	0.00
16	TAME + NC5	0.93	8.95	0.00	0.00
17	TAME + MCYC6	0.21	2.76	3.21	6.36
18	DME + MEO	0.31	3.01	1.66	27.66
19	DEE + H2O	1.00	8.00	0.00	0.00
20	MEO + ETH	0.08	1.15	0.46	0.49
21	NC4 + MEO	0.64	5.71	2.22	12.07
22	MEO + NC7	0.38	4.93	3.66	10.50
23	IC4 + MEO	0.70	5.71	5.48	30.53
24	NC5 + MEO	0.71	7.83	9.45	23.33
25	NC5- + MEO	0.55	6.19	3.86	13.75
26	IC5- + MEO	0.33	3.58	1.59	5.41
27	ISOPRENE + MEO	0.52	5.78	6.28	11.96
28	ISOPRENE + DEE	0.23	2.46	10.24	2.97
29	MEO + 1C7-	0.31	3.84	2.98	7.32
30	MEO + H2O	0.11	1.53	0.46	0.67
31	NC4 + ETH	0.46	3.81	0.00	0.00
32	ETH + H2O	0.16	2.53	5.39	2.22
33	NC6 + TBA	0.23	2.95	1.12	1.24
34	TBA + NC7	0.08	1.19	1.50	2.48

Table B.5: Results of the NRTL-QSPR model (Contd.)

System No.	System	% AAD			
		T, K	P, bar	K_1	K_2
35	NC8 + TBA	0.18	2.90	0.00	0.00
36	TBA + IC5	0.24	2.56	9.61	2.30
37	TBA + IC5-	0.37	3.97	8.42	4.76
38	ISOPRENE + TBA	0.75	7.89	2.67	12.07
39	TBA + H2O	1.68	35.67	20.77	27.24
40	TOH + NC5	0.32	3.01	0.00	0.00
41	MTB + ACTN	0.11	1.31	1.76	3.16
42	MTB + 13BD	0.30	3.46	6.00	2.26
43	MEO + TBA	0.30	4.91	4.47	7.19
44	MEO + IC4-	0.90	7.01	8.68	0.77
45	MEO + ACTN	0.13	1.73	1.63	2.15
46	MEO + PPN	0.07	0.79	0.66	1.57
47	ETH + TBA	0.12	1.93	0.40	1.33
48	TOH + H2O	0.91	13.53	8.70	6.04
49	NC4 + TBA	1.13	9.29	9.99	20.00
50	NC4 + NC5	0.17	1.78	12.98	8.28
51	NC5 + ETH	0.83	8.00	2.81	10.19
52	NC5 + 2M2B	0.25	2.96	0.00	0.00
53	NC5 + ACTN	0.34	3.09	0.00	0.00
54	IC4 + NC4	0.47	4.56	4.39	6.69
55	IC4- + NC4	0.08	0.72	0.00	0.00
56	IC4- + IC4	0.08	0.65	0.00	0.00
57	1C4- + NC4	0.08	0.64	1.59	2.82
58	1C4- + IC4	0.43	3.58	0.00	0.00
59	1C4- + 13BD	0.20	1.73	0.58	0.91
60	C2B- + NC4	0.81	6.32	0.00	0.00
61	T2B- + NC4	0.03	0.29	0.00	0.00
62	2M1B + MEO	0.72	7.57	2.00	7.63
63	2M1B + NC5	0.08	0.94	0.00	0.00
64	2M1B + 2M2B	0.08	0.95	0.43	0.42
65	2M2B + MEO	0.66	7.05	2.89	8.50
66	2M2B + ETH	0.86	8.97	0.00	0.00
67	2M2B + ACTN	0.31	2.93	1.39	3.90
68	ACTN + ETH	0.16	2.09	1.10	1.37
69	ACTN + TBA	0.11	1.42	1.19	2.51

Table B.5: Results of the NRTL-QSPR model (Contd.)

System No.	System	% AAD			
		T, K	P, bar	K_1	K_2
70	ACTN + NC4	0.44	3.10	4.48	0.43
71	ACTN + DISB	0.22	2.80	0.00	0.00
72	ACTN + H2O	0.13	1.62	0.85	1.60
73	PPN + NC5	1.15	7.67	0.00	0.00
74	PPN + H2O	0.11	1.29	2.40	3.34
75	13BD + MEO	0.66	5.79	1.09	12.02
76	13BD + NC4	0.15	1.25	1.99	1.67
77	13BD + IC4	0.10	0.83	0.00	0.00
78	13BD + C2B-	1.19	8.58	0.00	0.00
79	13BD + T2B-	0.20	1.85	0.00	0.00
80	13BD + ACTN	0.51	4.21	0.00	0.00
81	C13P + MEO	0.22	2.53	3.43	7.62
82	T13P + MEO	0.33	3.85	4.96	9.64
83	T13P + ACTN	0.23	2.66	0.00	0.00
84	TBA + 2M1B	0.73	7.23	8.55	2.08
85	TBA + 2M2B	0.37	4.01	8.48	4.77
86	DME + MEO	0.31	3.01	1.66	27.66
87	MEO + H2O	0.11	1.53	0.46	0.67
88	MEM + MEO	0.64	7.44	0.00	0.00
89	DMS + MEO	2.12	22.52	0.00	0.00
90	H2S + MEO	1.52	12.05	1.85	33.08
91	MEO + DMDS	0.10	1.29	0.70	3.53
92	MEM + H2O	0.47	3.34	0.00	0.00
93	DMDS + MEM	0.98	10.66	19.17	4.79
94	H2S + MEM	0.56	4.07	0.68	56.92
95	H2S + DMS	0.47	3.54	2.10	26.97
96	MEM + DMS	0.18	1.92	0.09	2.34
97	BENZ + TOL	0.09	0.92	1.45	2.58
98	NC7 + ETHBENZ	0.02	0.27	0.59	1.44
99	NC8 + ETHBENZ	0.73	8.53	9.95	12.76
100	1C7- + TOL	0.06	0.80	1.38	1.99
101	NC7 + PXYL	0.23	3.42	1.71	3.77
102	BENZ + CYC6	0.43	5.28	4.85	7.56
103	MCYC5 + BENZ	0.33	3.97	3.36	3.20
104	CYC6 + TOL	0.21	2.90	2.45	5.91

Table B.5: Results of the NRTL-QSPR model (Contd.)

System No.	System	% AAD			
		T, K	P, bar	K_1	K_2
105	ISOPRENE + 2M2B	0.12	1.27	1.35	1.45
106	HFBENZ + TOL	0.45	6.79	5.27	9.85
107	TETCHMETH + BENZ	0.33	3.42	5.57	5.08
108	CS2 + CYC6	0.16	1.89	0.67	3.24
109	CS2 + CYC5	0.22	2.63	2.92	3.17
110	CS2 + TETCHMETH	0.09	1.08	1.23	1.43
111	HFBENZ + PXYL	0.87	13.93	5.57	21.51
112	HFBENZ + CYC6	0.01	0.18	0.71	0.54
113	TOL + 4M2P	0.04	0.57	1.51	1.20
114	TOL + 2PENT	0.09	1.28	1.22	2.11
115	BENZ + ACETONE	0.30	3.26	5.66	5.61
116	BENZ + 2BUTANONE	0.27	2.55	1.62	2.67
117	BENZ + THIOPHENE	0.32	3.81	3.49	2.46
118	HFBENZ + DIPE	0.55	7.16	9.90	7.66
119	TETCHMETH + 2BUTANONE	0.22	2.49	4.47	5.00
120	CYC6 + 2BUTANONE	0.12	1.30	3.06	3.03
121	NC7 + THIOPHENE	0.09	1.17	6.33	1.85
122	NC7 + 3PENTANONE	0.15	1.77	3.15	3.46
123	NC7 + 2BUTANONE	0.36	3.89	6.64	6.85
124	NC10 + ACETONE	0.30	3.30	3.10	0.03
125	TETCHMETH + FURF	1.49	13.49	2.11	33.66
126	TETCHMETH + ACETONE	0.13	1.57	8.21	2.04
127	BENZ + 12DICHMETH	0.37	3.95	3.56	4.50
128	TOL + 12DICHMETH	0.15	1.64	2.23	1.07
129	BENZ + DIETHAMINE	0.16	1.84	1.62	0.78
130	BENZ + TRIETHAMINE	0.13	1.38	1.54	1.20
131	ETHBENZ + ACRYL	0.56	8.46	9.02	1.37
132	TOL + NITROBENZ	0.12	1.39	0.30	6.14
133	NC7 + BUTYLCH	0.11	1.35	3.53	2.84
134	CYC5 + CHLOROFORM	0.03	0.39	1.47	1.14
135	NC7 + TRIETHAMINE	0.11	1.35	0.83	1.12
136	23DMETHBUT + CHLOROFORM	0.10	1.08	1.44	0.86
137	ETHBENZ + NITROBENZ	1.25	14.40	5.46	24.02
138	BENZ + NITROMETH	0.04	0.57	1.36	1.16
139	BENZ + TBUT	0.10	1.37	2.45	3.47

Table B.5: Results of the NRTL-QSPR model (Contd.)

System No.	System	% AAD			
		T, K	P, bar	K_1	K_2
140	BENZ + ETH	0.13	1.68	1.62	1.94
141	BENZ + 2PROP	0.18	2.20	1.98	3.76
142	NC7 + ETHIOD	0.10	1.20	4.88	1.60
143	CYC6 + PYRD	0.11	1.14	1.09	5.31
144	NC8 + PYRD	0.07	0.90	1.51	0.99
145	NC8 + MEO	0.46	5.44	10.13	1.32
146	CYC6 + ETH	0.09	1.18	2.17	3.15
147	NC5 + 1BUT	0.53	5.64	0.57	5.37
148	TETCHETHY + ETH	0.30	3.72	3.95	1.49
149	HFBENZ + 1PROP	0.23	3.69	1.60	7.01
150	HFBENZ + MEO	0.18	2.73	4.31	3.41
151	PROPANAL + ACETONE	0.24	2.75	4.82	2.79
152	PROPANAL + 2BUTANONE	0.31	3.83	5.80	5.62
153	ACETONE + VIACETATE	0.03	0.36	1.19	1.56
154	ACETALD + PROPACETATE	0.24	2.57	2.74	3.30
155	ACETALD + VIACETATE	0.26	2.74	0.22	0.99
156	ACETALD + METHACETATE	0.63	7.11	8.41	14.20
157	DEE + ACETONE	0.44	4.85	6.34	8.24
158	ACETALD + DEE	0.17	1.85	2.46	3.59
159	DEE + METHIOD	0.11	1.20	2.22	3.00
160	DEE + DICHMETH	0.23	2.59	1.50	1.35
161	14DIOX + 2PROP	0.15	1.89	5.51	3.13
162	EPE + CHLOROFORM	0.08	0.95	2.78	3.44
163	DEE + CHLOROFORM	0.83	9.53	17.69	17.27
164	ACETONE + CHLOROFORM	0.10	1.30	2.05	2.75
165	PROPACETATE + 1PROP	0.10	1.31	2.13	1.31
166	ETHACETATE + 2PROP	0.24	3.27	5.82	5.14
167	DEE + ETH	0.85	12.23	1.86	17.47
168	FURF + ETH	0.51	7.78	5.52	0.86
169	ACETONE + MEO	0.39	4.62	3.72	6.23
170	14DIOX + MEO	0.09	1.25	2.05	0.67
171	ETH + TRIETHAMINE	0.09	1.43	2.36	2.49
172	TBUT + 1BUT	0.28	4.96	2.44	8.78
173	1PROP + 2M1P	0.10	1.59	1.61	2.10
174	ETH + 2PROP	0.03	0.36	1.58	1.98

Table B.5: Results of the NRTL-QSPR model (Contd.)

System No.	System	% AAD			
		T, K	P, bar	K_1	K_2
175	MEO + 2M1P	0.62	8.79	1.42	5.46
176	ETH + 2M1P	0.51	7.68	2.87	7.32
177	BUTAMINE + 1BUT	0.12	1.74	1.74	2.79
178	DIETHAMINE + ETH	0.20	2.80	6.03	5.68
179	ETH + ACTN	0.09	1.27	3.54	3.26
180	BUTAMINE + 1PROP	0.19	2.77	1.73	2.90
181	BROMOBENZ + CYC6	0.16	2.34	2.57	3.38
182	12DICHETH + 2M1P	0.47	6.37	1.25	5.76
183	MEO + 12DICHETH	0.12	1.70	1.85	2.67
184	H2O + DIETHAMINE	0.36	4.49	8.79	1.68
185	H2O + PYRD	0.11	1.41	4.07	6.60
186	H2O + MEO	0.12	1.59	3.60	1.57
187	H2O + 2PROP	0.19	3.21	2.56	3.97
188	H2O + ETH	0.07	0.93	3.36	3.82
189	ACETALD + PROPOX	0.42	4.51	39.82	10.73
190	ACETALD + BENZ	1.63	19.79	4.36	18.79
191	PROPANAL + CYC6	0.33	3.68	5.57	8.28
192	CHLOROFORM + FURF	2.02	18.16	10.89	46.49
193	1C4- + FURF	0.55	4.63	0.14	26.99
194	TOL + FURF	0.28	3.05	6.50	9.84
195	ETHBENZ + FURF	0.29	3.19	2.55	5.17
196	PXYL + FURF	0.30	3.40	1.32	2.08
197	NC5 + ACETONE	0.62	7.48	4.66	8.04
198	FURF + NC10	0.41	5.02	8.99	9.65
199	TOL + BENZALD	0.17	2.20	0.93	16.69
200	BENZALD + BENZACETATE	1.17	14.63	18.16	29.54
201	ACETONE + TETCHMETH	0.13	1.50	3.59	9.01
202	CS2 + ACETONE	3.84	34.49	24.09	26.32
203	ACETONE +ACTN	0.08	0.94	0.71	1.59
204	ACETONE + 12DICHETH	0.12	1.31	2.65	6.02
205	ACETONE + ETHIOD	0.21	2.61	0.00	0.00
206	METHACETATE + ACETONE	1.58	16.29	22.25	22.29
207	ACETONE + METHACETATE	0.14	1.84	2.21	2.10
208	ACETONE + 2BUTANONE	0.12	1.27	4.94	8.73
209	ACETONE + ETHACETATE	0.21	2.36	3.41	3.32

Table B.5: Results of the NRTL-QSPR model (Contd.)

System No.	System	% AAD			
		T, K	P, bar	K_1	K_2
210	DEE + ACETONE	0.17	2.12	0.00	0.00
211	ACETONE + PYRD	0.76	8.83	4.84	8.20
212	ISOPRENE + ACETONE	0.19	2.05	2.48	5.98
213	2M2B + ACETONE	0.71	7.36	2.39	5.76
214	2MB + ACETONE	0.36	3.71	1.32	4.04
215	ACETONE + PROPACETATE	0.24	2.57	2.76	3.34
216	ACETONE + 112TRICHETH	0.33	3.57	4.56	12.48
217	CYC6 + 4M2P	0.31	3.43	3.93	16.13
218	BENZ + 4M2P	0.52	6.12	3.52	13.64
219	CHLOROFORM + 4M2P	0.18	1.91	4.34	10.00
220	CYC6 + CYCHEXANONE	0.22	2.55	0.37	6.72
221	NC7 + 3PENTANONE	0.15	1.83	3.04	3.87
222	3PENTANONE + 4M2P	0.21	2.37	3.46	5.64
223	ETHACETATE + 3PENTANONE	0.09	1.03	4.89	5.47
224	METHACETATE + 3PENTANONE	0.50	5.45	4.87	2.65
225	2BUTANONE + ETHBENZ	0.39	5.16	3.12	8.51
226	2BUTANONE + NC8	1.58	22.26	7.35	15.20
227	2BUTANONE + NC7	0.78	9.41	12.94	21.04
228	2BUTANONE + TOL	0.09	1.06	1.43	3.53
229	2BUTANONE + BENZ	0.29	3.03	4.33	3.79
230	BENZ + 2BUTANONE	0.12	1.55	2.94	4.12
231	2M2B + 2BUTANONE	0.72	7.29	0.00	0.00
232	ETHACETATE + 2BUTANONE	0.19	2.17	4.35	5.51
233	CHLOROFORM + 2BUTANONE	1.65	16.16	21.25	27.89
234	TETCHMETH + 2BUTANONE	0.09	1.08	5.01	5.41
235	ACETONE + NC10	1.46	19.58	0.31	38.46
236	DEE + BENZ	0.12	1.45	0.00	0.00
237	DEE + HFBENZ	0.03	0.34	0.57	4.60
238	DEE + ETHACETATE	0.24	3.14	0.00	0.00
239	14DIOX + NC8	0.17	2.00	3.08	8.76
240	14DIOX + TOL	0.47	5.37	4.40	4.63
241	NC7 + 14DIOX	0.12	1.40	1.98	2.00
242	BENZ + 14DIOX	0.29	3.83	1.37	4.75
243	DIETHAMINE + 14DIOX	0.44	4.67	3.20	3.48
244	ETHACETATE + 14DIOX	0.21	2.37	3.61	3.13

Table B.5: Results of the NRTL-QSPR model (Contd.)

System No.	System	% AAD			
		T, K	P, bar	K_1	K_2
245	CS2 + 14DIOX	3.00	28.88	0.00	0.00
246	TETCHMETH + 14DIOX	0.30	3.91	0.00	0.00
247	DIPE + ETHBENZ	0.59	6.91	2.35	16.26
248	DIPE + TOL	0.15	1.74	2.23	5.94
249	DIPE + BENZ	0.24	2.61	1.99	1.39
250	DIPE + HFBENZ	0.02	0.32	0.75	1.26
251	CHLOROFORM + DIPE	0.32	3.47	3.13	5.18
252	DIPE + NC7	1.35	15.50	8.46	20.77
253	ACETALD + DEE	0.17	1.84	2.95	4.31
254	PROPANAL + METHACETATE	0.20	2.53	4.01	2.50
255	PROPANAL + ETHACETATE	0.06	0.78	2.75	4.54
256	PROPANAL + BENZ	0.60	6.80	8.36	15.76
257	NC5 + PROPANAL	0.34	3.69	4.31	6.30
258	ISOPRENE + BUTYRALD	1.82	21.97	0.00	0.00
259	DICHMETH + FURF	0.53	5.39	2.01	6.23
260	12DICHETH + FURF	0.08	0.87	3.03	5.56
261	ACETONE + FURF	0.24	2.51	0.66	36.27
262	ETHACETATE + FURF	0.19	1.98	0.96	16.91
263	NC4 + FURF	3.21	21.28	0.07	16.01
264	4M2P + FURF	0.23	3.00	2.67	5.16
265	TETCHETHY + FURF	0.07	0.82	1.93	2.90
266	ETHBENZ + BENZALD	1.10	13.80	7.18	17.50
267	DEE + TETCHMETH	0.30	3.44	2.41	5.46
268	DEE + CYC6	0.42	4.75	0.00	0.00
269	DEE + TOL	1.39	14.79	4.99	19.13
270	2MB + DEE	0.15	1.59	1.08	2.54
271	MTBE + TETCHMETH	0.22	2.60	2.32	2.61
272	MTBE + CHLOROFORM	1.05	13.84	27.87	16.73
273	MTBE + METHACETATE	0.14	1.43	1.66	1.37
274	MTBE + ETHACETATE	0.15	1.50	1.70	4.68
275	MTBE + BENZ	0.17	1.88	0.34	0.57
276	MTBE + CYC6	0.39	4.46	0.00	0.00
277	MTBE + DIPE	0.17	1.92	3.99	1.88
278	MTBE + TOL	0.10	1.14	1.04	6.47
279	MTBE + NC7	1.80	25.21	8.73	12.67

Table B.5: Results of the NRTL-QSPR model (Contd.)

System No.	System	% AAD			
		T, K	P, bar	K_1	K_2
280	DICHMETH + MTBE	0.33	3.97	3.92	6.92
281	NC4 + MTBE	0.69	6.77	0.00	0.00
282	ISOPRENE +MTBE	0.19	2.10	0.00	0.00
283	2M2B + MTBE	0.18	1.99	0.00	0.00
284	2MB + MTBE	0.48	5.08	0.00	0.00
285	2MB + ETBE	0.74	7.85	1.76	5.06
286	ETBE + TOL	0.81	12.04	2.90	2.30
287	ETBE + NC8	0.30	3.66	0.00	0.00
288	DME + METHAMINE	0.14	1.46	0.00	0.00
289	DME + NC4	2.46	19.19	18.28	31.96
290	DME + MTBE	0.28	2.71	0.65	10.81
291	CHLOROFORM + BENZ	0.77	8.02	3.24	3.48
292	CS2 + BENZ	0.27	3.04	2.37	3.01
293	BUTAMINE + BENZ	0.44	5.14	9.30	20.31
294	DIETHAMINE + BENZ	0.17	1.86	6.35	11.49
295	BENZ + ACTN	0.16	2.45	2.35	2.11
296	BENZ + PYRD	1.57	24.82	6.83	15.60
297	BENZ + HFBENZ	0.72	4.68	2.60	4.21
298	BENZ + BROMOBENZ	0.18	2.21	4.02	14.57
299	BENZ + NITROBENZ	1.17	18.10	0.38	38.70
300	BENZ + ETHBENZ	0.05	0.49	3.42	7.07
301	BENZ + PXYL	0.33	3.55	3.92	5.16
302	TOL + NITROETH	0.95	12.41	0.00	0.00
303	TOL + ETHDIAMINE	0.32	3.67	3.72	3.91
304	TOL + PYRD	1.10	17.67	1.75	2.52
305	CHLOROFORM + TOL	0.24	2.51	4.07	5.77
306	CS2 + TOL	0.36	4.20	0.00	0.00
307	ACTN + TOL	0.17	2.04	2.54	3.04
308	12DICHETH + TOL	0.31	3.56	5.13	4.39
309	TETCHMETH + ETHBENZ	0.21	2.56	1.18	2.66
310	ACTN + ETHBENZ	0.62	6.88	10.28	15.38
311	DIETHAMINE + ETHBENZ	0.46	5.75	0.90	12.59
312	TETCHMETH + PXYL	0.38	5.34	2.03	4.01
313	ACTN + PXYL	1.18	14.01	19.68	23.06
314	12DICHETH + PXYL	0.05	0.68	0.00	0.00

Table B.5: Results of the NRTL-QSPR model (Contd.)

System No.	System	% AAD			
		T, K	P, bar	K_1	K_2
315	ACETALD + TOL	4.76	69.07	6.94	64.06
316	BUTYRAL + TOL	0.12	1.31	7.98	14.65
317	2M1B + ACETONE	0.58	5.99	0.00	0.00
318	PROPOX + ACETONE	0.58	6.67	8.54	10.31
319	3HEXANONE + 4 HEPTANONE	0.07	0.94	2.47	4.62
320	TOL + CYCHEXANONE	0.29	3.25	5.29	6.94
321	NC6 + 3 PENTANONE	0.24	2.69	1.28	3.02
322	3PENATANONE + 4HEPTANONE	0.10	1.21	3.53	18.15
323	NC6 + 2BUTANONE	0.38	4.22	3.81	4.60
324	NC6 + 14DIOX	1.59	15.63	11.74	23.53
325	ACETALD + ACETONE	0.27	2.89	3.67	12.20
326	PROPOX + PROPANAL	0.39	4.21	7.83	10.81
327	METHACETATE + BUTYRAL	0.11	1.38	2.56	2.02
328	BUTYRAL + PROPACETATE	0.08	1.08	2.22	3.15
329	BUTYRAL + BENZ	0.28	3.16	5.47	4.42
330	BUTYRAL + NC7	1.50	21.65	14.75	22.90
331	13BD + MTBE	0.75	8.60	4.61	9.93
332	ETBE + NC7	1.41	13.47	6.76	7.46

References

1. Acosta, R.G., Rodrigues, E.R., P.M. De La Guardia, *Rev. Inst. Mex. Petrol* (1980).
2. Alm, K., M. Ciprian, *J. Chem. Eng. Data*, 25, 100 (1980).
3. Churkin, V.N., Gorshkov, V.A., S. Yu. Pavlov, *Prom-St Sint Kauch*, 4, 2 (1979).
4. Velasco, E., Cocero, M.J., F. J. Mato, *J. Chem. Eng. Data*, 35, 21 (1990).
5. Wang, Y., *Petrochem Tech (Rep China)*, 7, 442 (1989).
6. Mullins, S.R., Oehlert, L., Wileman, K.P., Manley,D.B., *AIChE Symposium Series*, 85, 271, 94 (1997).
7. Zong, Z., Yang, X., Zheng, X., *Ranliao Huaxue Xuebao*, 15, 32 (1987).
8. Phillips Data Files (1995).
9. Pavlova, et al., *Prom.-st Sint. Kauch.,* 6, 2 (1981).
10. Cervenkova and Bublik (1984).
11. Palczewska-Tulinska et al. (1990).
12. Churkin, V.N., Gorshkov, V.A., Pavlov, S. Yu., Basher, M.E., *Prom-St. Sint. Kauch.,* 4, 2 (1979).
13. Semar, S., Sandler, I.S., Antosik, M., private communication
14. Churkin, V.N., Gorshkov, V.A., S. Yu. Pavlov, Zh Fiz Khim, 52, 488 (1978).
15. Leu, A.D., Chen, C.J., Robinson, D.B., *AIChE Symposium Series*, 85, 271 (1982).
16. Mervart, Z., Kubilnova, M., Zelikova, V., *Collect. Czech. Chem. Comm.,* 26, 2129 (1961).
17. Vilin, O., *Collect. Czech. Chem. Comm.,* 26, 2480 (1961).
18. Kharin, S.E., et. al., *Khim Technol.,* 12, 1695 (1969).
19. Kojima, K. and M. Kato, Kagaku Kogaku, 33, 769 (1969).
20. Holderbaum, T., Utzig, A., Gmehling, J., *Fluid Phase Equilibria,* 63, 219 (1991).
21. Kirschbaum, E., Gestner, H., Z. Vdi. Beih. Verfahrenstechnik, 1, 10, (1939).
22. Dalager P.J., *J. Chem. Eng. Data*, 14, 298, (1969).

23. Govindaswamy, S., Andiappan, A.N., Lakshmanan, S.M., *J. Chem. Eng. Data*, 22, 264 (1977).
24. Janaszewki, B., Oracz, P., Goral, M., Warycha, S., *Fluid Phase Equilibria*, 9, 295 (1982).
25. Kumar, A., S.S. Katti, *Indian J. Chem. Eng.,* 19A, 795 (1980).
26. Lesteva, T.M., Ogorodnikov, S.K., Kazakova, S.V.,, *Zhikl. Khim. Leningrad*, 43, 1574 (1970).
27. Edwards, D., Marucco, J., Ratouis, M., Dode, M.J., *J. Chim. Phys. Physiochim. Biol.,* 63, 239(1966).
28. Villamanan M.A., Allawi A.J., Van Ness H.C., *J. Chem. Eng. Data*, 29, 431, (1984).
29. Signer, R., Arm, H., Daeniker, H., *Helv. Cheim. Acta*,52, 2347(1969).
30. Ogordonikov, S.K., Kogan, V.B., Nemstov, M.S., *Zh. Prikl. Khim.,* 33, 2685 (1960).
31. Budantseva, L.S., Lesteva, T.M., Nemtsov, M.S., *Zh. Fiz. Khim*., 49, 1844 (1975).
32. Benedict, M., Johnson, C.A., Solomon, E., Rubin, L.C., *Trans. Am. Inst. Chem. Eng.*, 41, 371(1945).
33. Budantseva, L.S., Lesteva, T.M., Nemtsov, M.S., *Zh. Fiz. Khim.*, 49, 1844(1975).
34. Yasuda, M., Kawade, H., Katayama, T., *Kakaku Kogaku Ronbunshu,* 1, 172(1975).
35. Tenn, F.G., Missen, R.W., *Can. J. Chem. Eng.,* 41, 12 (1963).
36. Haywood, J. K., *J. Am. Chem. Soc.,* 21, 994 (1899).
37. Kooner, Z. S., Fenby, D.V., *Aust. J. Chem.,* 33, 1943 (1980).
38. Oracz, P., *Int. Data Series, Sel. Data Mixtures Ser. A,* 2 (1986).
39. Chang E., Calado J. C. C., Street, W.B., *J. Chem. Eng. Data,* 27, 293 (1982).
40. Leu, A. D., Robinson, D.B., *J. Chem. Eng. Data,* 37, 10 (1992).
41. Ogorodnikov, S.K., Kogan, V.B., Nemtsov, M.S., *Zh. Prikl. Khim,* 33, 2685(1960).
42. Dobson, H.J.E., *J. Chem. Soc.,* 2866(1925).
43. D'Avilla, S.G., Cotrim, M. L., *Rev. Bras. Technol.*, 4, 191(1973).
44. Huey, S., *J. Chem. Eng. Data,* 37, (1991).

45. Antosik, M., Sandler, S.I., *J. Chem. Eng. Data,* 39, 584 (1994).
46. Bernshtein, L. A., *J. Chem. Eng. Data,* 37, (1979).
47. Steinhagen, V., Sandler, S.I., 8, *J. Chem. Eng. Data,* 39, 584 (1994).
48. Leu, A. D., *AIChE Symposium Series*, 85, 11 (1989).
49. Mato, F. A., Charles B., *J. Chem. Eng. Data,* 36, 262 (1991).
50. Pascal, P., *Bull. Soc. Chim. Fr.,* 29, 9 (1921).
51. Ziak, J., Zavodska, M., Jurik, J., *Petrochemia,* 14, 41 (1974).
52. Polak, J., *Can. J. Chem.,* 48, 2457 (1970).
53. Oracz, P., *Int. Data Ser., Sel. Data Mixtures, Ser. A,* 286 (1989).
54. Joukovsky, N. I., *Bull. Soc. Chim. Belg.,* 43, 397 (1934).
55. Dohnal, V., Holub, R., Pick, J., *Collect. Czech. Chem. Commun.,* 42(5), 1445 (1977).
56. Tamir, A., Wisniak, J., *J. Chem. Eng. Data,* 31(3), 363 (1986).
57. Mato, F., GonzalezBenito, G., *An. Quim., Ser. A,* 81(1), 116 (1985).
58. Martin, M. C, Cocero, M. J., Mato, F., *Fluid Phase Equilibria,* 74, 243 (1992).
59. Suska, J., *Collect. Czech. Chem. Commun.,* 35(2), 385 (1970).
60. Oracz, P., *Int. Data Ser., Sel. Data Mixtures, Ser. A,* 289 (1989).
61. Andreeva, N. G., *Zh. Prikl. Khim. (Leningrad),* 49(5), 1155 (1976).
62. Melpolder, F. W., *Fluid Phase Equilibria,* 26(3), 279 (1986).
63. Calingaert, G., Hitchcock, L.B., *J. Am. Chem. Soc.,* 49, 750 (1927).
64. Ishii, N., *J. Soc. Chem. Ind. Japan,* 38, 705 (1935).
65. McCracken, P. G., Storvick, T. S., Smith, J.M., *J. Chem. Eng. Data,* 5, 130 (1960).
66. Campbell, S. W., Wilsak, R. A., Thodos, G., *J. Chem. Thermodyn.,* 19(5), 449 (1987).
67. Gumpert, H. J., Wiss. Z., *Tech. Hochsch. Chem. Leuna-Merseburg,* 15, 179 (1973).
68. Zawiska, A. C., Glowka, S., *Bull. Acad. Pol. Sci. Chim.,*17, 373 (1969).
69. Rodriguez, A. T., McLure, I.A., *Fluid Phase Equilibria,* 12(3), 297 (1983).
70. Hirata, M., Suda, S., *Bull. Japan Petrol. Inst.,* 10, 20 (1968).
71. Martinez-Ortiz, J. A., Manley, D.B., *J. Chem. Eng. Data,* 23, 165 (1978).

72. Lawrence, D. R., Swift, G.W., *J. Chem. Eng. Data,* 19, 61 (1974).
73. Sage, B. H., Lacey, W.N., *Ind. Eng. Chem.,* 40(7), 1300 (1948).
74. Steele, K., Poling, B. E., Manley, D.B., *J. Chem. Eng. Data,* 21, 399 (1976).
75. Leu, A., Carroll, J. C., Robinson, D.B., *Fluid Phase Equilibria*, 72, 163 (1992).
76. Flebbe, J. L., Barclay, D. A., Manley, D.B., *J. Chem. Eng. Data,* 27(4), 405 (1982).
77. Dolejsek, Z., *Chem. Prumsyl.,* 11, 361 (1961).
78. Smirnov, V.V., *Prom-St. Sint. Kauch.,* 2, 1 (1976).
79. Ogorodnikov, S.K., *Zh. Prikl. Khim.,* 34, 1096 (1961).
80. Nagahama, K., Hirata, M., *Bull. Jap. Petrol. Inst.,* 18, 80 (1976).
81. Sugi, H., Katayama, T., *J. Chem. Engg. of Japan,* 11(3), 167 (1978).
82. Wilson, R. W., *J. Chem. Eng. Data,* 24(2), 130 (1979).
83. Vierk, A. L., *Anorg. Chem.,* 261, 283 (1950).
84. Muthu, O., Maher, P. J., Smith, B.D., *J. Chem. Eng. Data,* 25(2), 163 (1980).
85. Dohnal, V., *Collect. Czech. Chem. Commun.,* 47(12), 3177 (1982).
86. Raviprasad, A., *J. Chem. Eng. Data,* 23, 26 (1978).
87. Nagata, I., *J. Chem. Thermodyn.,* 21(3), 225 (1989).
88. Rodriguez, A. T., McLure, I.A., *Fluid Phase Equilibria,* 12(3), 297 (1983).
89. Nhu, N.V., Svejda, P., *Fluid Phase Equilibria,* 49, 127 (1989).
90. Trejo, A., Zepeda, M.C., *Fluid Phase Equilibria,* 47, 265 (1989).
91. Taramasso, M., M. De Malde, *Chim. Ind. (Milan),* 49, 820 (1967).
92. Laird, D. G., Howat, C.S., *Fluid Phase Equilibria,* 60, 173 (1990).
93. Gromov, G.P., Movzumsade, M. M., Sadykov, R.K., *Izv. Vyssh. Uceb. Zaved. Neft. Gaz.,* 12, 57 (1969).
94. Wilding, W.V., DIPPR Project 805/93, (1993).
95. Kilner, J., Mcbain, S. E., Roffey, M.G., *J. Chem. Thermodyn.,* 22 (2), 203 (1990).
96. Wilding, W. V., Wilson, L. C., Wilson, G.M., DIPPR Data Series No. 1, 6 (1991).
97. DIPPR Project 801; *Physical and Thermodynamic Properties of Pure Chemicals.*
98. Gmehling, J., Onken, U., Arlt, W., Vapor-Liquid Equilibrium Data Collection, *Chemistry Data Series*, Vol. 1-8, DECHEMA, (1979).

VITA

Devipriya Ravindranath

Candidate for the Degree of

Master of Science

Thesis: STRUCTURE-BASED GENERALIZED MODELS FOR PURE-FLUID SATURATION PROPERTIES AND ACTIVITY COEFFICIENTS

Major Field: Chemical Engineering

Biographical:

Personal Data: Born in Mettupalayam, Tamil Nadu, India, April 25th, 1981, the daughter of P.V.Ravindranath and Indra Ravindranath.

Education: Graduated from St. Ann's High School, Secundrabad, India, in June 1996; received Bachelor of Technology Degree in Chemical Engineering from Osmania University, Hyderabad, India, in June 2002; completed requirements for the Master of Science Degree from Oklahoma State University, Stillwater, in December, 2005.

Experience: Employed by Oklahoma State University, School of Chemical Engineering as a Graduate assistant, 2003-2005.

Professional Memberships: American Institute of Chemical Engineers.

Name: Devipriya Ravindranath Date of Degree: December, 2005

Institution: Oklahoma State University Location: Stillwater, Oklahoma

Title of Study: STRUCTURE-BASED GENERALIZED MODELS FOR PURE-FLUID SATURATION PROPERTIES AND ACTIVITY COEFFICIENTS

Pages in Study: 154 Candidate for the Degree of Master of Science

Major Field: Chemical Engineering

Scope and Method of Study:

Structure-based generalized models were developed for *a priori* predictions of pure-fluid saturation properties, and for vapor-liquid equilibrium (VLE) of binary mixtures. Specifically, Quantitative Structure-Property Relationships (QSPR) modeling was used to provide structure-based parameters for (a) the Scaled-Variable-Reduced-Coordinate (SVRC) saturation property model, and (b) the Non-Random Two-Liquid (NRTL) and the Universal Quasi-Chemical (UNIQUAC) activity coefficient models. A representative database comprised of diverse molecular species was utilized for these generalizations

Findings and Conclusions:

The SVRC-QSPR model generalizations for vapor pressure and saturated phase densities yielded predictions with absolute average deviation (AAD) of 1%. Similarly, the NRTL-QSPR and UNIQUAC-QSPR activity coefficient models produced VLE predictions within twice the AAD of the data regressions.

The results of this preliminary study demonstrate the efficacy of using theory-framed QSPR modeling for generalizing saturation property and phase equilibrium models.

ADVISOR'S APPROVAL: _____